Reducing uncertainties in image-guided radiotherapy of rectal cancer

Ende, R.P.J. van den

Cover Page

Universiteit Leiden

The handle http://hdl.handle.net/1887/137099 holds various files of this Leiden University dissertation.

Author: Ende, R.P.J. van den
Title: Reducing uncertainties in image-guided radiotherapy of rectal cancer
Issue date: 2020-10-22

Reducing uncertainties in image-guided radiotherapy of rectal cancer

Roy Pieter Johannes van den Ende

Reducing uncertainties in image-guided radiotherapy of rectal cancer

Roy Pieter Johannes van den Ende

Reducing uncertainties in image-guided radiotherapy of rectal cancer

Reducing uncertainties in image-guided radiotherapy of rectal cancer

Proefschrift

ter verkrijging van
de graad van Doctor aan de Universiteit Leiden
op gezag van Rector Magnificus prof. mr. C.J.J.M. Stolker,
volgens besluit van het College voor Promoties
te verdedigen op donderdag 22 oktober 2020
klokke 13:45 uur

door

Roy Pieter Johannes van den Ende
geboren te Delft
in 1991

CONTENTS

Chapter 1

Introduction

INTRODUCTION

Rectal cancer epidemiology

Worldwide, the incidence of colorectal cancer has increased in the last decade, especially in Western countries. This increase in incidence may be explained by modifiable lifestyle factors, such as smoking, alcohol intake, physical inactivity, obesity, low consumption of fruits and vegetables and high consumption of red meat and processed meat [1]. In addition, the introduction of population screening has contributed to an increased incidence. In the Netherlands, the incidence of colorectal cancer is one of the highest of all cancer types, with 15.306 new cases in 2016, of which 4461 were diagnosed as rectal cancer [2]. Since the early nineties, the incidence of rectal cancer has doubled and the 5-year survival has increased from 53% to 67% in recent years.

Survival of rectal cancer patients is mainly dependent on the disease stage at the time of diagnosis, with a better prognosis for early diagnosed patients. Unfortunately, most patients are unaware of their disease until clinical symptoms occur, with an already advanced stage as a result. In order to improve survival for colorectal cancer patients, population screening was introduced in the Netherlands in 2014. This has led to an increased incidence, leading to more early stage colorectal cancer patients at diagnosis. Apart from possibly less aggressive treatment in some patients, improved overall survival of colorectal cancer patients has been anticipated [3].

Treatment
Surgery

Treatment advances in the last decades have led to improved local control and overall survival of rectal cancer patients. Surgery is the mainstay of treatment and a major step in surgical quality was made with the introduction of standardized total mesorectal excision (TME) surgery by Heald [4]. In a TME procedure, the entire mesorectal compartment is excised along anatomical planes. The specimen includes the rectum, surrounding mesorectum and perirectal lymph nodes, enclosed by the mesorectal fascia (MRF). The introduction of this standardized technique reduced local recurrence rates from over 25% to approximately 10% [4–6].

Generally, two approaches of TME surgery are used. An abdominoperineal resection (APR) is generally used in patients with low lying tumors and involves removal of the anus, rectum and part of the sigmoid colon along with the complete mesorectum. Due to the removal of the anal sphincter complex, an APR always results in a permanent stoma. A low anterior resection (LAR) involves removal of the part of the rectum in which the tumor is located along with the surrounding mesorectum. An anastomosis is then performed to attach the colon to the remaining part of the rectum. To reduce the risk of anastomotic leakage, patients may have a temporary stoma, which can be reverted later on [7].

For early stage rectal cancer patients with T1N0, an alternative to TME surgery might be a local excision. In this procedure, the tumor is locally excised through the anus using transanal endoscopic microsurgery (TEM), thereby saving the rectum and sphincter complex. Local excision surgery is associated with lower morbidity and mortality rates compared to TME surgery [8]. However, TEM has an increased risk of a non-radical resection [9] as well as a risk of leaving involved lymph nodes behind. As a result, local recurrence rates are substantially higher after TEM compared to TME [10].

(Chemo)radiotherapy

For more advanced cases, the addition of (chemo)radiotherapy to TME surgery further reduced local recurrence rates to 5-8% [11–14]. Two general treatment schedules are used as a neoadjuvant treatment. For intermediate risk patients, i.e. cT1-3N1 or cT3N0 with >5 mm extramural invasion and no involved mesorectal fascia (MRF), short-course radiotherapy (SC-RT) is given with 25 Gy in 5 fractions within one week in northern European countries.

The MRF is the resection plane of a TME resection and involvement of the MRF leads to positive circumferential resection margins (CRM) in a large number of patients. Several studies have demonstrated an increased local and distant recurrence risk after resections with a positive CRM [15]. If the distance of the primary tumor or involved lymph node to the MRF is smaller than or equal to 1 mm, it is considered an involved MRF and the patient is not eligible for direct TME surgery. For high risk patients, being cT4, cT3 with involved MRF, and/or cN2 or extramesorectal pathological nodes, long-course chemoradiotherapy (LC-CRT) is given with 45-50 Gy in fractions of 1.8-2 Gy.

The addition of preoperative SC-RT in stage I-III patients has been investigated in the TME trial and the MRC CR07 trial. In the TME trial, patients with resectable rectal cancer were randomized between SC-RT followed by immediate surgery or surgery alone [11]. In the MRC CR07 trial, patients with resectable rectal cancer were randomized between SC-RT with direct TME surgery or TME surgery with selective adjuvant chemoradiotherapy [14]. In both trials, a significant reduction in local recurrence rate was observed in patients with a negative CRM after TME in the radiotherapy group compared to the TME alone group. Because of the short interval between radiotherapy and TME surgery, no downstaging was observed [16].

The addition of chemotherapy to radiotherapy was investigated in the FFCD 9203 and EORTC 22921 trials. In the EORTC 22921 trial, patients with resectable, T3-T4 rectal cancer were randomized between preoperative long-course radiotherapy with or without fluorouracil based chemotherapy. In addition, the role of adjuvant chemotherapy was investigated, resulting in a 2x2 design [12]. In the FFCD 9203 trial, patients with resectable T3-4 rectal cancer were randomized between preoperative long-course radiotherapy with or without concomitant chemotherapy [17]. Time between (chemo)radiotherapy and surgery was 3-10 weeks. In both trials, the addition of chemotherapy resulted in lower local recurrence rates compared to long-course radiotherapy only. Ten year local recurrence was 22.4% vs 11.8% in the

EORTC 22921 trial and 5-year local recurrence was 16.5% vs 8.1% in the FFCD 9203 trial. In addition, more tumor downstaging was observed in the chemoradiotherapy group.

The Stockholm III trial investigated the optimal fractionation of neoadjuvant radiotherapy and timing to surgery by randomizing patients with resectable rectal cancer between short-course radiotherapy with immediate surgery, short-course radiotherapy with delayed surgery and chemoradiotherapy with delayed surgery. Interim analyses showed that patients in the SC-RT with delayed surgery group had a greater degree of tumor regression and a higher pathological complete response rate compared to the SC-RT with immediate surgery group [18,19]. After a follow-up of a minimum of 2 years, no differences in local recurrences, distal recurrences and overall survival were observed. In addition, the risk of surgical complications was lower in the delayed surgery groups. Preoperative toxicity was however higher.

Frail patients that are considered unfit for surgery are usually also unfit for chemotherapy. For these patients, definitive radiotherapy can be offered. Literature describes varying schedules and techniques, including external beam radiotherapy (EBRT), contact therapy and brachytherapy [20].

Toxicity and complications

The introduction of standardized TME surgery led to a substantial reduction in local recurrence rates. However, after TME surgery a permanent stoma is required in about 10-20% of cases and a temporary stoma is required in 60-70% of cases of which many are not reversed [21,22]. In addition, TME surgery can result in substantial morbidity, including bowel leaks (16%), urinary incontinence or retention (25-34%), sexual dysfunction, and daily symptoms of urgency, incomplete emptying and stool frequency (30-40%) [23–27]. Thirty-days operative mortality is around 3-6% for patients <75 years of age and around 10-14% for patients >75 years of age [28].

While pre-operative (chemo)radiotherapy reduced local recurrence rates, it is also associated with an increased risk of side effects such as bowel and sexual dysfunction [29]. In the TME trial, 10-year local recurrence rates were lower in the radiotherapy group (5% vs 11%, p<0.0001), but no benefit in overall survival was observed (48% vs 49%). In a subgroup analysis, a benefit in overall survival was observed in the radiotherapy group in TNM stage III patients (50% vs 40%) with negative CRM. However, in TNM stage I and II patients, overall survival was lower in the radiotherapy group (65 vs 72% for stage I and 51 vs 57% for stage II) [11]. Although one has to be careful with interpretation of unplanned subgroup analyses, these results seem to suggest that EBRT can cause a systemic effect. It has to be noted that patients in the TME trial were treated with a box technique with conventional 2D treatment planning, which may have contributed to the systemic effect. The results also show that patient selection based on disease stage could be useful, as overall survival was lower in stage I-II rectal cancer patients in the SC-RT group. In addition, reducing the integral dose and/or the dose to the organs at risk may reduce the side-effects associated with radiotherapy.

Reducing treatment related toxicity and morbidity

Improvements in the treatment of rectal cancer patients have led to increased survival. As a result, long-term outcome has become an increasingly important factor. In addition, the introduction of population screening will lead to earlier detection of the disease with probably improved survival as a result [3]. Both preoperative (chemo)radiotherapy and TME surgery are associated with toxicity and complications. As a result, research for rectal cancer treatment has focused on the reduction of radiation dose to (healthy) tissue and less extensive surgery or omission of surgery in selected patients.

Neoadjuvant radiotherapy

The target volume for neoadjuvant radiotherapy for rectal cancer typically encompasses the primary tumor, with elective irradiation of the whole mesorectum and presacral and internal iliac nodes, with the cranial border around the level of the sacral promontory and the caudal border at least 2 cm below the primary tumor. The most important organs at risk are the small bowel and the sphincter complex. Due to the large target volume and the proximity of these organs at risk to the target volume, dose is deposited in these organs at risk which causes part of the radiotherapy treatment related toxicity. In addition, dose deposition in nerves located in the pelvis may attribute to decreased functional outcome.

Reduction of dose to healthy tissue can be achieved by decreasing treatment margins, or by using an alternative treatment technique. Research on the interfraction displacement of the CTV resulted in guidelines on required margins for rectal cancer radiotherapy. These required margins reduced the PTV volumes on average with 16% (SC-RT) and 24% (LC-CRT) compared to previous standard practice [30].

EBRT is currently the standard treatment modality for neoadjuvant radiotherapy for rectal cancer. With EBRT, the patient is irradiated using an external beam, in which radiation dose is deposited in the healthy tissue surrounding the target volume before it reaches the target volume. An attractive alternative treatment technique is intracavitary irradiation, that offers the advantage of delivering a high dose to the tumor from the inside while sparing surrounding organs at risk due to a steep dose gradient. Intracavitary irradiation for rectal cancer is an experimental and specialized treatment technique that is not widely available. It can be applied using either contact therapy or brachytherapy. Contact therapy is performed using a 50 kV handheld tube under direct visual control of the tumor [31]. Due to the low energy and therefore a steep dose fall-off, a very localized treatment can be applied. Brachytherapy can be given endoluminally, with an applicator inserted in the rectum. A number of different rectal applicators are available, ranging from single channel rigid applicators to flexible multichannel applicators [32]. With an afterloading system, an irradiation source can be guided through the channels in order to irradiate the region of interest. The multichannel flexible applicator is often used for high-dose rate endorectal brachytherapy (HDREBT) and has the advantage that the eight channels are placed circumferential near the edge of the applicator, which allows conformal treatment planning by using the channels that are located near the tumor. Although HDREBT is an invasive procedure as opposed to EBRT, it is well tolerated by most patients [33].

Compared to the target volume in neoadjuvant EBRT, brachytherapy reduces the irradiated volume considerably, leading to less dose to normal tissue. In addition, the dose in the tumor itself is significantly higher. However, potential positive lymph nodes that are further away from the tumor are not irradiated or receive a lower dose compared to EBRT. Nonetheless, the role of HDREBT as a neoadjuvant treatment was demonstrated by the group of Vuong *et al*. In a single center study, neoadjuvant HDREBT (4x 6.5 Gy) was given for mainly T3 tumors (88.8%) with 34% of patients having N+. A final pathologic stage of T0N0-2 was reached in 27% and 5-year local control was 95% [34]. In a recent retrospective chart review that compared HDREBT to EBRT (mainly chemoradiotherapy), pathological complete response rates were similar (18.8% in the HDREBT group vs 17.1% in the EBRT group) and T-stage downstaging was significantly higher in the HDREBT group (59.4% vs 28.5%, p<0.01) [35]. Hesselager *et al*. performed a matched comparison of 318 patients treated with preoperative HDREBT (4x 6.5 Gy, TME after 4-8 weeks), preoperative SC-RT (5x5 Gy, direct TME) and TME only [36]. Less perioperative bleeding was reported in the HDREBT group compared to the SC-RT and TME only group (380 mL, 947 mL and 919 mL, respectively). In addition, less re-interventions were performed in the HDREBT group than in the SC-RT and TME only group (4.1%, 14.2% and 12.3%, respectively). Although it was not the primary endpoint of the study, a pathological complete response rate of 23.6% was reported after HDREBT. However, it is difficult to draw firm conclusions based on these non-randomized trials.

Organ preservation

The reported negative effects of rectal cancer surgery led to increased interest for organ preservation, in which surgery might be omitted if the patient experiences a complete response after neoadjuvant therapy. In these patients, a 'watch and wait' strategy with omission of surgery and a strict follow-up protocol seems to be a safe alternative to surgery [37]. Surgery and the related morbidy and mortality are then avoided.

A pathological complete response (pCR) is observed in 15-25% of patients after standard chemoradiotherapy [38,39]. Complete response rates up to 50% are observed in centers with a dedicated watch and wait protocol, probably due to better patient selection [40,41]. Complete response rates might be increased by delivering a higher dose to the tumor [42,43]. This may therefore be beneficial in organ preservation strategies in order to increase the chance of a complete response. Tumor dose can be increased by applying a boost using EBRT or intracavitary irradiation.

A randomized trial comparing 13x3 Gy radiotherapy with or without an endocavitary boost using X-ray contact therapy (85 Gy in 3 fractions) reported an improved clinical complete response rate (24% vs 2%) in the boost group [44]. No difference in local relapse and acute or postoperative toxicity were reported and 2-year overall survival was similar. Another randomized trial compared LC-CRT (28 x 1.8 Gy) with- or without HDREBT boost (2 x 5 Gy) in resectable T3 and T4 rectal cancer patients [45]. The R0 resection rate was higher in the boost group (99% vs 90%) as was the major response rate defined as tumor regression grade 1 and 2 (44% vs 29%). No difference was found in toxicity or surgical

complications. Unfortunately, no difference in pCR rate was reported. The HERBERT trial was a dose escalation trial in which a HDREBT boost in 3 weekly fraction of 5-8 Gy was applied after 13 x 3 Gy EBRT in inoperable and elderly patients [46]. The maximum tolerated dose was determined at 7 Gy. Overall, a CR rate of 60% was observed. However, the treatment came with substantial risk of toxicity, with 40% grade ≥3 proctitis.

In order to facilitate organ preservation in early stage rectal cancer patients, (chemo)radiotherapy has to be given in order to control the tumor. This group of patients would normally not receive neoadjuvant treatment as the standard of care for these patients is TME surgery. The risk of pelvic lymph node involvement or distal mesorectal nodal involvement is very low in early rectal cancer patients. Therefore, it is doubtful whether the typically used large target volumes are required for these patients and reduction of the target volume to only include the peritumoral region of the primary tumor and mesorectum seems reasonable. The significant volume reduction might lead to decreased treatment-related toxicity without compromising oncological outcome. This is currently being investigated in the STAR-TReC trial, which assesses the feasibility of short-course radiotherapy or long-course chemoradiotherapy with subsequent two-stage response assessment as an alternative to TME surgery. Patients with T1-3bN0M0 rectal cancer are randomized between TME, organ preservation utilizing LC-CRT and organ preservation utilizing SC-RT. The radiotherapy target volume only includes the mesorectum [47].

Treatment delivery techniques

In order to deliver radiotherapy safely, a target volume needs to be defined to steer the treatment planning. In general, three target volumes are defined: the gross tumor volume (GTV), the clinical target volume (CTV) and the planning target volume (PTV). The GTV is defined as macroscopic tumor tissue which can be seen, palpated or imaged. The CTV is defined as the GTV plus the volume that is expected to contain any microscopic tumor deposits. Since microscopic tumor deposits in the tissue surrounding the tumor cannot be imaged, guidelines have been developed for delineation of the CTV for rectal cancer based on local recurrence patterns in the pelvis [48].

To ensure full coverage of the CTV by the prescribed dose, geometrical deviations of the treatment process should be taken into account. These deviations for example include CTV delineation errors, setup errors of the patient with respect to the treatment machine, and inter- and intrafraction CTV motion. Geometrical deviations are separated into two components: treatment preparation (systematic errors) and treatment execution (random errors). Systematic errors result in a shift of the dose distribution with respect to the target volume, while random errors result in blurring of the dose distribution [49]. The geometrical deviations are taken into account by adding a PTV margin to the CTV. Increasing the margin size will increase the chance that the CTV receives full coverage by the prescribed dose. However, with increasing margin size, more healthy tissue will be irradiated with risk of side-effects.

Image-guided external beam radiotherapy

EBRT delivery techniques have evolved in the past decades to deliver radiation doses with increasing conformality. During the mid-nineties, a box technique was commonly used. It utilizes multiple (e.g. 3 or 4) rectangular beams, aimed at the target at any angle in the transverse plane. Each beam was homogeneous in terms of intensity. This technique was replaced by 3D conformal radiotherapy. Using a multileaf collimator, the shape of each beam could be adapted to the shape of the PTV. A more conformal approach is intensity-modulated radiotherapy (IMRT), in which each beam is divided into segments. The beam intensity can be varied individually for each segment, resulting in more conformal treatment plans with a more homogeneous dose distribution within the PTV compared to the more conventional delivery techniques [50,51]. IMRT can also be delivered with a rotating gantry, in which rotation speed and beam intensity can be modulated, called volumetric arc therapy. Each improvement in radiotherapy delivery technique led to more conformal treatment plans, with higher dose gradients at the edges of the target volume. As a result, the treatment plans will be less forgiving in terms of geometrical deviations. Small deviations can lead to underdosage of the target volume if insufficient margins are used as the target volume will move out of the high dose region.

In image-guided radiotherapy (IGRT), corrections are applied based on measurements of the geometrical deviations. The imaging devices that are used to measure the geometrical deviations have evolved in the past years. In the nineties, an electronic portal imaging device (EPID) was used to acquire 2D projection images by measuring the exit dose [52]. The bony anatomy of the patient could be visualized and the position of the bony anatomy with respect to the treatment field could be corrected to match that of the treatment plan, if necessary.

New imaging modalities that could be used for setup correction were introduced in the last decade, including in-room CT, kV-CBCT on a linear accelerator and MV-CT on a helical radiotherapy unit. All these modalities have in common that they could perform three-dimensional (3D) imaging of the patient on the treatment table. However, the soft tissue contrast of these modalities is limited, which makes setup correction based on any other tissue than bony anatomy challenging [53]. In a GTV boost setting, setup correction can therefore not be performed on the GTV itself. As an alternative, fiducial markers could be used as a surrogate for the GTV. Fiducials have been used for setup correction of the target volume in prostate cancer and esophageal cancer [54,55]. The most recent advancement in onboard imaging is the MR-guided radiotherapy system [56]. With the superior soft tissue contrast of MRI, setup correction could be performed based on a direct visualization of the GTV. However, MR-guided radiotherapy systems are not widely available yet.

With increased interest for organ preservation and GTV dose escalation, improvements aimed at boost delivery for rectal cancer are timely. Although extensive research has been performed on the inter- and intrafraction displacement of the CTV relative to the bony anatomy, limited research was performed on the inter- and intrafraction displacement of the GTV relative to bony anatomy to determine margins for

a GTV boost [57–59]. As a result, a wide range of clinically used PTV margins of 7-30 mm is described in literature [60–64].

Setup correction could potentially be performed based on the fiducials instead of bony anatomy. To do so, the fiducials need to be representative of the GTV and the fiducials should be visible on MRI to accurately determine the fiducial-GTV spatial relationship. Literature on the use of fiducials in rectal cancer patients focuses on insertion technique, retention rate and complications [65,66]. The stability of fiducials with respect to the GTV has not been investigated. MRI visibility of fiducials has been evaluated in phantoms, but no in-vivo analysis has been reported [67,68].

Image-guided brachytherapy

The HDREBT procedure using the flexible multichannel applicator has been described first by Vuong *et al.* [69]. During endoscopy, the length and size of the tumor is assessed and endoluminal clips are attached to the rectal wall near the tumor to be able to visualize the tumor extent on radiographs for position verification. The target volume and endoluminal clips are delineated on a planning CT scan with applicator in situ and the applicator is reconstructed, which means that the position of the eight catheter channels in the applicator are denoted on the CT scan. Before irradiation, position verification of the applicator is performed. Dummy catheters containing tungsten markers that can be visualized on a radiograph are inserted into three channels of the applicator. Subsequently, anterior-posterior and lateral radiographs are acquired of the patient with applicator in situ. The position of the endoluminal clips and tungsten markers are used to check the insertion depth and rotation of the applicator. If the applicator is positioned correctly, irradiation is initiated.

Due to the steep dose gradient of HDREBT, interfractional anatomical variations of millimetres can have a substantial impact on dose to the target volume or organs at risk. Most publications on the use of HDREBT describe oncological outcomes, but do not report on the technical aspects of the brachytherapy procedure [70–72]. Initial publications describe a procedure using a single planning CT scan for all subsequent fractions [69,73]. More recent publications describe a more adaptive approach, acquiring a planning CT scan at each fraction [74,75]. So far, the possible dosimetric benefit of using an adaptive approach has not been reported.

HDREBT treatment planning is currently performed using a planning CT, on which accurate localization of the tumor is difficult due to limited soft tissue contrast. MRI could be used to accurately determine the tumor location due to its superior soft tissue contrast [76]. Given that the endoluminal clips that are used for position verification create large artifacts on MRI [77], alternative MRI-compatible fiducial markers may be used. However, similar to the potential application of fiducial markers in an EBRT boost, the visibility on MRI and the stability with respect to the GTV has not been investigated.

A further improvement in the HDREBT procedure would be to omit the planning CT scan and perform delineation and treatment planning on MRI only. MRI-only brachytherapy is already the standard for brachytherapy of cervical cancer [78]. Reconstruction of the rigid applicator is performed by rigidly registering a model of the applicator to the applicator on the MRI scan. However, such an approach is not available for the flexible rectum applicator. In addition, the applicator causes a signal void on the currently used anatomical sequences and the individual channels cannot be identified. Therefore, the challenge in MRI-only HDREBT lies in the reconstruction of the flexible applicator on MRI.

Thesis outline

As described, both TME surgery and radiotherapy are associated with increased risk of side-effects. As a result, research is focused on increasing the dose to the tumor to achieve higher response rates for possible organ preservation and on the reduction of irradiated (healthy) tissue. The purpose of this thesis is to reduce uncertainties in image-guided radiotherapy of rectal cancer to increase the accuracy of external beam radiotherapy boosting and high-dose rate endorectal brachytherapy.

Initial publications on HDREBT for rectal cancer describe the use of a single planning CT for all subsequent fractions, while more recent literature describes a procedure using a planning CT at each fraction. However, a dosimetric comparison between the two approaches has not been performed to date. The question is whether the increased patient burden of a planning CT scan at each fraction is justified by any dosimetric improvement in terms of target volume coverage and dose to organs at risk. **Chapter 2** describes the difference between the two approaches in terms of target volume coverage and dose to the organs at risk.

MRI-compatible fiducial markers can be used for HDREBT as an alternative to the endoluminal clips. This would allow the use of MRI for treatment planning for HDREBT. For EBRT, setup correction based on fiducial markers could potentially increase the accuracy of a GTV boost compared to setup correction on bony anatomy. To accomplish this, the fiducial markers need to be visible on MRI to determine the spatial relationship between fiducials markers and the GTV. **Chapter 3** evaluates the MRI visibility of four different gold fiducial markers.

To enable MRI-only planning for HDREBT, the applicator and the individual channels need to be visible on MRI. However, the applicator creates a signal void on currently used anatomical MRI sequences. **Chapter 4** investigates whether an ultrashort echo time sequence can be used to visualize the individual channels within the applicator and reports on the geometric fidelity.

To use fiducials as a surrogate for the GTV, the stability of the fiducials with respect to the GTV needs to be determined. In **Chapter 5**, the stability of implanted gold fiducial markers relative to the GTV is determined. Furthermore, the inter- and intrafraction displacement of the GTV is characterized and required margins for different setup correction scenarios in a EBRT GTV boost setting are suggested.

In the STAR-TReC trial, a novel target volume is used which includes only the mesorectum. Mesorectum only planning is intended for early stage rectal cancer with the aim of reducing the CTV and thereby reducing dose to the healthy tissue while maintaining local control. **Chapter 6** describes the results of a quality assurance program for mesorectum only planning.

REFERENCES

1. Arnold M, Sierra MS, Laversanne M, Soerjomataram I, Jemal A, Bray F. Global patterns and trends in colorectal cancer incidence and mortality. *Gut* 2017;66:683–91.

2. Nederlandse Kankerregistratie (NKR), IKNL 2019.

3. Morris EJA, Whitehouse LE, Farrell T, Nickerson C, Thomas JD, Quirke P, *et al.* A retrospective observational study examining the characteristics and outcomes of tumours diagnosed within and without of the English NHS Bowel Cancer Screening Programme. *Br J Cancer* 2012;107:757–64.

4. Heald RJ, Ryall RD. Recurrence and survival after total mesorectal excision for rectal cancer. *Lancet* 1986;1:1479–82.

5. Havenga K, Enker WE, Norstein J, Moriya Y, Heald RJ, Van Houwelingen HC, *et al.* Improved survival and local control after total mesorectal excision or D3 lymphadenectomy in the treatment of primary rectal cancer: An international analysis of 1411 patients. *Eur J Surg Oncol* 1999;25:368–74.

6. Ridgway PF, Darzi AW. The Role of Total Mesorectal Excision in the Management of Rectal Cancer. *Cancer Control* 2003;10:205–11.

7. Bakker IS, Snijders HS, Wouters MW, Havenga K, Tollenaar RAEM, Wiggers T, *et al.* High complication rate after low anterior resection for mid and high rectal cancer; results of a population-based study. *Eur J Surg Oncol* 2014;40:692–8.

8. Restivo A, Zorcolo L, D'Alia G, Cocco F, Cossu A, Scintu F, *et al.* Risk of complications and long-term functional alterations after local excision of rectal tumors with transanal endoscopic microsurgery (TEM). *Int J Colorectal Dis* 2016;31:257–66.

9. Endreseth BH, Myrvold HE, Romundstad P, Hestvik UE, Bjerkeset T, Wibe A, *et al.* Transanal excision vs. major surgery for T1 rectal cancer. *Dis Colon Rectum* 2005;48:1380–8.

10. De Graaf EJR, Doornebosch PG, Tollenaar RAEM, Meershoek-Klein Kranenbarg E, de Boer AC, Bekkering FC, *et al.* Transanal endoscopic microsurgery versus total mesorectal excision of T1 rectal adenocarcinomas with curative intention. *Eur J Surg Oncol* 2009;35:1280–5.

11. Van Gijn W, Marijnen CAM, Nagtegaal ID, Kranenbarg EMK, Putter H, Wiggers T, *et al.* Preoperative radiotherapy combined with total mesorectal excision for resectable rectal cancer: 12-year follow-up of the multicentre, randomised controlled TME trial. *Lancet Oncol* 2011;12:575–82.

12. Bosset JF, Calais G, Mineur L, Maingon P, Stojanovic-Rundic S, Bensadoun RJ, *et al.* Fluorouracil-based adjuvant chemotherapy after preoperative chemoradiotherapy in rectal cancer: Long-term results of the EORTC 22921 randomised study. *Lancet Oncol* 2014;15:184–90.

13. Sauer R, Liersch T, Merkel S, Fietkau R, Hohenberger W, Hess C, *et al.* Preoperative versus postoperative chemoradiotherapy for locally advanced rectal cancer: Results of the German CAO/ARO/AIO-94 randomized phase III trial after a median follow-up of 11 years. *J Clin Oncol* 2012;30:1926–33.

14. Sebag-Montefiore D, Stephens RJ, Steele R, Monson J, Grieve R, Khanna S, *et al.* Preoperative radiotherapy versus selective postoperative chemoradiotherapy in patients with rectal cancer (MRC CR07 and NCIC-CTG C016): a multicentre, randomised trial. *Lancet* 2009;373:811–20.

15. Nagtegaal ID, Quirke P. What Is the Role for the Circumferential Margin in the Modern Treatment of Rectal Cancer? *J Clin Oncol* 2008;26:303–12.

16. Marijnen CAM, Nagtegaal ID, Klein Kranenbarg E, Hermans J, Van de Velde CJH, Leer JWH, *et al.* No downstaging after short-term preoperative radiotherapy in rectal cancer patients. *J Clin Oncol* 2001;19:1976–84.

17. Gérard JP, Conroy T, Bonnetain F, Bouché O, Chapet O, Closon-Dejardin MT, *et al.* Preoperative radiotherapy with or without concurrent fluorouracil and leucovorin in T3-4 rectal cancers: Results of FFCD 9203. *J Clin Oncol* 2006;24:4620–5.

18. Pettersson D, Cederniark B, Holm T, Radu C, Pahhnan L, Glimelius B, *et al.* Interim analysis of the Stockholm III trial of preoperative radiotherapy regimens for rectal cancer. *Br J Surg* 2010;97:580–7.

19. Pettersson D, Lörinc E, Holm T, Iversen H, Cedermark B, Glimelius B, *et al.* Tumour regression in the randomized Stockholm III Trial of radiotherapy regimens for rectal cancer. *Br J Surg* 2015;102:972–8.

20. Wang SJ, Hathout L, Malhotra U, Maloney-Patel N, Kilic S, Poplin E, *et al.* Decision-Making Strategy for Rectal Cancer Management Using Radiation Therapy for Elderly or Comorbid Patients. *Int J Radiat Oncol Biol Phys* 2018;100:926–44.

21. Anderin K, Gustafsson UO, Thorell A, Nygren J. The effect of diverting stoma on long-term morbidity and risk for permanent stoma after low anterior resection for rectal cancer. *Eur J Surg Oncol* 2016;42:788–93.

22. Kim MJ, Kim YS, Park SC, Sohn DK, Kim DY, Chang HJ, *et al.* Risk factors for permanent stoma after rectal cancer surgery with temporary ileostomy. *Surg (United States)* 2016;159:721–7.

23. Marijnen CAM, Kapiteijn E, van de Velde CJH, Martijn H, Steup WH, Wiggers T, *et al.* Acute Side Effects and Complications After Short-Term Preoperative Radiotherapy Combined With Total Mesorectal Excision in Primary Rectal Cancer: Report of a Multicenter Randomized Trial. *J Clin Oncol* 2002;20:817–25.

24. Hendren SK, O'Connor BI, Liu M, Asano T, Cohen Z, Swallow CJ, *et al.* Prevalence of male and female sexual dysfunction is high following surgery for rectal cancer. *Ann Surg* 2005;242:212–23.

25. Wallner C, Lange MM, Bonsing BA, Maas CP, Wallace CN, Dabhoiwala NF, *et al.* Causes of fecal and urinary incontinence after total mesorectal excision for rectal cancer based on cadaveric surgery: A study from the cooperative clinical investigators of the Dutch total mesorectal excision trial. *J Clin Oncol* 2008;26:4466–72.

26. Engel J, Kerr J, Schlesinger-Raab A, Eckel R, Sauer H, Hölzel D, *et al.* Quality of Life in Rectal Cancer Patients: A Four-Year Prospective Study. *Ann Surg* 2003;238:203–13.

27. Temple LK, Bacik J, Savatta SG, Gottesman L, Paty PB, Weiser MR, *et al.* The development of a validated instrument to evaluate bowel function after sphincter-preserving surgery for rectal cancer. *Dis Colon Rectum* 2005;48:1353–65.

28. Tekkis PP, Poloniecki JD, Thompson MR, Stamatakis JD. Operative mortality in colorectal cancer: Prospective national study. *Br Med J* 2003;327:1196–9.

29. Wiltink LM, Chen TYT, Nout RA, Meershoek-Klein Kranenbarg E, Fiocco M, Laurberg S, *et al.* Health-related quality of life 14years after preoperative short-term radiotherapy and total mesorectal excision for rectal cancer: Report of a multicenter randomised trial. *Eur J Cancer* 2014;50:2390–8.

30. Nijkamp J, Swellengrebel M, Hollmann B, De Jong R, Marijnen C, Van Vliet-Vroegindeweij C, *et al.* Repeat CT assessed CTV variation and PTV margins for short- and long-course pre-operative RT of rectal cancer. *Radiother Oncol* 2012;102:399–405.

31. Gérard JP, Myint AS, Croce O, Lindegaard J, Jensen A, Myerson R, *et al.* Renaissance of contact x-ray therapy for treating rectal cancer. *Expert Rev Med Devices* 2011;8:483–92.

32. Myint AS. Novel radiation techniques for rectal cancer. *J Gastrointest Oncol* 2014;5:212–7.

33. Néron S, Perez S, Benc R, Bellman A, Rosberger Z, Vuong T. The experience of pain and anxiety in rectal cancer patients during high-dose-rate brachytherapy. *Curr Oncol* 2014;21:89–95.

34. Vuong T, Richard C, Niazi T, Liberman S, Letellier F, Morin N, *et al.* High dose rate endorectal brachytherapy for patients with curable rectal cancer. *Semin Colon Rectal Surg* 2010;21:115–9.

35. Garfinkle R, Lachance S, Vuong T, Mikhail A, Pelsser V, Gologan A, *et al.* Is the pathologic response of T3 rectal cancer to high-dose-rate endorectal brachytherapy comparable to external beam radiotherapy? *Dis Colon Rectum* 2019;62:294–301.

36. Hesselager C, Vuong T, Påhlman L, Richard C, Liberman S, Letellier F, *et al.* Short-term outcome after neoadjuvant high-dose-rate endorectal brachytherapy or short-course external beam radiotherapy in resectable rectal cancer. *Color Dis* 2013;15:662–6.

37. van der Valk MJM, Hilling DE, Bastiaannet E, Meershoek-Klein Kranenbarg E, Beets GL, Figueiredo NL, *et al.* Long-term outcomes of clinical complete responders after neoadjuvant treatment for rectal cancer in the International Watch & Wait Database (IWWD): an international multicentre registry study. *Lancet* 2018;391:2537–45.

38. Maas M, Nelemans PJ, Valentini V, Das P, Rödel C, Kuo LJ, *et al.* Long-term outcome in patients with a pathological complete response after chemoradiation for rectal cancer: A pooled analysis of individual patient data. *Lancet Oncol* 2010;11:835–44.

39. Sanghera P, Wong DWY, McConkey CC, Geh JI, Hartley A. Chemoradiotherapy for Rectal Cancer: An Updated Analysis of Factors Affecting Pathological Response. *Clin Oncol* 2008;20:176–83.

40. Maas M, Lambregts DMJ, Nelemans PJ, Heijnen LA, Martens MH, Leijtens JWA, *et al.* Assessment of Clinical Complete Response After Chemoradiation for Rectal Cancer with Digital Rectal Examination, Endoscopy, and MRI: Selection for Organ-Saving Treatment. *Ann Surg Oncol* 2015;22:3873–80.

41. Habr-Gama A, Gama-Rodrigues J, São Julião GP, Proscurshim I, Sabbagh C, Lynn PB, *et al.* Local recurrence after complete clinical response and watch and wait in rectal cancer after neoadjuvant chemoradiation: Impact of salvage therapy on local disease control. *Int J Radiat Oncol Biol Phys* 2014;88:822–8.

42. Appelt AL, Ploen J, Vogelius IR, Bentzen SM, Jakobsen A. Radiation dose-response model for locally advanced rectal cancer after preoperative chemoradiation therapy. *Int J Radiat Oncol Biol Phys* 2013;85:74–80.

43. Burbach JPM, Den Harder AM, Intven M, Van Vulpen M, Verkooijen HM, Reerink O. Impact of radiotherapy boost on pathological complete response in patients with locally advanced rectal cancer: A systematic review and meta-analysis. *Radiother Oncol* 2014;113:1–9.

44. Gerard JP, Chapet O, Nemoz C, Hartweig J, Romestaing P, Coquard R, *et al.* Improved sphincter preservation in low rectal cancer with high-dose preoperative radiotherapy: The Lyon R96-02 randomized trial. *J Clin Oncol* 2004;22:2404–9.

45. Jakobsen A, Ploen J, Vuong T, Appelt A, Lindebjerg J, Rafaelsen SR. Dose-effect relationship in chemoradiotherapy for locally advanced rectal cancer: A randomized trial comparing two radiation doses. *Int J Radiat Oncol Biol Phys* 2012;84:949–54.

46. Rijkmans EC, Cats A, Nout RA, van den Bongard DHJG, Ketelaars M, Buijsen J, *et al.* Endorectal Brachytherapy Boost After External Beam Radiation Therapy in Elderly or Medically Inoperable Patients With Rectal Cancer: Primary Outcomes of the Phase 1 HERBERT Study. *Int J Radiat Oncol Biol Phys* 2017;98:908–17.

47. Rombouts AJM, Al-Najami I, Abbott NL, Appelt A, Baatrup G, Bach S, *et al.* Can we Save the rectum by watchful waiting or TransAnal microsurgery following (chemo) Radiotherapy versus Total mesorectal excision for early REctal Cancer (STAR-TREC study)?: protocol for a multicentre, randomised feasibility study. *BMJ Open* 2017;7:e019474.

48. Roels S, Duthoy W, Haustermans K, Penninckx F, Vandecaveye V, Boterberg T, *et al.* Definition and delineation of the clinical target volume for rectal cancer. *Int J Radiat Oncol Biol Phys* 2006;65:1129–42.

49. Van Herk M, Remeijer P, Rasch C, Lebesque J V. The probability of correct target dosage: Dose-population histograms for deriving treatment margins in radiotherapy. *Int J Radiat Oncol Biol Phys* 2000;47:1121–35.

50. Urbano MTG, Henrys AJ, Adams EJ, Norman AR, Bedford JL, Harrington KJ, *et al.* Intensity-modulated radiotherapy in patients with locally advanced rectal cancer reduces volume of bowel treated to high dose levels. *Int J Radiat Oncol Biol Phys* 2006;65:907–16.

51. Mok H, Crane CH, Palmer MB, Briere TM, Beddar S, Delclos ME, *et al.* Intensity modulated radiation therapy (IMRT): Differences in target volumes and improvement in clinically relevant doses to small bowel in rectal carcinoma. *Radiat Oncol* 2011;6:63.

52. El-Gayed AAH, Bel A, Vijlbrief R, Bartelink H, Lebesque J V. Time trend of patient setup deviations during pelvic irradiation using electronic portal imaging. *Radiother Oncol* 1993;26:162–71.

53. Tan J, Lim Joon D, Fitt G, Wada M, Lim Joon M, Mercuri A, *et al.* The utility of multimodality imaging with CT and MRI in defining rectal tumour volumes for radiotherapy treatment planning: A pilot study. *J Med Imaging Radiat Oncol* 2010;54:562–8.

54. Jin P, van der Horst A, de Jong R, van Hooft JE, Kamphuis M, van Wieringen N, *et al.* Marker-based quantification of interfractional tumor position variation and the use of markers for setup verification in radiation therapy for esophageal cancer. *Radiother Oncol* 2015;117:412–8.

55. Beltran C, Herman MG, Davis BJ. Planning Target Margin Calculations for Prostate Radiotherapy Based on Intrafraction and Interfraction Motion Using Four Localization Methods. *Int J Radiat Oncol Biol Phys* 2008;70:289–95.

56. Oelfke U. Magnetic Resonance Imaging-guided Radiation Therapy: Technological Innovation Provides a New Vision of Radiation Oncology Practice. *Clin Oncol* 2015;27:495–7.

57. Brierley JD, Dawson LA, Sampson E, Bayley A, Scott S, Moseley JL, *et al.* Rectal motion in patients receiving preoperative radiotherapy for carcinoma of the rectum. *Int J Radiat Oncol Biol Phys* 2011;80:97–102.

58. Kleijnen J-PJE, van Asselen B, Burbach JPM, Intven M, Philippens MEP, Reerink O, *et al.* Evolution of motion uncertainty in rectal cancer: implications for adaptive radiotherapy. *Phys Med Biol* 2016;61:1–11.

59. Kleijnen J-PJE, van Asselen B, Van den Begin R, Intven M, Burbach JPM, Reerink O, *et al.* MRI-based tumor inter-fraction motion statistics for rectal cancer boost radiotherapy. *Acta Oncol (Madr)* 2019;58:232–6.

60. Vestermark LW, Jacobsen A, Qvortrup C, Hansen F, Bisgaard C, Baatrup G, *et al.* Long-term results of a phase II trial of high-dose radiotherapy (60 Gy) and UFT/l-leucovorin in patients with non-resectable locally advanced rectal cancer (LARC). *Acta Oncol (Madr)* 2008;47:428–33.

61. Seierstad T, Hole KH, Sælen E, Ree AH, Flatmark K, Malinen E. MR-guided simultaneous integrated boost in preoperative radiotherapy of locally advanced rectal cancer following neoadjuvant chemotherapy. *Radiother Oncol* 2009;93:279–84.

62. Mohiuddin M, Paulus R, Mitchell E, Hanna N, Yuen A, Nichols R, *et al.* Neoadjuvant chemoradiation for distal rectal cancer: 5-year updated results of a randomized phase 2 study of neoadjuvant combined modality chemoradiation for distal rectal cancer. *Int J Radiat Oncol Biol Phys* 2013;86:523–8.

63. Engineer R, Mohandas KM, Shukla PJ, Shrikhande S V., Mahantshetty U, Chopra S, *et al.* Escalated radiation dose alone vs. concurrent chemoradiation for locally advanced and unresectable rectal cancers: Results from phase II randomized study. *Int J Colorectal Dis* 2013;28:959–66.

64. Burbach JM, Verkooijen HM, Intven M, Kleijnen J-PPJEJ, Bosman ME, Raaymakers BW, *et al.* RandomizEd controlled trial for pre-operAtive dose-escaLation BOOST in locally advanced rectal cancer (RECTAL BOOST study): study protocol for a randomized controlled trial. *Trials* 2015;16:58.

65. Vorwerk H, Liersch T, Rothe H, Ghadimi M, Christiansen H, Hess CF, *et al.* Gold markers for tumor localization and target volume delineation in radiotherapy for rectal cancer. *Strahlentherapie Und Onkol* 2009;185:127–33.

66. Moningi S, Walker AJ, Malayeri AA, Rosati LM, Gearhart SL, Efron JE, *et al.* Analysis of fiducials implanted during EUS for patients with localized rectal cancer receiving high-dose rate endorectal brachytherapy. *Gastrointest Endosc* 2015;81:765–9.

67. Chan MF, Cohen GN, Deasy JO. Qualitative Evaluation of Fiducial Markers for Radiotherapy Imaging. *Technol Cancer Res Treat* 2015;14:298–304.

68. Gurney-Champion OJ, Lens E, Van Der Horst A, Houweling AC, Klaassen R, Van Hooft JE, *et al.* Visibility and artifacts of gold fiducial markers used for image guided radiation therapy of pancreatic cancer on MRI. *Med Phys* 2015;42:2638–47.

69. Vuong T, Devic S, Moftah B, Evans M, Podgorsak EB. High-dose-rate endorectal brachytherapy in the treatment of locally advanced rectal carcinoma: Technical aspects. *Brachytherapy* 2005;4:230–5.

70. Smith JA, Wild AT, Singhi A, Raman SP, Qiu H, Kumar R, *et al.* Clinicopathologic comparison of high-dose-rate endorectal brachytherapy versus conventional chemoradiotherapy in the neoadjuvant setting for resectable stages II and III low rectal cancer. *Int J Surg Oncol* 2012;2012:406568.

71. Corner C, Bryant L, Chapman C, Glynne-Jones R, Hoskin PJ. High-dose-rate afterloading intraluminal brachytherapy for advanced inoperable rectal carcinoma. *Brachytherapy* 2010;9:66–70.

72. Chuong MD, Fernandez DC, Shridhar R, Hoffe SE, Saini A, Hunt D, *et al.* High-dose-rate endorectal brachytherapy for locally advanced rectal cancer in previously irradiated patients. *Brachytherapy* 2013;12:457–62.

73. Devic S, Vuong T, Moftah B, Evans M, Podgorsak EB, Poon E, *et al.* Image-guided high dose rate endorectal brachytherapy. *Med Phys* 2007;34:4451–8.

74. Vuong T, Devic S. High-dose-rate pre-operative endorectal brachytherapy for patients with rectal cancer. *J Contemp Brachytherapy* 2015;7:181–6.

75. Nout RA, Bekerat H, Devic S, Vuong T. Is Daily CT-Based Adaptive Endorectal Brachytherapy of Benefit Compared to Using a Single Treatment Plan for Preoperative Treatment of Locally Advanced Rectal Cancer? *Brachytherapy* 2016;15:S83–4.

76. Khoo VS, Joon DL. New developments in MRI for target volume delineation in radiotherapy. *Br J Radiol* 2006;79.

77. Swellengrebel HAM. Evaluating long-term attachment of two different endoclips in the human gastrointestinal tract. *World J Gastrointest Endosc* 2010;2:344.

78. Pötter R, Haie-Meder C, Van Limbergen E, Barillot I, De Brabandere M, Dimopoulos J, *et al.* Recommendations from gynaecological (GYN) GEC ESTRO working group (II): Concepts and terms in 3D image-based treatment planning in cervix cancer brachytherapy - 3D dose volume parameters and aspects of 3D image-based anatomy, radiation physics, radiobiolo. *Radiother Oncol* 2006;78:67–77.

Chapter 2

Benefit of adaptive CT-based treatment planning in high-dose-rate endorectal brachytherapy for rectal cancer

Roy P.J. van den Ende

Eva C. Rijkmans

Ellen M. Kerkhof

Remi A. Nout

Martijn Ketelaars

Mirjam S. Laman

Corrie A.M. Marijnen

Uulke A. van der Heide

ABSTRACT

Purpose

In this planning study, we investigated the dosimetric benefit of repeat CT-based treatment planning at each fraction versus the use of a single CT-based treatment plan for all fractions for high-dose rate endorectal brachytherapy (HDREBT) for rectal cancer.

Methods and materials

We included eleven patients that received a CT scan with applicator in situ for all three fractions. The treatment plan of the first fraction was projected on the repeat CT scans to simulate the use of a single treatment plan. Additionally, replanning was performed on the repeat CT scans and these were compared to the corresponding projected treatment plans.

Results

Repeat CT-based treatment planning resulted on average in a 21% higher (p=0.01) conformity index compared to single CT-based treatment planning. Projecting the initial treatment plan to the repeat CT scans of fraction two and three, 12/22 fractions reached a CTV D98 of 85% of the prescribed dose of 7 Gy, which increased to 14/22 using replanning. For the remaining fractions, median CTV D98 was 4.2 Gy and an intervention would be necessary to correct applicator balloon setup or to remove remaining air and/or feces between the CTV and the applicator.

Conclusions

Using a single CT-based treatment plan for all fractions may result in a suboptimal treatment at later fractions. Therefore, repeat CT imaging should be the minimal standard practice in HDREBT for rectal cancer to determine whether an intervention would be necessary. Replanning based on repeat CT imaging resulted in more conformal treatment plans and is therefore recommended.

INTRODUCTION

Total mesorectal excision is the mainstay in the treatment of rectal cancer. For more advanced cases, the addition of neoadjuvant (chemo)radiotherapy has resulted in lower local recurrence rates, but none of the recent trials has demonstrated a benefit in overall survival [1–4]. Unfortunately, (chemo) radiotherapy is associated with an increased risk of side effects such as bowel and sexual dysfunction [5]. Vuong *et al.* introduced high-dose rate endorectal brachytherapy (HDREBT) as a replacement of neo-adjuvant external beam radiation therapy (EBRT) with promising results in local control [6,7]. For patients unfit or unwilling to undergo surgery, definitive or palliative radiotherapy are alternatives. Rijkmans *et al.* demonstrated the feasibility of a HDREBT boost after EBRT in inoperable patients [8]. Compared to EBRT, HDREBT can deliver high doses to the tumor while sparing surrounding organs due

to a steeper dose gradient [7]. As a consequence, HDREBT has the potential to decrease morbidity and reduce the risk of side effects [9]. However, the steeper dose gradient means that an anatomical inter-fraction variation of millimeters can have a high impact on the delivered dose to the target volume or surrounding organs. Therefore, high precision is required in imaging, contouring and treatment planning.

For HDREBT treatment planning, the conventional approach is to use the treatment plan generated at the first fraction, for all later fractions [10,11]. Alternatively, an adaptive approach could be used by creating a new treatment plan based on new imaging acquired at each fraction, taking into account inter-fraction anatomical variation [12,13]. For cervical cancer, several studies on image-guided brachytherapy compared the use of one treatment plan for all fractions to an adaptive approach using a newly generated treatment plan at each fraction [14,15]. The treatment plan for the first fraction was simulated on the imaging of the later fractions. The results showed that the treatment plan based on imaging of the first fraction did not lead to comparable target volume coverage and dose to organs at risk at later fractions [14,15]. Nowadays, repeat MR imaging is therefore recommended in brachytherapy for cervical cancer [16].

Most studies on the use of HDREBT for rectal cancer focus on oncological outcome and treatment related toxicity in the pre-operative setting, with limited detail on treatment planning. They do not address the question of using a non-adaptive or adaptive approach [9,17–19]. Vuong *et al.* initially reported a non-adaptive approach using one planning CT scan with applicator in situ on which a treatment plan is generated and used for all later fractions [10,11]. Recent publications by the same group describe an adaptive approach generating a new treatment plan based on a new CT scan for each fraction [12,13]. A recent abstract concludes that an adaptive approach resulted in a more conformal dose distribution [20].

In our study, we further investigated the comparison between a non-adaptive and an adaptive approach and added a quantification of conformity. Additionally, we analyzed the repeat CT scans and reported causes of insufficient target volume coverage. The aim of this study was to determine the differences regarding treatment plan conformity, target volume coverage and dose to organs at risk between using a single treatment plan for all fractions versus a new treatment plan at each fraction in HDREBT for rectal cancer.

METHODS AND MATERIALS

Patient selection
For the current study, we selected eleven patients from the HERBERT trial in whom repeat CT scans with applicator in situ were available at each fraction (the HERBERT trial, registered with the Dutch Central Committee on Research Involving Human Subjects; registration no. NL17037.031.07) [8,21].

Treatment

All patients were treated with 13x3 Gy EBRT at four fractions per week, followed by three weekly fractions of HDREBT using a prescription dose of 5-8 Gy starting six weeks after conclusion of EBRT. We adapted the brachytherapy equipment, application and positioning procedures from Devic *et al.* as described in Rijkmans *et al.* [8,11]. Patients received an enema prior to the CT scan with applicator in situ at each fraction.

We acquired a planning CT scan with applicator in situ prior to the first fraction. An inflatable balloon around the applicator on the opposite side of the clinical target volume (CTV) was used to fixate the applicator and to decrease the dose to the normal rectal wall. Treatment planning was performed using Oncentra Brachy (Elekta, Veenendaal, The Netherlands). The aim for treatment planning was to cover the CTV with the 100% isodose while containing the 400% isodose within the applicator. Repeat CT scans with applicator in situ were acquired for research purposes. In case of obvious differences compared to the CT scan of the first fraction, the treatment plan was adapted accordingly. These adapted treatment plans were not used in this study.

Delineation

The CTV was defined as residual macroscopic tumor and scarring after EBRT. CTV, anus, mesorectum and healthy rectal wall were delineated by two observers with help of diagnostic MRI, rectoscopy images and inserted endoluminal clips at the proximal and distal border of the tumor. The rectoscopy images were acquired before EBRT and before the first brachytherapy fraction. Comparing CTV delineations between fractions of the same patient was allowed to check for consistency. In case of discrepancy between delineations, consensus was sought.

Projection and replanning

To determine the differences in conformity, CTV coverage and dose to organs at risk between the use of a single treatment plan for all fractions and a new treatment plan at each fraction, the treatment plan of the first fraction and the new treatment plan were compared for each repeat CT scan. In order to obtain the dose distribution of the initial treatment plan on the repeat CT scans, the treatment plan of the first fraction was projected on the repeat CT scans. For this purpose, the most cranial activated dwell position was identified on the repeat CT scans in the same location with respect to the most cranial slice of the CTV delineation as on the CT scan of the first fraction. Subsequently, the dwell position pattern and dwell times were copied.

An experienced radiation treatment technologist created new treatment plans based on the repeat CT scans. As a result, for each repeat CT scan we thus obtained both a projected treatment plan of the first fraction and a new treatment plan.

Analysis

To quantify dose conformity, the COnformal INdex (COIN) parameter was used, as defined by Baltas *et al.* in the following equation [22]:

$$COIN = \frac{TV_{RI}}{TV} \times \frac{TV_{RI}}{V_{RI}} \times \prod_{i=1}^{N_{CO}} \left[1 - \frac{V_{COref,i}}{V_{CO,i}} \right]$$

With TV_{RI} the tumor volume covered by the reference isodose, TV the tumor volume, V_{RI} the reference isodose volume, N_{CO} the number of critical organs, $V_{COref,i}$ the volume of the critical organ with index i covered by the reference isodose and $V_{CO,i}$ the volume of the critical organ with index i (Figure 1). The healthy rectal wall, mesorectum and anus were considered critical organs. The COIN parameter ranges from 0-1, with 0 representing no conformity and 1 representing full conformity.

The HERBERT trial was a dose escalation study and patients were treated with a prescription dose of 5-8 Gy [8]. Therefore, for reporting of dose parameters, we chose to scale the dose distributions to a prescription dose of 7 Gy. To quantify CTV coverage, the CTV D98 parameter (i.e. the minimal dose to
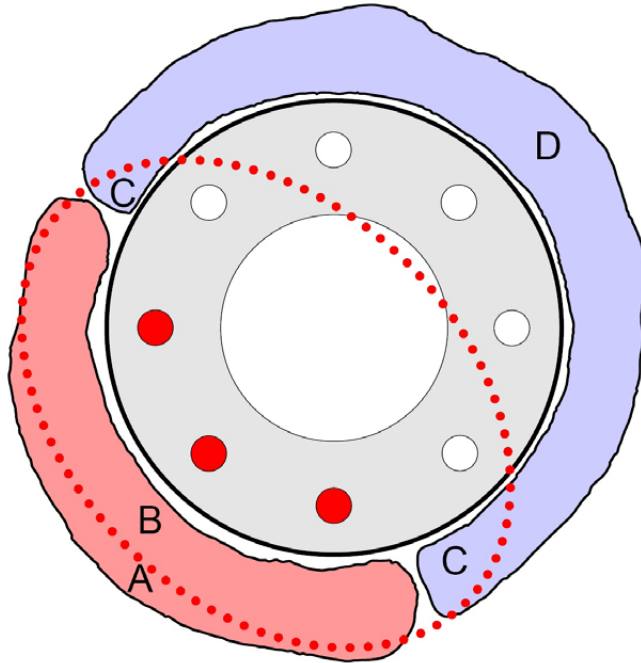
Figure 1. Schematic representation of the parameters of the COIN equation: tumor volume (TV, A + B), tumor volume covered by the 100% isodose (TV$_{RI}$, B), healthy rectal wall (V$_{CO}$, C + D), and healthy rectal wall covered by the 100% isodose (V$_{COref}$, C). V$_{RI}$ is the volume encompassed by the 100% reference isodose, represented by the dotted line. The three filled dots on the lower left side of the applicator represent activated dwell positions.

98% of the CTV volume) was collected for each treatment plan. For the dose to organs at risk, the D2cc (i.e. the minimal dose to the 2 cc of the organ at risk that receives the highest dose) for mesorectum and anus were collected. Additionally, a point dose on the healthy rectal wall directly opposing the delineated CTV within the center slice of the CTV was chosen to quantify dose to the healthy rectal wall.

We visually analyzed all CT scans and if a suboptimal applicator balloon orientation or air and/or feces between the CTV and the applicator were observed, an intervention would be required to correct applicator balloon orientation or to remove air and/or feces.

Statistics

We used SPSS Statistics 23 (IBM Corp. Released 2015. IBM SPSS Statistics for Windows, Version 23.0. Armonk, NY: IBM Corp.) for statistical analysis. The Friedman test was used to test for volume differences of the CTV delineations between the three CT scans. A univariate analysis of variance was performed for each dependent variable (COIN, CTV D98, healthy rectal wall dose and D2cc of the mesorectum and anus). Included independent variables were *plan type* (projection or replanning), *intervention required* (yes or no), *timepoint* (fraction two or three) and *patient* (one through eleven). All tests were two-sided and the significance threshold was set at 0.05.

RESULTS

CTV delineation

The average delineated CTV volume for all CT scans was 6.8 cc (range 2.4–13.0). Delineated CTV volumes did not differ significantly between the three CT scans for each patient (p=0.31).

Initial treatment planning

Table 1 shows the results for COIN and CTV D98 for the treatment plan of the first fraction, all projections and all new treatment plans. Results are presented as median (range). The median COIN for treatment plans of the first fraction was 0.14 (0.04–0.20) and the median CTV D98 was 5.8 Gy (3.6–7.3). On four of the eleven CT scans, air and/or feces was seen between the CTV and the applicator. As a result of this, combined with the constraint of the 400% isodose within the applicator, the CTV coverage and conformity were lower in the corresponding four treatment plans (Figure 2). The median COIN and CTV D98 were 0.09 (0.04–0.13) and 5.6 Gy (3.6–5.8), respectively. An intervention would be necessary to remove air and/or feces before creating a more conformal treatment plan with higher CTV coverage. The median COIN and CTV D98 for the seven remaining treatment plans was 0.15 (0.13–0.20) and 6.3 Gy (4.6–7.3), respectively.

Table 1. Conformity (COIN) and target volume coverage (CTV D98) for the initial treatment plan of the first CT scan and the projection and replanning for the repeat CT scans of all patients. Results are presented as median (range) unless indicated differently.

Parameter	Initial treatment plan	Projections	Replanning	Mean difference projections and replanning (mean (range))	Effect of plan type (p-value)	Mean ratio (projection vs. replanning)
Number of CT scans						
All	11	22	22			
Only interventions	4	8	8			
Excl. interventions	7	14	14			
COIN (-)						
All	0.14 (0.04 – 0.20)	0.13 (0.01 – 0.18)	0.15 (0.02 – 0.19)	0.02 (-0.02 – 0.08)	0.01	1.21
Only interventions	0.09 (0.04 – 0.13)	0.08 (0.01 – 0.15)	0.11 (0.02 – 0.16)	0.02 (-0.02 – 0.08)	0.17	1.31
Excl. interventions	0.15 (0.13 – 0.20)	0.14 (0.07 – 0.18)	0.15 (0.11 – 0.19)	0.02 (-0.01 – 0.04)	< 0.001	1.15
CTV D98 (Gy)						
All	5.8 (3.6 – 7.3)	6.4 (3.3 – 7.8)	6.6 (2.8 – 7.6)	0.3 (-1.0 – 2.4)	0.11	1.07
Only interventions	5.6 (3.6 – 5.8)	4.2 (3.3 – 6.9)	5.0 (2.8 – 5.9)	0.1 (-1.0 – 1.7)	0.89	1.03
Excl. interventions	6.3 (4.6 – 7.3)	6.9 (3.7 – 7.8)	7.0 (6.1 – 7.6)	0.5 (-0.8 – 2.4)	0.06	1.10

Projection

The treatment plan of the first fraction was projected on the repeat CT scans of the second and third fraction for each patient, resulting in 22 projections. The median COIN and CTV D98 of all projections were 0.13 (0.01–0.18) and 6.4 Gy (3.3–7.8), respectively. In some of the 22 repeat CT scans, air and/or feces was seen between the CTV and the applicator (5/22), a suboptimal orientation of the applicator balloon was observed (2/22) or the applicator balloon was not inflated (1/22). For the projections on these eight repeat CT scans (from six patients), the median COIN and CTV D98 were 0.08 (0.01–0.15) and 4.2 Gy (3.3–6.9), respectively. An intervention would be necessary to remove air and/or feces or to correct applicator balloon orientation before creating a more conformal treatment plan with higher CTV coverage. For the remaining 14 projections (from nine patients), the median COIN and CTV D98 were 0.14 (0.07–0.18) and 6.9 Gy (3.7–7.8), respectively. Figure 3 shows an example of a patient in which the projections lead to similar conformity and CTV coverage as the initial treatment plan and a patient in which air and feces is seen on the CT scan of the third fraction leading to lower conformity and CTV coverage.

Replanning

New treatment plans were generated based on the repeat CT scans for each patient, resulting in 22 new treatment plans. The median COIN and CTV D98 were 0.15 (0.02–0.19) and 6.6 Gy (2.8–7.6), respectively.
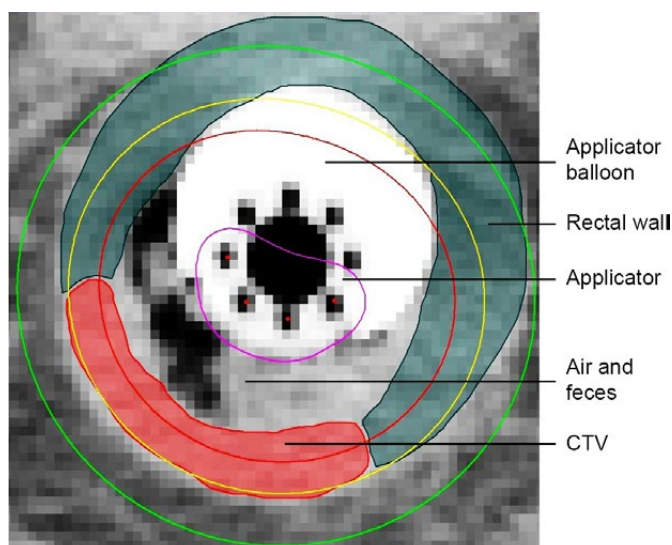
Figure 2. Example of a CT scan in which full coverage of the CTV was not possible considering the constraint of the 400% isodose within the applicator. Air and feces are seen between the CTV and the applicator. The 400%, 100%, 75% and 50% isodoses are shown.

For the new treatment plans based on the eight repeat CT scans that required an intervention, the median COIN and CTV D98 were 0.11 (0.02–0.16) and 5.0 Gy (2.8–5.9), respectively. For the remaining 14 new treatment plans, the median COIN and CTV D98 were 0.15 (0.11–0.19) and 7.0 Gy (6.1–7.6), respectively.

Projection versus replanning

There was a statistically significant effect of *plan type* (p=0.01) and *intervention required* (p=0.002) on the COIN parameter considering all cases. The COIN was on average 21% higher after replanning compared to the projected treatment plans. Considering the cases that did not require an intervention, COIN was on average 15% higher after replanning (Table 1).

There was a statistically significant effect of *intervention required* (p=0.001) on CTV D98, considering all cases. Only borderline significance was reached on the effect of *plan type* in the subgroup of cases that did not require an intervention (p=0.06). In those cases, CTV D98 was on average 10% higher after replanning. One case showed an increase of CTV D98 of 2.4 Gy (66%, from 3.7 Gy to 6.1 Gy) after replanning and another case showed an increase of CTV D98 of 1.7 Gy (42%, from 4.0 Gy to 5.7 Gy). In one case, replanning resulted in a CTV D98 decrease of 1.0 Gy (-15%, from 6.9 to 5.9 Gy).
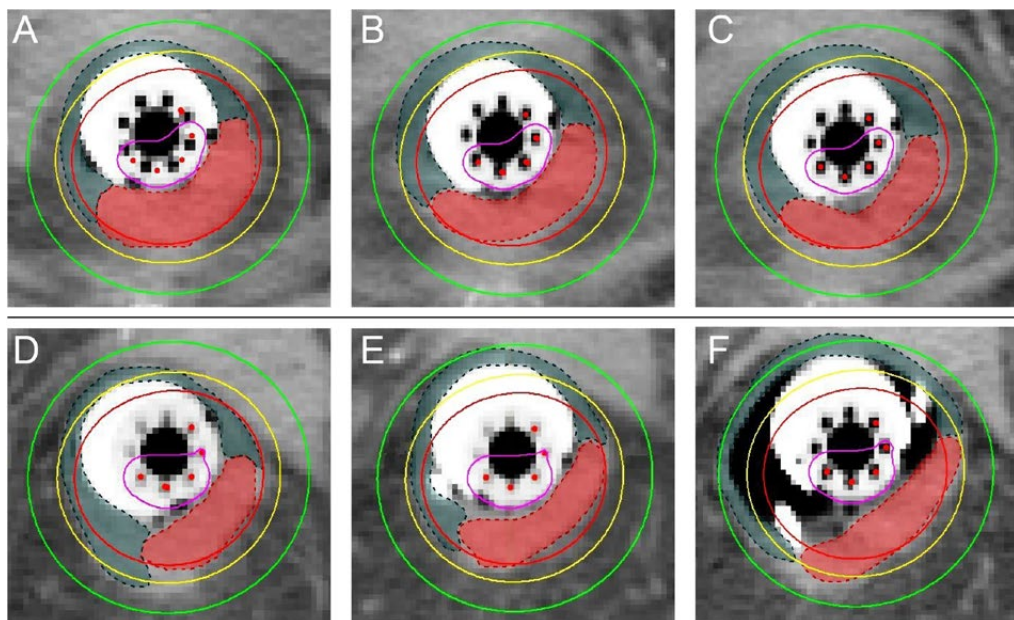
Figure 3. An example of a patient in which the projections (B+C) lead to similar conformity and CTV coverage as the initial treatment plan (A), and a patient in which the projections lead to similar conformity and CTV coverage (E) and lower conformity and CTV coverage (F, due to air and feces) compared to the initial treatment plan (D). The 400%, 100%, 75% and 50% isodoses are shown.

All other differences in CTV D98 were smaller than 1.0 Gy.

When considering a plan acceptable when the CTV D98 is at least 85% of the prescribed dose and at least 90% of the initial treatment plan at the first fraction, 12/22 projections were considered acceptable versus 14/22 new treatment plans. In the eight remaining unacceptable treatment plans, an intervention would have been necessary to achieve an acceptable treatment plan.

Dose to organs at risk

The dose to organs at risk is presented in Table 2. There was a statistically significant effect of *intervention required* on D2cc of the mesorectum considering all cases (p<0.001). No other significant effects were observed. In one case, after replanning, a reduction of the rectal wall point dose larger than 1 Gy (3.1 Gy) was observed. In another case, a decrease of mesorectum D2cc of more than 1 Gy (1.3 Gy) was observed. In another patient with a very distal tumor, an increase of the anus D2cc of 2.3 Gy and 2.1 Gy for fraction two and three was observed. All other differences in anus D2cc were smaller than 1 Gy.

Table 2. Dose to organs at risk (rectal wall point dose and D2cc of mesorectum and anus) for the initial treatment plan of the first CT scan and the projection and replanning for the repeat CT scans of all patients. Results are presented as median (range) unless indicated differently.

Parameter	Initial treatment plan	Projection	Replanning	Mean difference projection and replanning (mean (range))	Effect of plan type (p-value)	Mean ratio (projection vs. replanning)
Number of CT scans						
All	11	22	22			
Only interventions	4	8	8			
Excl. interventions	7	14	14			
Rectal wall point dose (Gy)						
All	5.2 (2.7 – 6.9)	4.8 (2.8 – 10.6)	5.1 (3.0 – 7.5)	-0.2 (-3.1 – 0.9)	0.28	0.98
Only interventions	5.0 (3.6 – 6.4)	5.1 (4.5 – 10.6)	5.2 (4.0 – 7.5)	-0.5 (-3.1 – 0.8)	0.24	0.95
Excl. interventions	5.3 (2.7 – 6.9)	4.5 (2.8 – 6.5)	4.9 (3.0 – 6.2)	-0.1 (-0.8 – 0.9)	0.66	1.00
Mesorectum D2cc (Gy)						
All	6.1 (4.8 – 7.2)	6.1 (4.0 – 8.0)	5.8 (3.9 – 7.7)	-0.2 (-1.3 – 0.7)	0.15	0.98
Only interventions	5.2 (4.8 – 7.2)	5.5 (4.0 – 8.0)	5.2 (3.9 – 7.7)	-0.4 (-1.3 – 0.6)	0.08	0.94
Excl. interventions	6.4 (5.8 – 6.8)	6.2 (4.4 – 7.5)	5.9 (4.4 – 7.2)	-0.1 (-0.8 – 0.7)	0.65	1.00
Anus D2cc (Gy)						
All	1.7 (0.5 – 3.6)	2.7 (0.4 – 4.5)	3.0 (0.4 – 6.1)	0.2 (-0.8 – 2.3)	0.34	1.07
Only interventions	2.1 (0.9 – 2.6)	3.2 (0.9 – 4.3)	3.1 (0.9 – 6.1)	0.2 (-0.8 – 2.3)	0.66	1.05

DISCUSSION

The aim of this study was to determine the differences regarding treatment plan conformity, target volume coverage and dose to organs at risk between using a single treatment plan for all fractions versus a new treatment plan at each fraction in HDREBT for rectal cancer. In this study of eleven patients, replanning for each fraction resulted in a significantly more conformal treatment plan and in some cases a substantially higher CTV D98 (Table 1). This study shows that for 12/22 repeat CT scans, the projected treatment plans met the coverage criteria of CTV D98 being at least 85% of the prescribed dose and at least 90% of the CTV D98 of the first fraction. This improved to 14/22 after replanning. An important value of repeat CT at each fraction lies in verifying applicator balloon setup and absence of air and/or feces in the rectum. This is underlined by the significant effect of intervention required on COIN and CTV D98. Although replanning resulted on average in a 31% increase in COIN in the cases that needed an intervention, COIN and CTV D98 remain low and demonstrate the limited value of replanning in these cases (Table 1). If interventions would have been performed where needed, we expect that treatment plan conformity and target volume coverage would have been similar to those cases that did not need an intervention. After an intervention, a new repeat CT scan should always be acquired to verify its effect.

Adding repeat CT planning before each fraction adds approximately one hour per fraction. This includes acquiring the CT scan, delineation of target volume and organs at risk and treatment planning. We realize that this adaptive approach is labor intensive and may therefore be difficult to implement. Therefore, we report on the benefit of an adaptive approach in terms of treatment plan quality to aid in the decision whether to implement it or not. Even without replanning, acquiring a repeat CT scan is valuable to verify applicator balloon setup and absence of air and/or feces.

As reported, two cases show an increase of CTV D98 of 2.4 Gy and 1.7 Gy after replanning. In the first case, this was due to a different insertion angle of the applicator, which led to a different orientation of the CTV. In the second case, this was due to a suboptimal balloon orientation and a different insertion angle of the applicator, which led to a different orientation of the CTV on the repeat CT scan. Therefore, in these two cases, the projected treatment plan partly missed the CTV. Consequently, after replanning, the new treatment plan was adapted to the CTV on the repeat CT scan and this resulted in a higher CTV D98. One case showed a decrease of CTV D98 of 1.0 Gy and a reduction of the rectal wall point dose of 3.1 Gy because the applicator balloon was not inflated on the repeat CT scan, which resulted in a more conservative treatment planning for the new treatment plan. In another case, after replanning, a decrease of mesorectum D2cc of 1.3 Gy was observed because the CTV orientation was slightly different on the repeat CT scan. This resulted in the projected treatment plan partly missing the CTV and covering a part of the mesorectum instead. After replanning, the new treatment plan was adapted to the CTV on the repeat CT scan, resulting in a lower mesorectum D2cc. An increase of the anus D2cc of 2.3 Gy and 2.1 Gy for fraction two and three was observed in a patient with a distal tumor. For this specific patient, the most caudal slice of the CTV was larger on the repeat CT scans compared to the CTV on the CT scan of the first fraction, resulting in lower CTV coverage of the projected treatment plan. Consequently, after replanning, the new treatment plan was adapted to the larger CTV and this resulted in a higher anus D2cc.

Our conclusions are consistent with a congress abstract of Nout *et al.* on a cohort of 16 patients [20]. Additionally, we report on treatment plan conformity and causes of decreased target volume coverage. Similar studies have been performed for image-guided brachytherapy for cervical cancer, which conclude that an adaptive approach is necessary to correct for possible changes in applicator and anatomy geometry [14,15].

One paper by Devic *et al.* describes the distribution of the corrections in craniocaudal direction for a cohort of 62 patients and shows for one patient what effect it would have on the CTV dose if these corrections were not applied [11]. Our study did not evaluate variations in dose as a result of uncertainties in applicator positioning correction using X-rays.

Baltas *et al.* describe the COIN parameter for evaluation of implant quality and dose specification in brachytherapy [22]. With HDREBT using an endorectal applicator no implants are involved. As the

radiation source is brought next to the tumor instead of into the tumor, the reference isodose volume (V_{RI}) will always be substantially larger than the volume of the CTV that is covered by the reference isodose (TV_{RI}). The $\frac{TV_{RI}}{V_{RI}}$ component of the COIN equation is therefore very low, resulting in low COIN values. This explains the low COIN values reported in this study, compared to the values mentioned in Baltas *et al.* [22]. In our opinion, rather than the absolute value, the ratio of the COIN between projection and replanning is informative and a good measure for treatment plan conformity.

Two factors of the COIN equation are dependent on the absolute delineated volume of the tumor (TV) and organs at risk $(V_{CO,i})$. However, as comparisons are made between the projection and the replanning on the same CT scan, the delineated volumes of the tumor and organs at risk are the same for projection and replanning.

There are some limitations in this study. First, the number of patients was small. Secondly, the delineations of the CTV are difficult to perform on CT, even with the provided diagnostic MRI scan, rectoscopy images, digital rectal examination and inserted endoluminal clips at the proximal and distal border of the tumor. No MRI with applicator in situ was available because the endoluminal clips cause large artifacts on MRI. Consequently, there may be delineation variation among the CT scans of the three fractions. Third, we did not report cumulative dose in this study because only four patients did not require an intervention at all three fractions, on which no reliable conclusions can be drawn. Finally, it would be difficult to show the clinical benefit for patients in terms of local control or reduction in toxicity. However, our results show that without additional imaging, patients would have received a suboptimal treatment with substantial underdosage.

CONCLUSION

The results of this study show that using a single CT-based treatment plan for all fractions in HDREBT for rectal cancer may result in a suboptimal treatment at later fractions. Therefore, repeat CT imaging should be the minimal standard practice in HDREBT for rectal cancer to determine whether an intervention would be necessary. Replanning based on repeat CT imaging resulted in more conformal treatment plans and is therefore recommended.

REFERENCES

1. Van Gijn W, Marijnen CAM, Nagtegaal ID, Kranenbarg EMK, Putter H, Wiggers T, *et al.* Preoperative radiotherapy combined with total mesorectal excision for resectable rectal cancer: 12-year follow-up of the multicentre, randomised controlled TME trial. *Lancet Oncol* 2011;12:575–82.

2. Bosset JF, Calais G, Mineur L, Maingon P, Stojanovic-Rundic S, Bensadoun RJ, *et al.* Fluorouracil-based adjuvant chemotherapy after preoperative chemoradiotherapy in rectal cancer: Long-term results of the EORTC 22921 randomised study. *Lancet Oncol* 2014;15:184–90.

3. Sauer R, Liersch T, Merkel S, Fietkau R, Hohenberger W, Hess C, *et al.* Preoperative versus postoperative chemoradiotherapy for locally advanced rectal cancer: Results of the German CAO/ARO/AIO-94 randomized phase III trial after a median follow-up of 11 years. *J Clin Oncol* 2012;30:1926–33.

4. Sebag-Montefiore D, Stephens RJ, Steele R, Monson J, Grieve R, Khanna S, *et al.* Preoperative radiotherapy versus selective postoperative chemoradiotherapy in patients with rectal cancer (MRC CR07 and NCIC-CTG C016): a multicentre, randomised trial. *Lancet* 2009;373:811–20.

5. Wiltink LM, Chen TYT, Nout RA, Meershoek-Klein Kranenbarg E, Fiocco M, Laurberg S, *et al.* Health-related quality of life 14years after preoperative short-term radiotherapy and total mesorectal excision for rectal cancer: Report of a multicenter randomised trial. *Eur J Cancer* 2014;50:2390–8.

6. Vuong T, Belliveau PJ, Michel RP, Moftah BA, Parent J, Trudel JL, *et al.* Conformal preoperative endorectal brachytherapy treatment for locally advanced rectal cancer: early results of a phase I/II study. *Dis Colon Rectum* 2002;45:1485–6.

7. Vuong T, Richard C, Niazi T, Liberman S, Letellier F, Morin N, *et al.* High dose rate endorectal brachytherapy for patients with curable rectal cancer. *Semin Colon Rectal Surg* 2010;21:115–9.

8. Rijkmans EC, Cats A, Nout RA, van den Bongard DHJG, Ketelaars M, Buijsen J, *et al.* Endorectal Brachytherapy Boost After External Beam Radiation Therapy in Elderly or Medically Inoperable Patients With Rectal Cancer: Primary Outcomes of the Phase 1 HERBERT Study. *Int J Radiat Oncol Biol Phys* 2017;98:908–17.

9. Smith JA, Wild AT, Singhi A, Raman SP, Qiu H, Kumar R, *et al.* Clinicopathologic comparison of high-dose-rate endorectal brachytherapy versus conventional chemoradiotherapy in the neoadjuvant setting for resectable stages II and III low rectal cancer. *Int J Surg Oncol* 2012;2012:406568.

10. Vuong T, Devic S, Moftah B, Evans M, Podgorsak EB. High-dose-rate endorectal brachytherapy in the treatment of locally advanced rectal carcinoma: Technical aspects. *Brachytherapy* 2005;4:230–5.

11. Devic S, Vuong T, Moftah B, Evans M, Podgorsak EB, Poon E, *et al.* Image-guided high dose rate endorectal brachytherapy. *Med Phys* 2007;34:4451–8.

12. Vuong T, Devic S. High-dose-rate pre-operative endorectal brachytherapy for patients with rectal cancer. *J Contemp Brachytherapy* 2015;7:181–6.

13. Nout RA, Devic S, Niazi T, Wyse J, Boutros M, Pelsser V, *et al.* CT-based adaptive high-dose-rate endorectal brachytherapy in the preoperative treatment of locally advanced rectal cancer: Technical and practical aspects. *Brachytherapy* 2016;15:477–84.

14. Kirisits C, Lang S, Dimopoulos J, Oechs K, Georg D, Pötter R. Uncertainties when using only one MRI-based treatment plan for subsequent high-dose-rate tandem and ring applications in brachytherapy of cervix cancer. *Radiother Oncol* 2006;81:269–75.

15. Davidson MTM, Yuen J, D'Souza DP, Batchelar DL. Image-guided cervix high-dose-rate brachytherapy treatment planning: Does custom computed tomography planning for each insertion provide better conformal avoidance of organs at risk? *Brachytherapy* 2008;7:37–42.

16. Haie-Meder C, Pötter R, Van Limbergen E, Briot E, De Brabandere M, Dimopoulos J, *et al.* Recommendations from Gynaecological (GYN) GEC-ESTRO Working Group (I): Concepts and terms in 3D image based 3D treatment planning in cervix cancer brachytherapy with emphasis on MRI assessment of GTV and CTV. *Radiother Oncol* 2005;74:235–45.

17. Hoskin PJ, De Canha SM, Bownes P, Bryant L, Jones RG. High dose rate afterloading intraluminal brachytherapy for advanced inoperable rectal carcinoma. *Radiother Oncol* 2004;73:195–8.

18. Corner C, Bryant L, Chapman C, Glynne-Jones R, Hoskin PJ. High-dose-rate afterloading intraluminal brachytherapy for advanced inoperable rectal carcinoma. *Brachytherapy* 2010;9:66–70.

19. Chuong MD, Fernandez DC, Shridhar R, Hoffe SE, Saini A, Hunt D, *et al.* High-dose-rate endorectal brachytherapy for locally advanced rectal cancer in previously irradiated patients. *Brachytherapy* 2013;12:457–62.

20. Nout RA, Bekerat H, Devic S, Vuong T. Is Daily CT-Based Adaptive Endorectal Brachytherapy of Benefit Compared to Using a Single Treatment Plan for Preoperative Treatment of Locally Advanced Rectal Cancer? *Brachytherapy* 2016;15:S83–4.

21. Dutch Central Committee on Research Involving Human Subjects; registration no. NL17037.031.07

22. Baltas D, Kolotas C, Geramani K, Mould RF, Ioannidis G, Kekchidi M, *et al.* A conformal index (COIN) to evaluate implant quality and dose specification in brachytherapy. *Int J Radiat Oncol Biol Phys* 1998;40:515–24.

Chapter 3

MRI visibility of gold fiducial markers for image-guided radiotherapy of rectal cancer

Roy P.J. van den Ende
Lisanne S. Rigter
Ellen M. Kerkhof
Els L. van Persijn van Meerten
Eva C. Rijkmans
Doenja M.J. Lambregts
Baukelien van Triest
Monique E. van Leerdam
Marius Staring
Corrie A.M. Marijnen
Uulke A. van der Heide

ABSTRACT

Background and purpose

A GTV boost is suggested to result in higher complete response rates in rectal cancer patients, which is attractive for organ preservation. Fiducials may offer GTV position verification on (CB)CT, if the fiducial-GTV spatial relationship can be accurately defined on MRI. The study aim was to evaluate the MRI visibility of fiducials inserted in the rectum.

Methods and materials

We tested four fiducial types (two Visicoil types, Cook and Gold Anchor), inserted in five patients each. Four observers identified fiducial locations on two MRI exams per patient in two scenarios: without (scenario A) and with (scenario B) (CB)CT available. A fiducial was defined to be consistently identified if 3 out of 4 observers labeled that fiducial at the same position on MRI. Fiducial visibility was scored on an axial and sagittal T2-TSE sequence and a T1 3D GRE sequence.

Results

Fiducial identification was poor in scenario A for all fiducial types. The Visicoil 0.75 and Gold Anchor were the most consistently identified fiducials in scenario B with 7 out of 9 and 8 out of 11 consistently identified fiducials in the first MRI exam and 2 out of 7 and 5 out of 10 in the second MRI exam, respectively. The consistently identified Visicoil 0.75 and Gold Anchor fiducials were best visible on the T1 3D GRE sequence.

Conclusions

The Visicoil 0.75 and Gold Anchor fiducials were the most visible fiducials on MRI as they were most consistently identified. The use of a registered (CB)CT and a T1 3D GRE MRI sequence is recommended.

INTRODUCTION

Neoadjuvant radiotherapy plays an important role in the treatment of patients with rectal cancer since it reduces the rate of local recurrence [1–4]. After standard neoadjuvant chemoradiation, pathological complete response is observed in approximately 15-25% of patients [5,6]. In selected centers with a watch and wait approach, clinical complete response is observed in up to 50% of patients, probably due to better patient selection [7,8]. Dose response analyses suggest that higher tumor doses result in higher complete response rates in rectal cancer patients, which is attractive in the light of increased interest for organ preservation [6,9–11].

Tumor dose can be increased by applying a boost with external beam radiotherapy (EBRT), high-dose rate endorectal brachytherapy (HDREBT) or contact therapy. Current clinical practice for position

verification is megavolt imaging or cone beam computed tomography (CBCT) during EBRT and a radiograph or CT during HDREBT [12–15]. However, these imaging modalities suffer from limited soft tissue contrast which makes position verification of the gross tumor volume (GTV) difficult [16,17]. For HDREBT position verification, endoluminal clips have been used to indicate the proximal and distal borders of the tumor [18]. However, these clips create large artifacts on magnetic resonance imaging (MRI), which makes it impossible to determine the spatial relationship with the GTV accurately using MRI [19]. With the introduction of MR-guided radiotherapy systems, position verification of the GTV could be performed online with the superior soft-tissue contrast of MRI [20]. However, as MR-guided linear accelerators and in room MRI-HDR suites are not widely available, MRI compatible gold fiducials in combination with (CB)CT may offer an alternative for position verification of the GTV. The use of fiducials has been described for other tumor locations such as pancreas, esophagus and prostate and has been proven useful for position verification of the target volume during EBRT [21–23].

To determine the location of the GTV accurately on (CB)CT, the spatial relationship between the GTV and the fiducials should be determined on MRI and therefore the fiducials have to be visible on MRI. Several studies report good MRI visibility of fiducials in phantoms or other organs [24–26]. However, the presence of air and feces in the rectum may hamper fiducial visibility. Excellent fiducial visibility in the rectum has been reported on CT, but no analysis of MRI visibility has been performed to date [27,28]. The aim of this study was to evaluate the MRI visibility of different fiducials inserted in the tumor or mesorectum.

METHODS AND MATERIALS

Patient selection

Between July 2015 and September 2016, we included 20 patients at the Netherlands Cancer Institute (NKI) and at the Leiden University Medical Center (LUMC) with proven rectal adenocarcinoma who were scheduled for short-course radiotherapy (SC-RT; 5x5 Gy) or long course chemoradiotherapy (LC-CRT; 25x2 Gy combined with capecitabine 825 mg/m^2 twice daily) followed by a total mesorectal excision. Eleven patients received SC-RT and nine patients LC-CRT. Exclusion criteria were contraindication for fiducial insertion (coagulopathy or anticoagulants that cannot be stopped), prior pelvic irradiation, pelvic surgery or hip replacement surgery, pregnancy, world health organization performance status 3-4 and a contraindication for MRI. This study was registered at the Dutch Trial Registry (REMARK study, registration no. NTR4606) [29].

Fiducials

We tested four types of fiducials, inserted in five patients each (Visicoil 0.5 mm x 5 mm and Visicoil 0.75 mm x 5 mm [IBA Dosimetry, GmbH, Germany], Cook 0.64 mm x 3.4 mm [COOK Medical, Limerick, Ireland] and Gold Anchor 0.28 mm x 20 mm (unfolded length)[Naslund Medical AB, Sweden]. The

Visicoil and Cook fiducials were straight, only differing in diameter and length. The Gold Anchor fiducial was also straight but could be folded when inserted, depending on the insertion technique. We have inserted the Gold Anchor fiducial in a folded configuration as it improves MRI visibility [24].

Four experienced gastroenterologists (two in each center) inserted 64 fiducials in 20 patients in the tumor or mesorectum at least one day before the start of radiotherapy by sigmoidoscopy or endoscopic ultrasonography. The target lesion was visualized and the absence of intervening vascular structures was verified before inserting each fiducial. In the first 10 patients, we aimed to insert three fiducials in the tumor tissue. Due to limited fiducial retention in these patients, in the last 10 patients we aimed to insert at least two fiducials in the mesorectal fat (one proximal and one distal of the tumor) and one in the center of the tumor.

Imaging

We acquired a planning CT scan before the start of radiotherapy on a Siemens Sensation Open (slice thickness 3.0-5.0 mm, pixel spacing 0.98-1.27 mm x 0.98-1.27 mm, 120 kVp, tube current 74-307 mA (automatic exposure control), exposure time 1100 ms, convolution kernel B40s) or a Philips Brilliance Big Bore (slice thickness 3.0 mm, pixel spacing 0.98-1.14 mm x 0.98-1.14 mm, 120 kVp, tube current 271 mA, exposure time 923 ms, convolution kernel B (Philips)). To evaluate reproducibility of fiducial visibility on MRI, we performed a pre-treatment MRI exam before the start of radiotherapy (from now on called first MRI) and a second MRI exam after completion of a week of radiotherapy (from now on called second MRI). MRI exams were performed in supine position on a standard MR table. Due to logistical reasons, for one patient a second MRI was not performed. MRI exams were performed on a Philips Achieva 1.5T, Philips Achieva 3T, Philips Achieva dStream 3T or a Philips Ingenia 3T. Two MRI exams were performed on the 1.5T MRI scanner, all other MRI exams were performed on 3T MRI scanners. We selected three MRI sequences for the fiducial visibility scoring, including a transverse 2D T2 turbo spin echo sequence (tT2-TSE), a sagittal 2D T2-TSE sequence (sT2-TSE) and a T1 3D gradient echo sequence (T1 3D GRE). The T1 3D GRE sequence was acquired with fat suppression in 16/20 scans in the first MRI and 14/19 scans in the second MRI. Scan parameters for the different MRI sequences are reported in Table I in the supplementary materials.

During the first week of radiotherapy, we acquired daily pre- and post-irradiation CBCT scans (reconstructed slice thickness 1.0 mm, pixel spacing 1.0 mm x 1.0 mm, 120 kVp, tube current 32 mA, exposure time 40 ms). Before the planning CT and each radiotherapy fraction, patients were asked to void their bladder and subsequently drink 300 cc of water to reproduce bladder filling.

As all fiducials were well visible on (CB)CT, we registered and subsequently resampled a (CB)CT scan to the T1 3D GRE sequence of each MRI exam with a rigid registration with a mutual information metric using Elastix [30]. The registration was assessed by a single observer (RE) by checking the alignment of the bony anatomy. We used the (CB)CT scan that was acquired closest to the acquisition date of the MRI

exam. The T1 3D GRE sequence was chosen for the registration as it had the highest resolution. As all MRI sequences were acquired within the same MRI exam without table movement between sequences, no registration was performed between the sequences.

Images were visualized with an in-house developed user interface, created in MeVisLab 2.7.1 (MeVis Medical Solutions AG, Fraunhofer MEVIS, Bremen, Germany). The user interface automatically determines a window/level setting depending on the image set that is shown. The automatically determined window was defined as the difference between the minimum and maximum image pixel value and the level was defined as the mean of the minimum and maximum image pixel value. All observers were therefore presented with images with initially the same window/level settings when performing the fiducial visibility scoring. In addition, observers were able to manually change the window/level settings.

Fiducial visibility scoring

Fiducial visibility was scored by two radiologists with expertise in rectal imaging (EP and DL), a radiation-oncologist (BT) and a resident radiation-oncologist (ER). Observers were blinded for fiducial type and each other's results.

Fiducial visibility was scored according to two scenarios. In scenario A, only the MRI images and clinical information (endoscopic findings and number and location of inserted fiducials) were available to the observers. In scenario B, the MRI images, clinical information as well as the rigidly registered CB(CT) scan were at the observer's disposal. For the first MRI, visibility scoring according to scenarios A and B was subsequently performed within one scoring session; for the second MRI, only scenario B was performed.

For each scenario, the observers first scored the fiducials on the first MRI for each patient and at a later stage on the second MRI for each patient. For both MRI exams the observers analyzed patients in random patient order. The observers rated the fiducial visibility on each available MRI sequence (not visible, poor/average or good/excellent) and rated how confident they were that the identified fiducial position really represented a fiducial and not for example an air artifact (not very confident, moderately confident, or very confident). Observers were then instructed to identify and label fiducial positions on the MRI sequence on which they could identify the fiducial location most accurately. Identified fiducial positions were saved in world coordinates.

We used the (CB)CT as a reference to determine the number of fiducials present in a patient at the time of the MRI exam. In combination with the soft tissue information from the MRI scan, we determined whether the fiducial was inserted in the tumor or the mesorectum. (CB)CT was not used as a reference to determine the position of the fiducials on MRI because of the limited soft tissue contrast which made deformable registration with MRI not feasible. Instead, the standard of reference for fiducial location on MRI was defined as the consistent identification of a fiducial on the same position on MRI by at least three out of four observers. This was determined by calculating the distances between the identifications of

all observers using the world coordinates of the identifications. Identification pairs with a distance of less than 5 mm between observers were subsequently analyzed visually to check whether the same artifact was labeled.

Statistical analysis

We used SPSS Statistics 23 (IBM Corp. Released 2015. IBM SPSS Statistics for Windows, Version 23.0. Armonk, NY: IBM Corp.) for statistical analysis. The Wilcoxon signed rank test was used to test for differences in visibility rating between MRI sequences. All tests were two-sided and the significance threshold was set at 0.05.

RESULTS

A total of 64 fiducials was inserted in 20 patients. A planning CT with fiducials was available in 10/20 patients. In the other 10 patients, fiducials were inserted after the planning CT. Median time between fiducial insertion and the first MRI exam was 3 days (range 0-11 days), between any MRI exam and the corresponding reference scan 0 days (range 0-5 days) and between the first and second MRI exam 7 days (range 4-21). At the time of the first MRI, 39 fiducials were still in situ in the tumor or mesorectum, based on evaluation on (CB)CT. At the time of the second MRI, 35 fiducials were still in situ. The remaining 29 fiducials were either lost between insertion and the first MRI (n=18), lost between the two MRI exams (n=4), inadvertently inserted in the prostate (n=5), or simultaneously ejected during insertion and therefore so close together that they were analyzed as one fiducial (n=2). For the nine patients that received LC-CRT, the CBCT scans that were acquired after the first week of radiotherapy showed that no further fiducials were lost during the course of treatment. Nine fiducials were inserted in the mesorectum (one Visicoil 0.5, two Visicoil 0.75, three Cook and three Gold Anchor fiducials) and thirty fiducials were inserted in the tumor (eight Visicoil 0.5, seven Visicoil 0.75, six COOKs and nine Gold Anchors). In five out of nine mesorectum fiducials in four patients a T1 3D GRE sequence was performed with fat suppression and therefore these fiducials were excluded from further analyses (one Visicoil 0.5, three COOKs and one Gold Anchor). None of these fiducials were consistently identified. An overview of patient characteristics, type of reference scan and number of fiducials on reference scan is provided for each patient in Table 1. All registrations of (CB)CT scans to corresponding MRI exams were assessed by a single observer (RE) and considered to be sufficiently aligned for the purpose of this study: giving an approximate location of the fiducial on MRI.

Table 1. Patient characteristics, type of reference scan and number of fiducials on reference scan.

Patient	Sex	Age	cTNM	Tx	Fiducial type	Number of inserted fiducials	First MRI		Second MRI	
							Reference scan	Number of fiducials on reference scan*	Reference scan	Number of fiducials on reference scan*
1	M	71	T3N0M0	SC-RT	Visicoil 0.5	3	CT	2	CBCT	1
2	M	82	T3N0M0	SC-RT	Visicoil 0.5	3	CBCT	2	CBCT	2
3	M	63	T2N0M0	LC-CRT	Visicoil 0.5	3	CBCT	0	CBCT	0
4	M	60	T3N1M0	LC-CRT	Visicoil 0.5	3	CBCT	3	CBCT	3
5	F	60	T3N1M0	SC-RT	Visicoil 0.5	3	CBCT	1	CBCT	1
6	M	67	T3N2M0	LC-CRT	Visicoil 0.75	3	CT	3	CBCT	1
7	F	52	T3N1M0	SC-RT	Visicoil 0.75	3	CT	2	CBCT	2
8	M	75	T3N0M0	SC-RT	Visicoil 0.75	3	CBCT	2	CBCT	2
9	M	82	T2N1M0	SC-RT	Visicoil 0.75	3	CBCT	1	CBCT	1
10	M	63	T3N1M0	SC-RT	Visicoil 0.75	3	CBCT	1	CBCT	1
11	F	62	T2N1M0	SC-RT	COOK	3	CT	2	CBCT	2
12	M	58	T3N0M0	LC-CRT	COOK	4	CBCT	0	-	-
13	M	57	T3N2M0	LC-CRT	COOK	4	CBCT	1	CBCT	1
14	F	60	T3N1M0	SC-RT	COOK	4	CBCT	1	CBCT	1
15	M	59	T3N2M0	LC-CRT	COOK	4	CBCT	2	CBCT	2
16	M	63	T3N0M0	LC-CRT	Gold Anchor	3	CBCT	2	CBCT	2
17	M	65	T3N2M0	LC-CRT	Gold Anchor	3	CBCT	2	CBCT	1
18	M	59	T2N1M0	SC-RT	Gold Anchor	3	CBCT	2	CBCT	2
19	F	61	T3N1M0	SC-RT	Gold Anchor	3	CBCT	3	CBCT	3
20	M	51	T3N0M0	LC-CRT	Gold Anchor	3	CBCT	2	CBCT	2

M = male, F = female, Tx = treatment schedule, SC-RT = short course radiotherapy, LC-CRT = long course chemoradiotherapy.
*The number of fiducials on the reference scan excludes fiducials that were inadvertently inserted in the prostate and fiducials in the mesorectum in which the T1 3D GRE was performed with fat suppression.

Table 2 shows an overview of the consistent and inconsistent fiducial identifications with corresponding confidence levels. In scenario A of the first MRI, 2/9 Visicoil 0.75, 1/6 Cook and 5/11 Gold Anchor fiducials were consistently identified with an average distance between identifications of 1.8 mm (range 0.0 – 3.8 mm). Of those, two Visicoil 0.75, one Cook and four Gold Anchor fiducials were subsequently also consistently identified in scenario B. In scenario B of the first MRI, a total of 17 fiducials were consistently identified with an average distance between identifications of 2.0 mm (range 0.0 – 5.1 mm).

Table 2. Number of consistent and inconsistent identifications for all observers for scenario B with corresponding confidence levels, split according to fiducial type.

	Visicoil 0.5	Visicoil 0.75	COOK	Gold Anchor
FIRST MRI EXAM, scenario B				
Fiducials on corresponding (CB)CT	8	9	6	11
Total identifications by 4 observers*	22 (32)	34 (36)	26 (24)	43 (44)
Inconsistent identifications	19	13	22	14
Consistent identifications	3	21	4	29
Which represent number of consistently identified fiducials	1 / 8 (13%)	7 / 9 (78%)	1 / 6 (17%)	8 / 11 (73%)
Of which were already consistently identified in **scenario A**	0 / 8 (0%)	2 / 9 (22%)	1 / 6 (17%)	5 / 11 (45%)
Confidence level for all identifications				
not very confident	9 (41%)	2 (6%)	12 (46%)	6 (14%)
moderately confident	7 (32%)	10 (29%)	7 (27%)	7 (16%)
very confident	6 (27%)	22 (65%)	7 (27%)	30 (70%)
SECOND MRI EXAM, scenario B				
Fiducials on corresponding (CB)CT	7	7	6	10
Total identifications by 4 observers*	22 (28)	25 (28)	20 (24)	40 (40)
Inconsistent identifications	18	19	17	23
Consistent identifications	4	6	3	17
Which represent number of consistently identified fiducials	1 / 7 (14%)	2 / 7 (29%)	1 / 6 (17%)	5 / 10 (50%)
Confidence level for all identifications				
not very confident	4 (18%)	3 (13%)	9 (45%)	7 (18%)
moderately confident	3 (14%)	9 (39%)	7 (35%)	21 (52%)
very confident	15 (68%)	11 (48%)	4 (20%)	12 (30%)

*Numbers between brackets indicate the maximum number of correct identifications by four observers.
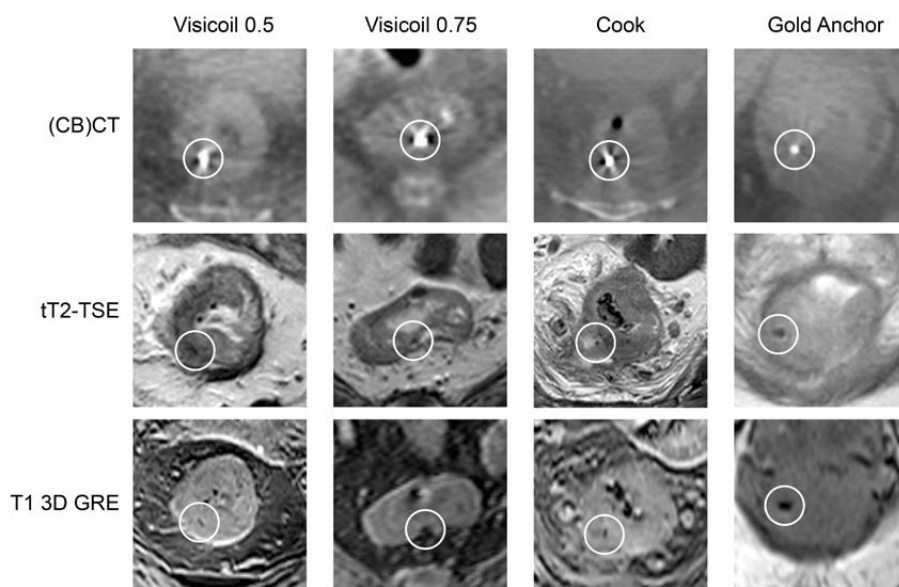
Figure 1. Examples of fiducials shown on (CB)CT and corresponding MRI sequences.

Because of the low number of consistently identified fiducials in scenario A compared to scenario B, scenario A was not performed for the second MRI. For the second MRI, nine fiducials were consistently identified with an average distance between identifications of 0.9 mm (range 0.0 – 1.9 mm). In scenario B, the Visicoil 0.75 and the Gold Anchor fiducials were the most consistently identified fiducial types with 7/9 fiducials in 4 patients and 8/11 fiducials in 5 patients in the first MRI and 2/7 fiducials in 2 patients and 5/10 fiducials in 4 patients in the second MRI, respectively. Examples of fiducials on (CB)CT and corresponding MRI sequences are shown in Figure 1. The fiducials shown in Figure 1 were consistently identified. Table 3 shows the difference between observers for the Visicoil 0.75 and Gold Anchor fiducial identifications. Observer 4 had a substantially lower number of consistently identified fiducials and labeled more fiducials on MRI than the number of fiducials present on the reference scan. For observer 3 and 4 in the second MRI of the Visicoil 0.75, one confidence level was missing.

Table 3. Number of consistently identified Visicoil 0.75 and Gold Anchor fiducials with corresponding confidence levels for each observer.

	Observer 1	Observer 2	Observer 3	Observer 4
Visicoil 0.75				
FIRST MRI EXAM, scenario B				
Number of identifications	7 / 9	7 / 9	9 / 9	11 / 9
Of which are consistently labeled identifications	6	7	7	1
Confidence level for all identifications				
not very confident	1 (14%)	0 (0%)	0 (0%)	1 (9%)
moderately confident	2 (29%)	2 (29%)	3 (33%)	3 (27%)
very confident	4 (57%)	5 (72%)	6 (67%)	7 (64%)
SECOND MRI EXAM, scenario B				
Number of identifications	5 / 7	4 / 7	7 / 7	9 / 7
Of which are consistently labeled identifications	2	2	2	0
Confidence level for all identifications				
not very confident	1 (20%)	1 (25%)	0 (0%)	1 (13%)
moderately confident	1 (20%)	3 (75%)	4 (67%)	1 (13%)
very confident	3 (60%)	0 (0%)	2 (33%)	6 (75%)
Gold Anchor				
FIRST MRI EXAM, scenario B				
Number of identifications	10 / 11	9 / 11	12 / 11	12 / 11
Of which are consistently labeled identifications	7	8	8	6
Confidence level for all identifications				
not very confident	2 (20%)	1 (11%)	1 (8%)	2 (17%)
moderately confident	2 (20%)	1 (11%)	2 (17%)	2 (17%)
very confident	6 (60%)	7 (78%)	9 (75%)	8 (67%)
SECOND MRI EXAM, scenario B				
Number of identifications	8 / 10	8 / 10	11 / 10	13 / 10
Of which are consistently labeled identifications	5	5	5	2
Confidence level for all identifications				
not very confident	3 (38%)	0 (0%)	0 (0%)	4 (31%)
moderately confident	3 (38%)	5 (63%)	5 (46%)	8 (62%)
very confident	2 (25%)	3 (38%)	6 (55%)	1 (8%)

The visibility rating for the consistently identified Visicoil 0.75 and Gold Anchor fiducials per MRI sequence for both MRI exams is shown in Table 4. For the Visicoil 0.75, in the first MRI the tT2-TSE scored better visibility compared to the sT2-TSE sequence (p=0.03). The T1 3D GRE sequence scored better visibility compared to the tT2-TSE (p=0.03) and the sT2-TSE (p=0.01). In the second MRI, T1 3D GRE scored better visibility compared to the sT2-TSE (p=0.04). For the Gold Anchor, in the first MRI the T1 3D GRE scored better visibility compared to the sT2-TSE (p=0.02). No other statistically significant differences were observed. In addition, Table 4 shows on which MRI sequence the fiducial positions were labeled, which is the sequence on which the fiducial could most accurately be identified according to the observers. For both the Visicoil 0.75 and the Gold Anchor fiducials, the T1 3D GRE sequence was chosen most often in both MRI exams.

DISCUSSION

The aim of this study was to evaluate the MRI visibility of different fiducials inserted in the tumor or mesorectum. The results show that there are substantial differences in the number of consistently identified fiducials between fiducial types. For both the Visicoil 0.5 and the COOK fiducials, only one fiducial was consistently identified in both MRI exams (Table 2). These fiducial types were the smallest included in this study, which may explain the poor MRI visibility. This result confirms that of a study by Chan *et al.* who described the visibility of different types of fiducials in a phantom on CBCT, CT, megavolt imaging and MRI [26]. The authors concluded that fiducials with a diameter of 0.5 mm are poorly visible on MRI, even in a phantom. The Visicoil 0.75 has a larger diameter compared to the Visicoil 0.5 and the Cook fiducial, which may explain the better performance of this fiducial. The performance of the Gold Anchor fiducial is in line with a study by Gurney-Champion *et al.*, who evaluated and characterized the visibility of different fiducials in a phantom on CT and MRI and included an in-vivo analysis of four patients in whom fiducials were inserted in the pancreas [24]. The authors recommend a Gold Anchor fiducial in a folded configuration when MRI visibility is desired.

The fiducial insertion strategy was changed during the study because insertion of fiducials in the tumor resulted in a low fiducial retention rate. Since only nine out of 39 fiducials were inserted in the mesorectum and five of those were scanned with fat suppression on the T1 3D GRE sequence, no firm conclusions can be drawn on the difference in fiducial detection between fiducials in the tumor and the mesorectum.

Table 4. Visibility rating per MRI sequence for the consistently identified Visicoil 0.75 and Gold Anchor fiducials in scenario B of both MRI exams. In addition, the MRI sequence on which the fiducial positions were labeled is shown.

	tT2-TSE	sT2-TSE	T1 3D GRE
Visicoil 0.75			
FIRST MRI EXAM, scenario B			
not visible	1 (5%)	6 (29%)	0 (%)
poor/average	12 (57%)	7 (33%)	9 (43%)
good/excellent	8 (38%)	8 (38%)	12 (57%)
Labeled sequence	2 / 21 (10%)	2 / 21 (10%)	17 / 21 (81%)
SECOND MRI EXAM, scenario B			
not visible	0 (0%)	4 (67%)	0 (0%)
poor/average	4 (67%)	1 (17%)	2 (33%)
good/excellent	2 (33%)	1 (17%)	4 (67%)
Labeled sequence	0 / 6 (0%)	1 / 6 (17%)	5 / 6 (83%)
Gold Anchor			
FIRST MRI EXAM, scenario B			
not visible	3 (10%)	4 (14%)	2 (7%)
poor/average	9 (31%)	10 (35%)	5 (17%)
good/excellent	17 (59%)	15 (52%)	22 (76%)
Labeled sequence	8 / 29 (28%)	4 / 29 (14%)	17 / 29 (59%)
SECOND MRI EXAM, scenario B			
not visible	1 (6%)	3 (18%)	1 (6%)
poor/average	5 (29%)	7 (41%)	6 (35%)
good/excellent	11 (65%)	7 (41%)	10 (59%)
Labeled sequence	0 / 17 (0%)	7 / 17 (41%)	10 / 17 (59%)

Eight out of eleven Gold Anchor fiducials were consistently identified in the first MRI, while only five out of ten Gold Anchors fiducials were consistently identified in the second MRI (Table 2). One identified Gold Anchor fiducial was lost in between the MRI exams, as evaluated on CBCT. For the two Gold Anchor fiducials in two patients that were no longer identified in the second MRI, the first and the second MRI were compared. Air or feces deformed the rectum which made correlation with the CBCT scan difficult. In addition, the artifacts caused by air further hampered fiducial detection. For the Visicoil 0.75, only two out of seven fiducials were consistently identified in the second MRI, compared to seven out of nine in the first MRI. Two consistently identified fiducials were lost in between the MRI exams. The remaining three fiducials were no longer consistently identified in the second MRI as they were identified by only two out of four observers.

Even with the two best visible fiducials in this study, it can be argued whether the obtained performance justifies the use of fiducials in the rectum in clinical practice. For instance, reproducibility of the observer identifications between the MRI exams was limited, as shown by the lower number of consistently identified fiducials in the second MRI for Visicoil 0.75 and Gold Anchor. In addition, inconsistencies between observers were observed, especially for the Visicoil 0.75 (Table 3). This suggests that it is worthwhile to have at least two observers to identify the fiducial positions on MRI. Furthermore, more fiducials may be inserted to increase the chance that sufficient fiducials will be identified for position verification (e.g. two or three).

The anatomical 2D T2-TSE sequences scored lower visibility with the Visicoil 0.75 fiducials compared to the Gold Anchor fiducials. This may be explained by the smaller size of the Visicoil 0.75 fiducials, which results in smaller signal voids on MRI. The signal voids may have been too small on the T2-TSE sequences. It is therefore not sufficient to use these MRI sequences alone to identify fiducial positions on MRI. The T1 3D GRE sequence scored higher fiducial visibility for both MRI exams for the Visicoil 0.75 and the first MRI exam for the Gold Anchor and was most often chosen to label the fiducial position on in all cases (Table 4). It is therefore recommended to include a T1 3D GRE sequence.

The T1 3D GRE sequence was a single-echo sequence acquired with a TE of about 2 ms. Two studies that evaluated fiducial visibility in the prostate reported promising results on the use of a multi-echo gradient echo sequence [25,31]. The multi-echo gradient echo sequence results in multiple image sets with increasing TE which results in increased signal void size. It could be worthwhile to include this sequence in future studies, possibly enhancing fiducial identification.

Moningi *et al.* evaluated the role of fiducials in patients receiving neo-adjuvant endorectal brachytherapy in 11 rectal cancer patients [28]. The visibility of two types of fiducials was evaluated on CT by a radiologist, in which a subjective scoring system similar to this study was used. The radiologist scored all fiducials as clearly visible. The authors mention that both types of fiducials created a void on MRI that could assist with treatment planning, but no similar visibility analysis was performed to support this statement.

This study focused on gold fiducials, while other types of fiducials might be of interest. Liquid markers such as a hydrogel marker were not included because of poor stability, most likely because of absorption in the tissue [32]. Recent studies report on a liquid marker that forms a semisolid gel after injection [33,34]. Rydhog *et al.* reports on 15 lung cancer patients in whom markers were injected in the lymph nodes or the tumor. The authors found that the markers were well visible on CT and CBCT and stable in size and position throughout the treatment [33]. Schneider *et al.* evaluated gold fiducials and the liquid marker in a gel phantom that mimics the relaxation properties of pancreatic tissue. The authors show that the liquid markers cause signal voids on MRI due to the absence of water protons, equally affecting all MRI sequences [34]. This is contrary to gold fiducials, which also cause signal voids due to their effect

on T2* of the surrounding tissue [24]. Therefore, the potential visibility of gold fiducials and the artifact size are correlated. As a result, better gold fiducial visibility because of increased TE also results in larger artifacts caused by air.

There are some limitations to this study. Only 39 fiducials were available for the visibility analysis because some fiducials were lost between insertion and the first MRI and five fiducials were inadvertently inserted in the prostate. Because of the low number of available fiducials per fiducial type, no statistical tests were performed to test for differences in consistent identifications between fiducial types.

The observers were blinded for fiducial type. As the artifact size differs substantially between fiducial types, results might have been better if observers had known what artifact size to look for [24]. Since we defined a fiducial consistently identified if at least three out of four observers identified that fiducial position on the same position on MRI, inconsistently identified fiducials may still be true fiducials, but only identified by one or two observers.

There is no gold standard for the location of the fiducials on MRI. The rigid registration with (CB)CT provides an estimation of the location and may be inaccurate when day-to-day differences in rectal position and shape occur. Non-rigid registration was attempted for both the planning CT and CBCT scans, but was not considered feasible because of limited soft-tissue contrast, particularly on CBCT (35 out of 39 reference scans). Additionally, differences in rectal filling and differences in the presence and volume of air in the rectum further hampered non-rigid registration. Clinical practice does not include instructions on a diet or voiding of the rectum before the radiotherapy fraction. In addition, voiding of the bladder and drinking instructions were not applied before the MRI exam. If the drinking protocol would be applied to MRI and instructions on a diet or voiding of the rectum would be used, the correspondence between patient anatomy on CBCT and MRI may improve.

In conclusion, the Visicoil 0.75 and Gold Anchor fiducials were the best visible fiducials on MRI as it were the most consistently identified fiducials. Anatomical 2D T2-TSE MRI sequences are not sufficient to identify fiducials. Therefore, a T1 3D GRE sequence is recommended. The use of a corresponding (CB) CT scan improves fiducial detection on MRI. However, even for the best two fiducial types in this study, fiducial identification on MRI is challenging as shown by limited reproducibility between MRI exams and inconsistencies between observers. It is therefore recommended to have at least two observers and to further optimize MRI sequences to enhance the visibility of the fiducials.

REFERENCES

1. Van Gijn W, Marijnen CAM, Nagtegaal ID, Kranenbarg EMK, Putter H, Wiggers T, *et al.* Preoperative radiotherapy combined with total mesorectal excision for resectable rectal cancer: 12-year follow-up of the multicentre, randomised controlled TME trial. *Lancet Oncol* 2011;12:575–82.

2. Bosset JF, Calais G, Mineur L, Maingon P, Stojanovic-Rundic S, Bensadoun RJ, *et al.* Fluorouracil-based adjuvant chemotherapy after preoperative chemoradiotherapy in rectal cancer: Long-term results of the EORTC 22921 randomised study. *Lancet Oncol* 2014;15:184–90.

3. Sauer R, Liersch T, Merkel S, Fietkau R, Hohenberger W, Hess C, *et al.* Preoperative versus postoperative chemoradiotherapy for locally advanced rectal cancer: Results of the German CAO/ARO/AIO-94 randomized phase III trial after a median follow-up of 11 years. *J Clin Oncol* 2012;30:1926–33.

4. Sebag-Montefiore D, Stephens RJ, Steele R, Monson J, Grieve R, Khanna S, *et al.* Preoperative radiotherapy versus selective postoperative chemoradiotherapy in patients with rectal cancer (MRC CR07 and NCIC-CTG C016): a multicentre, randomised trial. *Lancet* 2009;373:811–20.

5. Maas M, Nelemans PJ, Valentini V, Das P, Rödel C, Kuo LJ, *et al.* Long-term outcome in patients with a pathological complete response after chemoradiation for rectal cancer: A pooled analysis of individual patient data. *Lancet Oncol* 2010;11:835–44.

6. Sanghera P, Wong DWY, McConkey CC, Geh JI, Hartley A. Chemoradiotherapy for Rectal Cancer: An Updated Analysis of Factors Affecting Pathological Response. *Clin Oncol* 2008;20:176–83.

7. Maas M, Lambregts DMJ, Nelemans PJ, Heijnen LA, Martens MH, Leijtens JWA, *et al.* Assessment of Clinical Complete Response After Chemoradiation for Rectal Cancer with Digital Rectal Examination, Endoscopy, and MRI: Selection for Organ-Saving Treatment. *Ann Surg Oncol* 2015;22:3873–80.

8. Habr-Gama A, Gama-Rodrigues J, São Julião GP, Proscurshim I, Sabbagh C, Lynn PB, *et al.* Local recurrence after complete clinical response and watch and wait in rectal cancer after neoadjuvant chemoradiation: Impact of salvage therapy on local disease control. *Int J Radiat Oncol Biol Phys* 2014;88:822–8.

9. Appelt AL, Ploen J, Vogelius IR, Bentzen SM, Jakobsen A. Radiation dose-response model for locally advanced rectal cancer after preoperative chemoradiation therapy. *Int J Radiat Oncol Biol Phys* 2013;85:74–80.

10. Hall MD, Schultheiss TE, Smith DD, Fakih MG, Wong JYC, Chen YJ. Effect of increasing radiation dose on pathologic complete response in rectal cancer patients treated with neoadjuvant chemoradiation therapy. *Acta Oncol (Madr)* 2016;55:1392–9.

11. Ortholan C, Romestaing P, Chapet O, Gerard JP. Correlation in rectal cancer between clinical tumor response after neoadjuvant radiotherapy and sphincter or organ preservation: 10-year results of the Lyon R 96-02 randomized trial. *Int J Radiat Oncol Biol Phys* 2012;83.

12. Vuong T, Devic S. High-dose-rate pre-operative endorectal brachytherapy for patients with rectal cancer. *J Contemp Brachytherapy* 2015;7:181–6.

13. Nout RA, Devic S, Niazi T, Wyse J, Boutros M, Pelsser V, *et al.* CT-based adaptive high-dose-rate endorectal brachytherapy in the preoperative treatment of locally advanced rectal cancer: Technical and practical aspects. *Brachytherapy* 2016;15:477–84.

14. Nijkamp J, de Jong R, Sonke JJ, Remeijer P, van Vliet C, Marijnen C. Target volume shape variation during hypo-fractionated preoperative irradiation of rectal cancer patients. *Radiother Oncol* 2009;92:202–9.

15. Tournel K, De Ridder M, Engels B, Bijdekerke P, Fierens Y, Duchateau M, *et al.* Assessment of Intrafractional Movement and Internal Motion in Radiotherapy of Rectal Cancer Using Megavoltage Computed Tomography. *Int J Radiat Oncol Biol Phys* 2008;71:934–9.

16. O'Neill BDP, Salerno G, Thomas K, Tait DM, Brown G. MR vs CT imaging: Low rectal cancer tumour delineation for three-dimensional conformal radiotherapy. *Br J Radiol* 2009;82:509–13.

17. Khoo VS, Joon DL. New developments in MRI for target volume delineation in radiotherapy. *Br J Radiol* 2006;79.

18. Vuong T, Devic S, Moftah B, Evans M, Podgorsak EB. High-dose-rate endorectal brachytherapy in the treatment of locally advanced rectal carcinoma: Technical aspects. *Brachytherapy* 2005;4:230–5.

19. Swellengrebel HAM. Evaluating long-term attachment of two different endoclips in the human gastrointestinal tract. *World J Gastrointest Endosc* 2010;2:344.

20. Oelfke U. Magnetic Resonance Imaging-guided Radiation Therapy: Technological Innovation Provides a New Vision of Radiation Oncology Practice. *Clin Oncol* 2015;27:495–7.

21. Van Der Horst A, Wognum S, Dávila Fajardo R, De Jong R, Van Hooft JE, Fockens P, *et al.* Interfractional position variation of pancreatic tumors quantified using intratumoral fiducial markers and daily cone beam computed tomography. *Int J Radiat Oncol Biol Phys* 2013;87:202–8.

22. Jin P, van der Horst A, de Jong R, van Hooft JE, Kamphuis M, van Wieringen N, *et al.* Marker-based quantification of interfractional tumor position variation and the use of markers for setup verification in radiation therapy for esophageal cancer. *Radiother Oncol* 2015;117:412–8.

23. Beltran C, Herman MG, Davis BJ. Planning Target Margin Calculations for Prostate Radiotherapy Based on Intrafraction and Interfraction Motion Using Four Localization Methods. Int J Radiat Oncol Biol Phys 2008;70:289–95.

24. Gurney-Champion OJ, Lens E, Van Der Horst A, Houweling AC, Klaassen R, Van Hooft JE, *et al.* Visibility and artifacts of gold fiducial markers used for image guided radiation therapy of pancreatic cancer on MRI. *Med Phys* 2015;42:2638–47.

25. Schieda N, Avruch L, Shabana WM, Malone SC. Multi-echo gradient recalled echo imaging of the pelvis for improved depiction of brachytherapy seeds and fiducial markers facilitating radiotherapy planning and treatment of prostatic carcinoma. *J Magn Reson Imaging* 2015;41:715–20.

26. Chan MF, Cohen GN, Deasy JO. Qualitative Evaluation of Fiducial Markers for Radiotherapy Imaging. *Technol Cancer Res Treat* 2015;14:298–304.

27. Vorwerk H, Liersch T, Rothe H, Ghadimi M, Christiansen H, Hess CF, *et al.* Gold markers for tumor localization and target volume delineation in radiotherapy for rectal cancer. *Strahlentherapie Und Onkol* 2009;185:127–33.

28. Moningi S, Walker AJ, Malayeri AA, Rosati LM, Gearhart SL, Efron JE, *et al.* Analysis of fiducials implanted during EUS for patients with localized rectal cancer receiving high-dose rate endorectal brachytherapy. *Gastrointest Endosc* 2015;81:765–9.

29. Dutch Trial Registry; registration no. NL4473. Accessed September 16, 2019.

30. Klein S, Staring M, Murphy K, Viergever MA, Pluim JPW. Elastix: A toolbox for intensity-based medical image registration. *IEEE Trans Med Imaging* 2010;29:196–205.

31. Gustafsson C, Korhonen J, Persson E, Gunnlaugsson A, Nyholm T, Olsson LE. Registration free automatic identification of gold fiducial markers in MRI target delineation images for prostate radiotherapy. *Med Phys* 2017;44:5563–74.

32. Machiels M, Van Hooft J, Jin P, Van Berge Henegouwen MI, Van Laarhoven HM, Alderliesten T, *et al.* Endoscopy/EUS-guided fiducial marker placement in patients with esophageal cancer: A comparative analysis of 3 types of markers. *Gastrointest Endosc* 2015;82:641–9.

33. Rydhög JS, Mortensen SR, Larsen KR, Clementsen P, Jølck RI, Josipovic M, *et al.* Liquid fiducial marker performance during radiotherapy of locally advanced non small cell lung cancer. *Radiother Oncol* 2016;121:64–9.

34. Schneider S, Jølck RI, Troost EGC, Hoffmann AL. Quantification of MRI visibility and artifacts at 3T of liquid fiducial marker in a pancreas tissue-mimicking phantom. *Med Phys* 2018;45:37–47.

Chapter 4

Applicator visualization using ultrashort echo time MRI for high-dose-rate endorectal brachytherapy

Roy P.J. van den Ende
Ece Ercan
Rick Keesman
Ellen M. Kerkhof
Corrie A.M. Marijnen
Uulke A. van der Heide

ABSTRACT

Purpose

The individual channels in an endorectal applicator for high-dose-rate endorectal brachytherapy are not visible on standard MRI sequences. The aim of this study was to test whether an ultrashort echo time (UTE) MRI sequence could be used to visualize the individual channels to enable MR-only treatment planning for rectal cancer.

Methods and materials

We used a radial 3D UTE pulse sequence and acquired images of phantoms and two rectal cancer patients. We rigidly registered a UTE image and CT scan of an applicator phantom, based on the outline of the applicator. One observer compared channel positions on the UTE image and CT scan in five slices spaced 25 mm apart. To quantify geometric distortions, we scanned a commercial 3D geometric QA phantom and calculated the difference between detected marker positions on the UTE image and corresponding marker positions on two 3D T_1-weighted images with opposing readout directions.

Results

On the UTE images, there is sufficient contrast to discern the individual channels. The difference in channel positions on the UTE image compared to the CT was on average -0.1 ± 0.1 mm (LR) and 0.1 ± 0.3 mm (AP). After rigid registration to the 3D T_1-weighted sequences, the residual 95th percentile of the geometric distortion inside a 550 mm diameter sphere was 1.0 mm (LR), 0.9 mm (AP) and 0.9 mm (CC).

Conclusions

With a UTE sequence, the endorectal applicator and individual channels can be adequately visualized in both phantom and patients. The geometrical fidelity is within acceptable range.

INTRODUCTION

For rectal cancer patients, high-dose rate endorectal brachytherapy (HDREBT) can be used to deliver high doses to the tumor while sparing surrounding organs at risk due to a steep dose gradient [1]. HDREBT may be delivered using an intracavitary mold applicator set, such as the flexible eight-channel applicator (Elekta, Veenendaal, the Netherlands). Applicator reconstruction for the flexible eight-channel applicator is currently performed on CT [2,3], because the individual channels of the applicator are not visible on conventional MR images due to the short T_2-relaxation time of the applicator. However, CT suffers from limited soft-tissue contrast, which makes it challenging to delineate the target volume accurately [4,5]. MRI is the primary imaging modality for tumor visualization because of its superior soft-tissue contrast and it is therefore currently registered to CT imaging to aid in the tumor delineation on CT. However, acquiring both CT and MRI on the same day can be time consuming and changes in

applicator positioning between the scans may occur because of patient movement and/or differences in organ filling. An MRI-only approach in which applicator reconstruction, delineation of target volume and organs at risk, and treatment planning is performed on MRI is therefore preferred.

MRI-only brachytherapy treatment planning is already the standard for cervical cancer in Europe [6]. To perform applicator reconstruction on MRI, models of rigid applicators have been made available in commercial treatment planning systems and these can be rigidly registered to the applicator on MR images. However, for non-rigid applicators such as the flexible endorectal applicator, such models are not available. In addition, since the individual channels of the flexible endorectal applicator are not visible on MRI, the rotation of the applicator cannot be determined because of its cylindrical shape. In brachytherapy for cervical cancer, dummy catheters can be used to aid in applicator reconstruction. The dummy catheter is filled with a fluid that produces high signal intensity on MRI. However, such dummy catheters are not available for the flexible endorectal applicator. As an alternative, an ultrashort echo time (UTE) sequence [7,8] may be used to visualize the applicator and the individual channels. UTE uses very short echo times on the order of <0.5 ms and allows visualization of materials with very short T_2-relaxation times.

The aim of this study was to test if a UTE sequence can be used to visualize the individual channels within the flexible endorectal applicator for HDREBT treatment planning. To this end, we first evaluated the visibility of the individual channels in a phantom and determined the geometric fidelity of the UTE sequence. Finally, we acquired UTE images from two rectal cancer patients with applicator in situ to evaluate the visibility of the individual channels in an applicator in situ.

METHODS AND MATERIALS

Applicator
We used a commercial intracavitary mold applicator (OncoSmart, Elekta, Veenendaal, The Netherlands). This is a flexible cylindrical applicator made of silicon with a diameter of 20 mm and a length of 280 mm. The applicator has eight channels radially spaced along its circumference, which allows for an asymmetric dose distribution [9].

UTE sequence
All MRI scans in this study were performed on a 3T scanner (Ingenia, Philips Healthcare, Best, The Netherlands). We used a 3D stack of radials UTE pulse sequence for radial sampling of free induction decays, enabled by clinical science functionality under a research agreement. A cylindrical encoding scheme was performed with radial sampling in-plane and cartesian sampling through-plane. Radial sampling was used as it allows for very short echo times in the order of <0.5 ms. The sequence is similar to the stack of spirals UTE sequence described in Qian *et al.* [10]. For UTE excitation, a non-selective

hard radiofrequency pulse was applied for a very short duration (0.05 ms) and was followed by a phase-encoding gradient in craniocaudal (CC) direction for slice encoding. Immediately after the phase-encoding gradient, a radial read-out was performed to quickly sample the k-space in the two directions that are perpendicular to the slice direction. The radial k-space data acquisition started already during the ramp of the gradients [7]. The scan parameters for the UTE sequences used for imaging the applicator phantom, the two patients, and the geometric QA phantom are shown in Table 1. To ensure clinical feasibility, the scanning times for patients were kept below 6 minutes.

Applicator phantom

To optimize and evaluate the UTE sequence for applicator visualization, we prepared a phantom. We first filled a box (400 x 300 x 190 mm^3) halfway with agarose gel. The agarose gel consisted of 0.2 g Dotarem 0.5 mM (Guerbet, Villepinte, France), 10 grams agar (A1296, Sigma Aldrich, Saint Louis, USA), and 3 grams NaCl per liter water, aiming for a T_1 (spin-lattice relaxation time) of 1-2 seconds and a T_2 (spin-spin relaxation time) of >30 ms [11], which is on the same order of magnitude as the relaxation properties of human soft-tissue around the rectum. A balloon was placed around the applicator and subsequently filled with 20cc of water with 5% Telebrix Gastro (Guerbet, Villepinte, France), as in our clinical procedure. The applicator was then placed on top of the first layer of agarose gel and a second layer of agarose gel was applied to fill the box.

Individual channel visualization

To evaluate the visibility of the individual channels within the applicator, we acquired an axial UTE image of the phantom. To test whether the visualized channels on the UTE image actually represent the individual channels within the applicator, we acquired an axial CT scan (Brilliance Big Bore, Philips Healthcare, Best, The Netherlands) of the phantom (voxel size 0.63 x 0.63 x 1 mm^3, 120 kVp, tube current 346 mA, exposure time 887 ms). We performed a rigid registration of the CT scan to the UTE

Table 1. Scan parameters for the UTE sequences used for imaging the applicator phantom, the patients, and the geometric fidelity phantom.

Parameter	Applicator phantom	Patient 1	Patient 2	Geometric QA phantom
Voxel size (mm^3)	1.0x1.0x2.5	1.0x1.0x3.5	0.98x0.98x2.5	1.94x1.94x1.94
Echo time (ms)	0.14	0.14	0.14	0.14
Repetition time (ms)	5.26	4.97	5.22	4.22
Acquisition grid	376x376x126	376x376x90	384x384x90	288x288x206
Field of view (mm^3)	376x376x315	376x376x315	376x376x225	560x560x400
Readout bandwidth (Hz/mm)	886	886	886	895
SENSE factor	1.4	1.4	1.4	1.0
Flip angle (deg)	10	10	10	10
Acquisition duration (s)	499	337	353	643

image based on the outline of the applicator using Elastix, a toolbox for intensity-based medical image registration [12]. To determine channel positions, one observer manually aligned a 2D template of the channel configuration on the UTE image and the registered CT scan in five slices spaced 25 mm apart. We then calculated the in-plane difference in channel positions between the UTE image and the CT scan. To evaluate the visibility of the channels in a clinical setting, we acquired informed consent from two rectal cancer patients undergoing HDREBT within a clinical trial. In addition to the MRI sequences acquired for HDREBT treatment planning, we acquired an additional axial UTE image for these two patients with the applicator in situ. As part of sequence optimization, we acquired a UTE image with a slice thickness of 3.5 mm in the first patient and a slice thickness of 2.5 mm in the second patient. For one slice in each UTE image, we determined the contrast-to-noise ratio $\left(CNR = |S_C - S_A| / \sigma \right)$ of the channels relative to the applicator. Here, S_C and S_A are the average signal intensities of the channels and the applicator, respectively, and σ is the standard deviation of the image noise. Average signal intensities were extracted from regions of interest of 2 x 2 mm placed on and between the channels. In a similar fashion, σ was estimated from signal intensity variations inside a region of interest in the balloon surrounding the applicator.

Geometric fidelity

To quantify geometric distortions, we acquired MRI images of a commercial 3D geometric QA phantom (Philips Healthcare, Best, The Netherlands) [13,14]. The phantom was placed on the treatment table centered around the isocenter. It consists of seven plastic plates, placed 55 mm apart, each containing 276 spheres (markers) filled with oil with a diameter of 10 mm. Within each plate, the markers are located on a grid with a spacing of 25 mm. In total, the phantom is 330 mm long and has a diameter of 500 mm.

To determine the actual position of the markers within the phantom, we used two axial 3D T_1-weighted gradient-echo sequences (voxel size: 1.94 mm x 1.94 mm x 1.94 mm, field of view: 560 x 560 x 400 mm^3, TE: 3.40 ms, TR: 6.90 ms, readout bandwith: 828 Hz/mm) with opposing readout directions (anterior and posterior) to be able to correct for magnetic-field inhomogeneity. Subsequently, we acquired a UTE image with the same isotropic voxel size as the two axial 3D T_1-weighted images (Table 1). The marker detection algorithm described in Keesman *et al.* [13] was used to detect the markers, which produced lists of marker positions, one for each image.

To correct for magnetic-field inhomogeneity, the corresponding detected marker positions in the two 3D T_1-weighted images were averaged. To assess the distortion of the averaged 3D T_1-weighted marker positions, a regular reference grid (containing the ideal marker positions, defined according to the known geometry of the phantom) was rigidly registered per plate to the averaged 3D T_1-weighted marker positions. Residuals between the averaged 3D T_1-weighted marker positions and the registered reference grid (ref_grid$_{T1\_3D}$) were calculated.

To assess the geometric distortion of the UTE image relative to the 3D T_1-weighted images, we calculated the residuals between detected markers in the UTE image and ref_grid$_{T1\_3D}$. The 5th, 50th and 95th percentiles for the residuals are presented for various diameters of spherical volume (DSV) to evaluate the geometric fidelity for various distances from the isocenter.

RESULTS

Individual channel visualization

On the UTE image that was acquired of the applicator phantom, the channels have sufficient contrast relative to the applicator itself to be able to discern the individual channels (Figure 1). The difference in channel positions on the UTE image compared to the CT was on average -0.1 ± 0.1 mm (left-right (LR)) and 0.1 ± 0.3 mm (anteroposterior (AP)). In addition, individual channels are visible on the UTE patient images (Figure 2). CNR was calculated from the slices that contained the balloon (Figure 2, A2 and B2). The CNR was 1.9 for patient 1 and 2.4 for patient 2.

Geometric distortion

In total, 1428 corresponding markers out of the 1932 markers in the geometric QA phantom were detected by the marker detection algorithm in both the 3D T_1-weighted images and the UTE image. Marker appearance on the UTE image and the 3D T_1-weighted images with opposing readout directions is shown in Figure 3. The mean and standard deviation of the residuals between the averaged 3D T_1-weighted marker positions and ref_grid$_{T1\_3D}$ was 0.01 ± 0.42 mm (LR), -0.03 ± 0.36 mm (AP), and 0.02 ± 0.33 mm (CC). The 95th percentile of the residuals was 0.81 mm (LR), 0.68 mm (AP), and 0.65 mm (CC) within a DSV of 550 mm, which includes all detected markers. In Figure 4, the residuals are plotted as a function of distance to the isocenter in the LR, AP and CC directions, respectively.

The mean and standard deviation of the residuals between detected markers in the UTE image and ref_grid$_{T1\_3D}$ were 0.46 ± 0.46 mm (LR), -1.69 ± 0.50 mm (AP), and 0.07 ± 0.48 mm (CC). This indicates a systematic shift, mostly in the AP direction. In a clinical scenario, a rigid registration is performed between the UTE image and an anatomical image based on the outline of the applicator to correct for any changes in patient and/or applicator positioning that can occur within the scan session. To investigate effects of higher-order distortion patterns in the UTE image, we corrected this systematic shift by means of a global translation. Subsequently, we calculated the remaining residuals. The 5th, 50th and 95th percentiles for these residuals within various DSVs are presented in Table 2. A 95th percentile of 1.0 mm or lower is observed in all directions within a DSV of 550 mm. The magnitude of the distortions increases with increasing distance from the isocenter. This can also be observed in Figure 4, where the residuals are plotted as a function of distance to the isocenter in the LR, AP and CC directions, respectively.
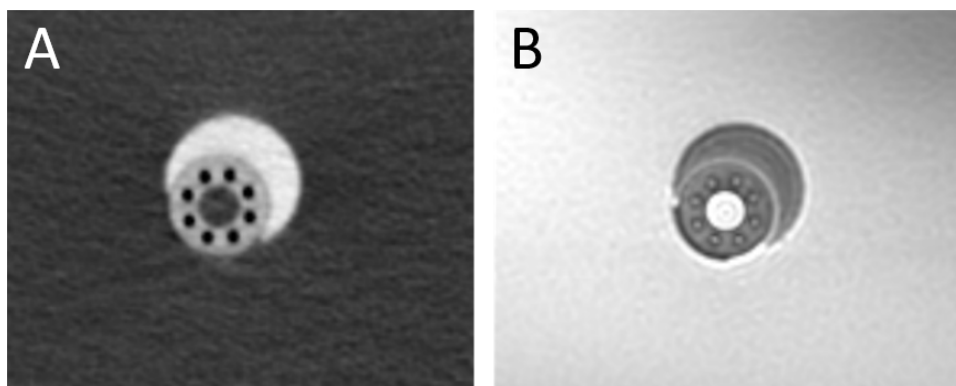
Figure 1. A CT scan (A) and UTE MR image (B) of the applicator phantom.
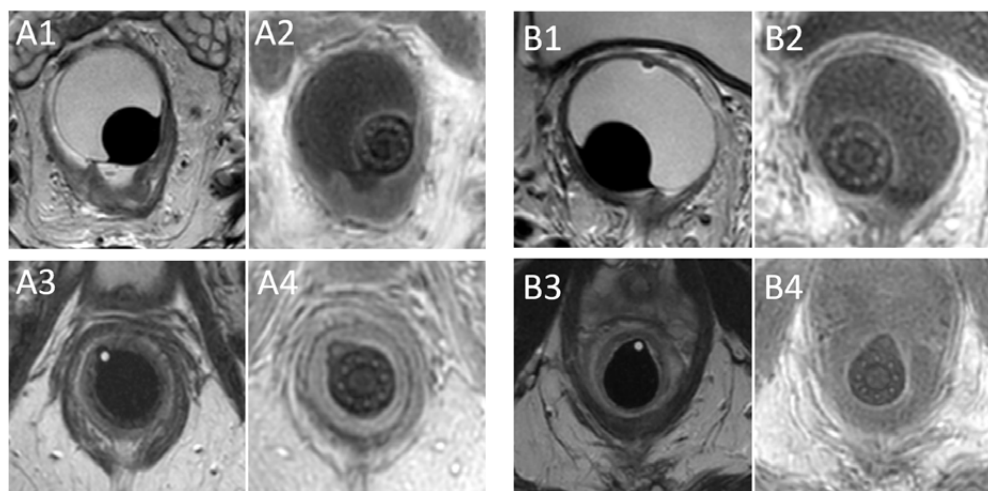
Figure 2. Axial slices of T2-TSE images (A1, A3, B1, B3) and UTE images (A2, A4, B2, B4) in two patients (A and B) with the applicator in situ.

DISCUSSION

Treatment planning for HDREBT for rectal cancer using the flexible endorectal applicator is currently not performed on MRI alone, as the individual channels within the applicator are not visible on MRI images. The aim of this study was to test if a UTE sequence can be used to visualize the individual channels within the flexible endorectal applicator for HDREBT treatment planning. We have shown that the individual channels are visible on UTE images, both in a phantom and in patients. The CNR of the channels and the

applicator was higher in patient 2. This may be explained by a partial volume effect due to a difference in slice thickness, which was 3.5 mm for patient 1 and 2.5 mm for patient 2.

We observed a systematic shift of the detected marker positions in the UTE image relative to ref_grid$_{T1\_3D}$, especially in the AP direction. In a clinical application, an anatomical image is used for delineation, while the UTE image would be used to visualize the individual channels within the applicator. A rigid registration would be performed based on the outline of the applicator and surrounding balloon, negating any systematic offsets. After correcting for the systematic shift, the 95th percentile of the residuals is 1.0 mm or lower in all directions within a DSV of 550 mm. In addition, within a volume that is typically of interest for applicator reconstruction (i.e., a DSV of 300 mm), the 95th percentile of the residuals was 0.3 mm (LR), 0.4 mm (AP) and 0.7 mm (CC), which is acceptable for HDREBT treatment planning.

In a UTE sequence, k-space data acquisition starts quickly after the radiofrequency excitation and is performed during the ramp up of the gradients [7]. This makes the UTE sequence prone to degraded image quality due to eddy currents and unbalanced hardware time delays, that lead to undesired k-space trajectory deviations [15]. This could have contributed to the systematic shift we have observed. Although for our application it suffices to correct for this shift by using a rigid registration, different techniques can be used to measure the actual k-space trajectory to improve the image reconstruction [15–17].
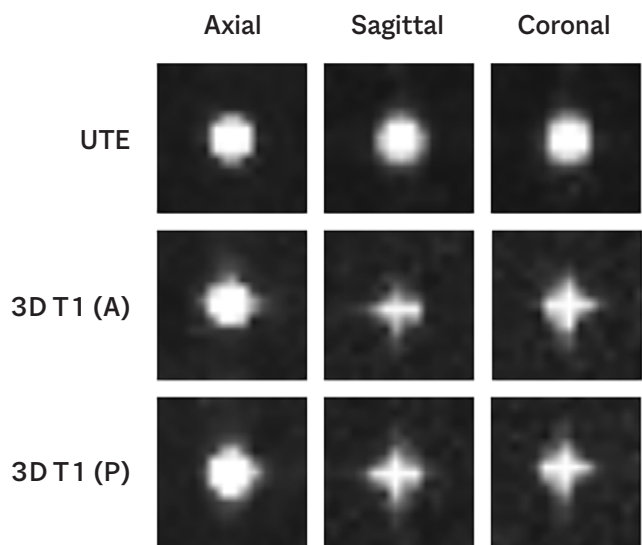
Figure 3. Appearance of a single marker of the 3D geometric QA phantom in the axial, sagittal and coronal plane on a UTE image and two 3D T$_1$-weighted images with opposing readout directions (A = anterior readout direction, P = posterior readout direction).
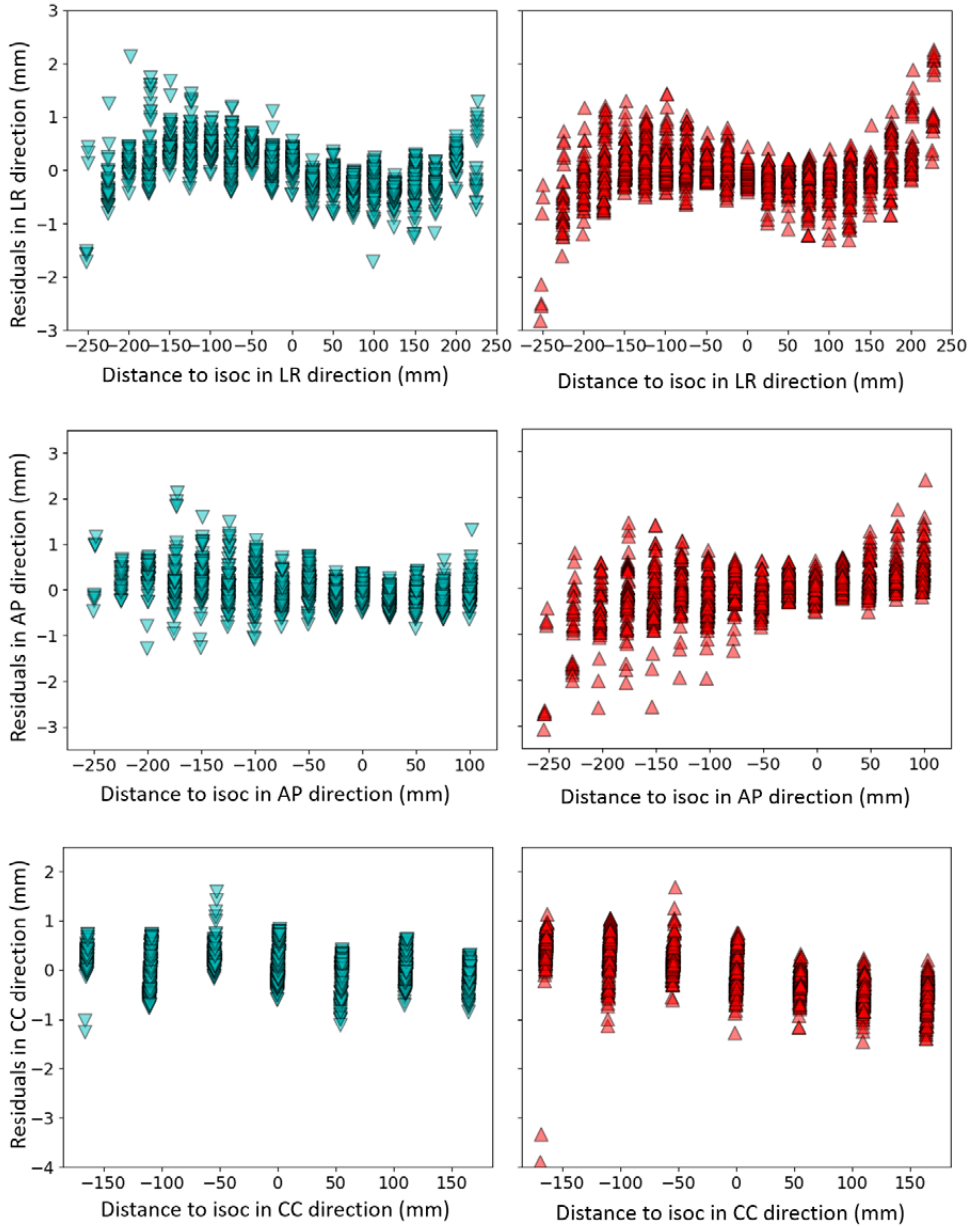
Figure 4. Residuals of the average detected marker positions of the 3D T_1-weighted images (blue) and residuals of detected markers in the UTE image (red) with respect to ref_grid$_{T1\_3D}$ in the LR-, AP- and CC-direction as a function of distance to isocenter (isoc) in the LR-, AP- and CC-direction, respectively.

Table 2. Measured residuals of detected marker positions in the UTE image relative to ref_grid$_{T1\_3D}$ in the LR, AP and CC direction after rigid registration of the detected markers in the UTE image to ref_grid$_{T1\_3D}$.

| DSV (mm)	Percentile	LR (mm)	AP (mm)	CC (mm)	No. of markers
100	5th	0.0	0.0	0.0	11
	50th	0.1	0.1	0.1	
	95th	0.2	0.4	0.7	
200	5th	0.0	0.0	0.0	121
	50th	0.1	0.1	0.2	
	95th	0.3	0.4	0.6	
300	5th	0.0	0.0	0.0	387
	50th	0.1	0.2	0.3	
	95th	0.3	0.4	0.7	
400	5th	0.0	0.0	0.0	862
	50th	0.1	0.2	0.3	
	95th	0.5	0.6	0.8	
550	5th	0.0	0.0	0.0	1428
	50th	0.2	0.3	0.3	
	95th	1.0	0.9	0.9	

CONCLUSIONS

The endorectal applicator and the individual channels can be adequately visualized using a UTE sequence in both a phantom and patients. After a rigid registration to an anatomical image, the geometric fidelity of the UTE sequence is within acceptable range. The UTE sequence is therefore suitable for HDREBT treatment planning.

REFERENCES

1. Vuong T, Richard C, Niazi T, Liberman S, Letellier F, Morin N, *et al.* High dose rate endorectal brachytherapy for patients with curable rectal cancer. *Semin Colon Rectal Surg* 2010;21:115–9.

2. Vuong T, Devic S. High-dose-rate pre-operative endorectal brachytherapy for patients with rectal cancer. *J Contemp Brachytherapy* 2015;7:181–6.

3. Nout RA, Devic S, Niazi T, Wyse J, Boutros M, Pelsser V, *et al.* CT-based adaptive high-dose-rate endorectal brachytherapy in the preoperative treatment of locally advanced rectal cancer: Technical and practical aspects. *Brachytherapy* 2016;15:477–84.

4. O'Neill BDP, Salerno G, Thomas K, Tait DM, Brown G. MR vs CT imaging: Low rectal cancer tumour delineation for three-dimensional conformal radiotherapy. *Br J Radiol* 2009;82:509–13.

5. Khoo VS, Joon DL. New developments in MRI for target volume delineation in radiotherapy. *Br J Radiol* 2006;79.

6. Pötter R, Haie-Meder C, Van Limbergen E, Barillot I, De Brabandere M, Dimopoulos J, *et al.* Recommendations from gynaecological (GYN) GEC ESTRO working group (II): Concepts and terms in 3D image-based treatment planning in cervix cancer brachytherapy - 3D dose volume parameters and aspects of 3D image-based anatomy, radiation physics, radiobiolo. *Radiother Oncol* 2006;78:67–77.

7. Holmes JE, Bydder GM. MR imaging with ultrashort TE (UTE) pulse sequences: Basic principles. *Radiography* 2005;11:163–74.

8. Bos C, Moerland MA, J. van den Brink, Seevinck PR. MR Image Guidance of Brachytherapy Needle Placement: Potential of 2D Ultrashort Echo Time Imaging. *Int J Radiat Oncol* 2013;87:S671.

9. Poon E, Reniers B, Devic S, Vuong T, Verhaegen F. Dosimetric characterization of a novel intracavitary mold applicator for 192Ir high dose rate endorectal brachytherapy treatment. *Med Phys* 2006;33:4515–26.

10. Qian Y, Boada FE. Acquisition-weighted stack of spirals for fast high-resolution three-dimensional ultrashort echo time MR imaging. *Magn Reson Med* 2008;60:135–45.

11. Shen Y, Goerner FL, Snyder C, Morelli JN, Hao D, Hu D, *et al.* T1 relaxivities of gadolinium-based magnetic resonance contrast agents in human whole blood at 1.5, 3, and 7T. *Invest Radiol* 2015;50:330–8.

12. Klein S, Staring M, Murphy K, Viergever MA, Pluim JPW. Elastix: A toolbox for intensity-based medical image registration. *IEEE Trans Med Imaging* 2010;29:196–205.

13. Keesman R, van de Lindt TN, Juan-Cruz C, van den Wollenberg W, van der Bijl E, Nowee ME, *et al.* Correcting geometric image distortions in slice-based 4D-MRI on the MR-linac. *Med Phys* 2019;46:3044–54.

14. Ranta I, Kemppainen R, Keyriläinen J, Suilamo S, Heikkinen S, Kapanen M, *et al.* Quality assurance measurements of geometric accuracy for magnetic resonance imaging-based radiotherapy treatment planning. *Phys Medica* 2019;62:47–52.

15. Atkinson IC, Lu A, Thulborn KR. Characterization and correction of system delays and eddy currents for MR imaging with ultrashort echo-time and time-varying gradients. *Magn Reson Med* 2009;62:532–7.

16. Latta P, Starčuk Z, Gruwel MLH, Weber MH, Tomanek B. K-space trajectory mapping and its application for ultrashort Echo time imaging. *Magn Reson Imaging* 2017;36:68–76.

17. Kronthaler S, Rahmer J, Börnert P, Karampinos D. Trajectory correction for ultrashort echo-time (UTE) imaging based on the measurement of the gradient impulse response function (GIRF) with a thin-slice method. Proc. Intl. Soc. Mag. Reson. Med. 27, 2019.

Chapter 5

Feasibility of gold fiducial markers as a surrogate for GTV position in image-guided radiotherapy of rectal cancer

Roy P.J. van den Ende
Ellen M. Kerkhof
Lisanne S. Rigter
Monique E. van Leerdam
Femke P. Peters
Baukelien van Triest
Marius Staring
Corrie A.M. Marijnen
Uulke A. van der Heide

ABSTRACT

Purpose

To evaluate the feasibility of fiducial markers as a surrogate for GTV position in image-guided radiotherapy of rectal cancer.

Methods and materials

We analyzed 35 fiducials in 19 rectal cancer patients who received short course radiotherapy or long-course chemoradiotherapy. A MRI exam was acquired before and after the first week of radiotherapy and daily pre- and post-irradiation CBCT scans were acquired in the first week of radiotherapy. Between the two MRI exams, the fiducial displacement relative to the center of gravity of the GTV (COG_{GTV}) and the COG_{GTV} displacement relative to bony anatomy was determined. Using the CBCT scans, inter- and intrafraction fiducial displacement relative to bony anatomy was determined.

Results

The systematic error of the fiducial displacement relative to the COG_{GTV} was 2.8, 2.4 and 4.2 mm in the left-right (LR), anterior-posterior (AP) and craniocaudal (CC) direction. Large interfraction systematic errors of up to 8.0 mm and random errors up to 4.7 mm were found for COG_{GTV} and fiducial displacements relative to bony anatomy, mostly in the AP and CC directions. For tumors located in the mid- and upper rectum these errors were up to 9.4 mm (systematic) and 5.6 mm (random) compared to 4.9 mm and 2.9 mm for tumors in the lower rectum. Systematic and random errors of the intrafraction fiducial displacement relative to bony anatomy were ≤2.1 mm in all directions.

Conclusions

Large interfraction errors of the COG_{GTV} and the fiducials relative to bony anatomy were found. Therefore, despite the observed fiducial displacement relative to the COG_{GTV}, the use of fiducials as a surrogate for GTV position reduces the required margins in the AP and CC direction for a GTV boost using image-guided radiotherapy of rectal cancer. This reduction in margin may be larger in patients with tumors located in the mid- and upper rectum compared to the lower rectum.

INTRODUCTION

Neoadjuvant radiotherapy reduces local recurrence rates after surgery in rectal cancer patients [1–4]. A pathological complete response is observed in 15-25% of patients after neoadjuvant chemoradiation [5,6]. In addition, dose escalation is suggested to result in higher complete response rates, which is attractive considering the increased interest in organ preservation [6–10].

The current clinical practice for setup correction in external-beam radiotherapy of rectal cancer is based on bony anatomy using cone beam computed tomography (CBCT) [11]. To ensure proper gross tumor volume (GTV) coverage in a GTV boost setting, a planning target volume (PTV) margin of 7-30 mm is used to accommodate delineation errors, setup errors and inter- and intrafraction motion of the GTV [12–16]. Setup correction based on the GTV instead of bony anatomy may decrease the required PTV margins. However, this is challenging due to the limited soft tissue contrast of CBCT [17]. MR-guided radiotherapy systems could be used to perform setup correction based on a direct visualization of the GTV with superior soft tissue contrast [18]. However, such systems are not widely available yet. Given that fiducial markers have been proven useful for setup correction in other tumor locations such as pancreas, esophagus and prostate [19–21], fiducials may be useful as a surrogate for GTV position in rectal cancer. Several studies have reported on the use of fiducials in the rectum and focus on marker visibility and migration [22], fiducial retention and adverse events [23,24] and the use of fiducials to aid in the delineation of the target volume [25]. However, none have investigated the potential benefit of fiducials for setup correction in radiotherapy of rectal cancer.

In order to use fiducials as a surrogate for the GTV, the position of the fiducials must be representative of the position of the GTV. The aim of this study was therefore to evaluate the feasibility of fiducials as a surrogate for GTV position in radiotherapy of rectal cancer.

METHODS AND MATERIALS

Patients
Between July 2015 and September 2016, we included 20 patients with proven rectal adenocarcinoma who were scheduled for short-course radiotherapy (SC-RT; 5x5 Gy) or long-course chemoradiotherapy (LC-CRT; 25x2 Gy combined with capecitabine 825 mg/m² twice daily on days of radiotherapy) followed by total mesorectal excision. Patients were treated in supine position. Before each radiotherapy fraction, patients were asked to void their bladder and subsequently drink 300 cc of water to reproduce bladder filling.

Exclusion criteria were contraindication for fiducial insertion (coagulopathy or anticoagulantia that could not be stopped), prior pelvic irradiation, pelvic surgery or hip replacement surgery, pregnancy, a contraindication for MRI or world health organization performance status 3-4. This study was registered at the Dutch Trial Registry (REMARK study, registration no. NL4473) [26].

Fiducials
We used four types of fiducials, inserted in five patients each (Visicoil 0.5x5 mm and Visicoil 0.75x5 mm [IBA Dosimetry, GmbH, Germany], Cook 0.64x3.4 mm [COOK Medical, Limerick, Ireland] and Gold Anchor 0.28x20 mm (unfolded length)[Naslund Medical AB, Sweden]). We endoscopically placed the

fiducials in the tumor and mesorectum at least one day before the start of radiotherapy. The fiducial insertion strategy is described in Rigter *et al.* [24].

MRI processing

We performed two multiparametric MRI exams for each patient on a Philips Achieva 1.5T, Philips Achieva 3T, Philips Achieva dStream 3T or Philips Ingenia 3T. Details of the scan protocol are listed in the supplementary materials. We acquired a first MRI exam up to two weeks before or up to one week after the start of radiotherapy and a second MRI exam between one and two weeks after the start of radiotherapy. In an earlier study, we evaluated the MRI visibility of the fiducials and we identified 17 out of 34 fiducials on the first MRI and 9 out of 30 fiducials on the second MRI [27]. The Visicoil 0.75 and the Gold Anchor were the best visible fiducials on MRI. In addition, a consensus meeting with a radiologist (EP) and a resident radiation oncologist (ER) was held to identify more fiducials for this study. We delineated the artifacts that the fiducials created on MRI on the tT2-TSE scan with help of the other available sequences. The coordinate of the center of gravity (COG) of this delineation represented the fiducial position.

The GTV was delineated on the tT2-TSE scan of both MRI exams by one observer (RE) and subsequently checked by a radiation oncologist (FP) in Oncentra (Elekta, Veenendaal, the Netherlands). We registered the tT2-TSE sequence of the second MRI exam to the tT2-TSE sequence of the first MRI exam using Elastix [28] with a rigid transformation based on the bony anatomy of the pelvis and the sacrum.

We selected both ischial spines and the pubic symphysis as anatomical landmarks on the bony anatomy on the MRI exams to assess registration accuracy. The registration accuracy was defined as the mean and standard deviation of the distances between a landmark position on the registered second MRI exam and the corresponding landmark position on the first MRI exam.

To determine the displacement of the fiducials relative to the GTV, we calculated the displacement for each fiducial relative to the center of gravity of the GTV delineation (COG_{GTV}) on the second MRI with respect to the first MRI. Subsequently, we determined the mean of means (M) by calculating the mean displacement over all fiducials and the group systematic error (Σ) by calculating the standard deviation over all fiducial displacements [29].

To determine the interfraction GTV displacement relative to bony anatomy, we calculated the displacement of the COG_{GTV} relative to bony anatomy on the second MRI with respect to the first MRI. Subsequently, we determined the mean of means by calculating the mean displacement over all COG_{GTV} displacements and the group systematic error by calculating the standard deviation over all COG_{GTV} displacements [29].

To test for differences in displacement between proximal and distal tumors, we calculated the interfraction COG$_{GTV}$ displacement relative to bony anatomy on MRI separately for patients with a tumor in the mid- and upper rectum (7-16 cm from anal verge) and the lower rectum (0-6 cm from anal verge) [30].

CBCT processing

During the first week of radiotherapy, we acquired daily pre- and post-irradiation CBCT scans (Elekta XVI, reconstructed slice thickness 1.0 mm, pixel spacing 1.0 mm x 1.0 mm). For the patients that were treated with LC-CRT, pre-irradiation CBCT scans were acquired weekly after the first week of radiotherapy.

The first pre-irradiation CBCT scan was used as the reference scan. We registered all subsequent CBCT scans to the reference scan using Elastix with a rigid registration based on the bony anatomy of the pelvis and the sacrum [28]. The registration accuracy was assessed using the same method as described for the MRI exams, with the promontory as an additional anatomical landmark.

We segmented fiducials on the reference and registered CBCT scans by manually selecting a point on each fiducial. A box of 12x12x12 mm was automatically created around each selected point and a threshold that was well above the image intensities of the surrounding soft tissue was applied to segment the fiducial. The coordinate of the COG for each fiducial segmentation was used as the position for each fiducial.

The displacement of the COG of all fiducials (COG$_{FID}$) as a result of changes in fiducial configuration was calculated as follows. For patients with two or more fiducials in situ, the position of each fiducial relative to the COG$_{FID}$ was determined on each pre-irradiation CBCT scan. To assess the resulting displacement of the COG$_{FID}$, we calculated the standard deviation of each fiducial position relative to COG$_{FID}$ over all pre-irradiation CBCT scans (SD$_{FID}$) and subsequently calculated the standard deviation (SD) of the COG$_{FID}$ for each patient with two or more fiducials in situ:

$$SD \ of \ COG_{FID} = \frac{\sqrt{SD^2_{FID_1} + SD^2_{FID_2} + \ldots + SD^2_{FID_n}}}{n}$$

with $SD^2_{FID_1}$, $SD^2_{FID_2}$, ..., $SD^2_{FID_n}$ the squared standard deviation of a fiducial position relative to COG$_{FID}$ over all pre-irradiation CBCT scans in the patient and n the number of fiducials in the patient. Subsequently, we determined the group random error (σ) by calculating the root-mean-square of all the standard deviations of COG$_{FID}$ [29].

To determine the interfraction fiducial displacement relative to bony anatomy, we calculated the displacement of each fiducial on each pre-irradiation CBCT scan with respect to the reference scan.

To determine the intrafraction fiducial displacement relative to bony anatomy, we calculated the displacement of each fiducial on the post-irradiation CBCT scan with respect to the pre-irradiation CBCT scan of the same fraction. For each fiducial, we calculated a mean displacement and corresponding standard deviation over all fractions for the inter- and intrafraction displacement in the left-right (LR), anterior-posterior (AP) and craniocaudal (CC) direction. Subsequently, we calculated for the inter- and intrafraction fiducial displacement the mean of means over all fiducials and the group systematic and random error by calculating the standard deviation of the mean displacements of all fiducials and the root-mean-square of the standard deviation of all fiducials [29].

To test for differences in displacement between proximal and distal tumors, we calculated the interfraction fiducial displacement relative to bony anatomy separately for patients with a tumor in the mid- and upper rectum (7-16 cm from anal verge) and the lower rectum (0-6 cm from anal verge) [30].

Treatment margins

To determine PTV margins, we quadratically added systematic and random errors of the different components to derive the combined errors for the GTV position in three image-guidance scenarios, using the Van Herk *et al.* margin recipe [31]. For setup correction based on bony anatomy, the inter- and intrafraction displacement of the GTV relative to the bony anatomy needs to be considered. We derived the interfraction displacement relative to bony anatomy in two ways. First from the COG_{GTV} displacement on MRI and second from the fiducial displacements on CBCT. Both were combined with the intrafraction fiducial displacement on CBCT to calculate the errors for setup correction based on bony anatomy. In a scenario of setup correction based on fiducials, we also need to consider the position uncertainty of the GTV relative to the fiducials. Therefore, we combined the fiducial displacement relative to the COG_{GTV} with the COG_{FID} displacement as a result of changes in fiducial configuration and the intrafraction fiducial displacement relative to bony anatomy on CBCT. In a scenario in which the GTV can be visualized directly for setup correction, we only used the errors of the intrafraction fiducial displacement relative to bony anatomy.

Statistical analysis

We used SPSS Statistics 23 (IBM Corp. Released 2015. IBM SPSS Statistics for Windows, Version 23.0. Armonk, NY: IBM Corp.) for statistical analysis. Because of the small sample size in this study, we used the non-parametric Mann-Whitney U test to test for differences between the mean and standard deviation of the fiducial displacements according to the distance from the anal verge.

RESULTS

Patients and fiducials

One patient was excluded as all fiducials were inadvertently inserted in the prostate. Therefore, 19 patients were available for analysis, of whom 8 received SC-RT and 11 received LC-CRT. Patient characteristics are shown in Table 1. The fiducial retention in the REMARK study was described earlier [32]. A total of 35 fiducials in situ were available for analysis on CBCT, of which 26 fiducials in the tumor and 9 in the mesorectum [27]. The consensus meeting resulted in 22 identified fiducials on the first MRI and 17 identified fiducials on the second MRI. All 17 fiducials identified on the second MRI were also identified on the first MRI. Of those, 14 fiducials were inserted in the tumor and 3 fiducials were inserted in the mesorectum. Examples of a GTV delineation and a fiducial on the T2-TSE sequence of both MRI exams and a fiducial on two CBCT scans is shown in Figure 1.

Imaging

Median time from the first MRI to the start of radiotherapy was 0 days (range -5 to 12 days). Median time between the first and second MRI exam was 7 days (range 4-21 days). For two patients who were treated with LC-CRT, the first MRI exam was acquired 2 days (2 fractions) and 5 days (3 fractions) after start of radiotherapy. The median delineated GTV volume was 22.8 cc (range 6.9 – 64.6 cc) for the first MRI and 15.2 cc (range 6.1 – 71.0 cc) for the second MRI. Median difference between the GTV volumes of the first and second MRI was -3.0 cc (range -26.5 – 6.4 cc), with a negative difference indicating a smaller volume in the second MRI. Fourteen out of nineteen delineated GTV volumes were smaller on the second MRI. The MRI registration error was on average 0.0 ± 0.6 mm (LR), 0.2 ± 1.4 mm (AP) and -0.1 ± 1.3 mm (CC).

A total of 219 CBCT scans were acquired in 19 patients (range 2 - 21 per patient), of which 132 pre-irradiation CBCT scans in 19 patients and 87 post-irradiation CBCT scans in 17 patients. The average time between pre- and post-irradiation CBCT scans was 9 ± 1 minutes. The CBCT registration error was on average -0.1 ± 0.7 mm (LR), -0.2 ± 0.9 mm (AP) and 0.0 ± 0.8 mm (CC).

Table 1. Patient characteristics

Patient	Sex	Age (years)	cTNM	Distance from anal verge (cm)	Tx	Fiducial type	Number of pre-irradiation CBCT scans	Number of post-irradiation CBCT scans	Number of implanted fiducials	Number of fiducials in situ at end of Tx*	Number of fiducials identified on both first and second MRI*
1	M	71	T3N0M0	5	SC-RT	Visicoil 0.5	5	5	3	1	1
2	M	82	T3N0M0	0	SC-RT	Visicoil 0.5	5	4	3	2	1
3	M	63	T2N0M0	2	LC-CRT	Visicoil 0.5	10	4	3	1	0
4	M	60	T3N1M0	8	LC-CRT	Visicoil 0.5	10	4	3	3	0
5	F	60	T3N1M0	2	SC-RT	Visicoil 0.5	2	0	3	1	1
6	M	67	T3N2M0	8	LC-CRT	Visicoil 0.75	10	6	3	1	1
7	F	52	T3N1M0	8	SC-RT	Visicoil 0.75	5	0	3	2	0
8	M	75	T3N0M0	10	SC-RT	Visicoil 0.75	4	2	3	2	2
9	M	82	T2N1M0	15	SC-RT	Visicoil 0.75	5	5	3	1	1
10	M	63	T3N1M0	15	SC-RT	Visicoil 0.75	5	5	3	1	1
11	F	62	T2N1M0	11	SC-RT	COOK	5	5	3	2	0
12	M	58	T3N0M0	1	LC-CRT	COOK	-	-	4	-	-
13	M	57	T3N2M0	7	LC-CRT	COOK	10	5	4	1	1
14	F	60	T3N1M0	2	SC-RT	COOK	5	5	4	3	0
15	M	59	T3N2M0	8	LC-CRT	COOK	11	8	4	3	0
16	M	63	T3N0M0	1	LC-CRT	Gold Anchor	9	5	3	2	2
17	M	65	T3N2M0	2	LC-CRT	Gold Anchor	9	5	3	1	1
18	M	59	T2N1M0	16	SC-RT	Gold Anchor	5	5	3	2	2
19	F	61	T3N1M0	10	SC-RT	Gold Anchor	5	5	3	3	1
20	M	51	T3N0M0	2	LC-CRT	Gold Anchor	12	9	3	3	2
Total							132	87	64	35	17

M = male, F = female, Tx = treatment schedule, SC-RT = short course radiotherapy, LC-CRT = long course chemoradiotherapy.
*Excludes fiducials that were inadvertently inserted in the prostate.

Inter- and intrafraction displacement

The systematic error of the interfraction fiducial displacement relative to the COG_{GTV} was 2.8 mm (LR), 2.4 mm (AP) and 4.2 mm (CC) as shown in Table 2. The random error of the interfraction displacement of the COG_{FID} was <1 mm in all directions.

The systematic error of the COG_{GTV} displacement relative to bony anatomy was substantially larger than the systematic error of the fiducial displacement relative to bony anatomy on CBCT in the AP (7.2 mm vs 4.8 mm) and CC direction (8.0 mm vs 4.6 mm). This was mainly due to two patients who showed a large COG_{GTV} displacement on MRI in the AP and CC direction: 15 mm and -20 mm (AP), and -16 mm and 20 mm (CC). After reviewing the MRI exams, we observed a large difference in the amount of air in the rectum which displaced the GTV. In one of these patients also a large difference in bladder filling was observed. In the other 17 patients, the group systematic error of the COG_{GTV} displacement relative to bony anatomy was 4.1 mm (AP) and 5.6 mm (CC), in line with the fiducial displacement relative to bony anatomy on CBCT.

Table 2. Mean of means, systematic error and random error for the different analyses

			LR (mm)	AP (mm)	CC (mm)	Available data	
Position uncertainty of GTV w.r.t. fiducials	Interfraction displacement fiducials w.r.t. COG_{GTV} (MRI)	M	-0.9	0.5	-0.2	MRI scans	26
		$\sum$	2.8	2.4	4.2	Fiducials	17
		σ	-	-	-	Patients	13
	Interfraction displacement of COG_{FID} as a result of changes in fiducial configuration (CBCT)	M	-	-	-	CBCT scans	76
		$\sum$	-	-	-	Fiducials	27
		σ	0.6	0.9	0.9	Patients	11
Interfraction displacement w.r.t. bony anatomy	Interfraction displacement of COG_{GTV} (MRI)	M	-0.2	0.5	-1.2	MRI scans	38
		$\sum$	2.8	7.2	8.0	Patients	19
		σ	-	-	-		
	Interfraction displacement of fiducials (CBCT)	M	0.4	-2.7	1.2	CBCT scans	132
		$\sum$	3.6	4.8	4.6	Fiducials	35
		σ	2.7	4.2	4.7	Patients	19
Intrafraction displacement w.r.t. bony anatomy	Intrafraction displacement of fiducials (CBCT)	M	-0.1	-0.5	1.1	CBCT scans	87
		$\sum$	0.8	1.4	1.6	Fiducials	32
		σ	1.4	1.7	2.1	Patients	17

LR = left-right, AP = anterior-posterior, CC = craniocaudal, M = mean of means, $\sum$ = systematic error, σ = random error
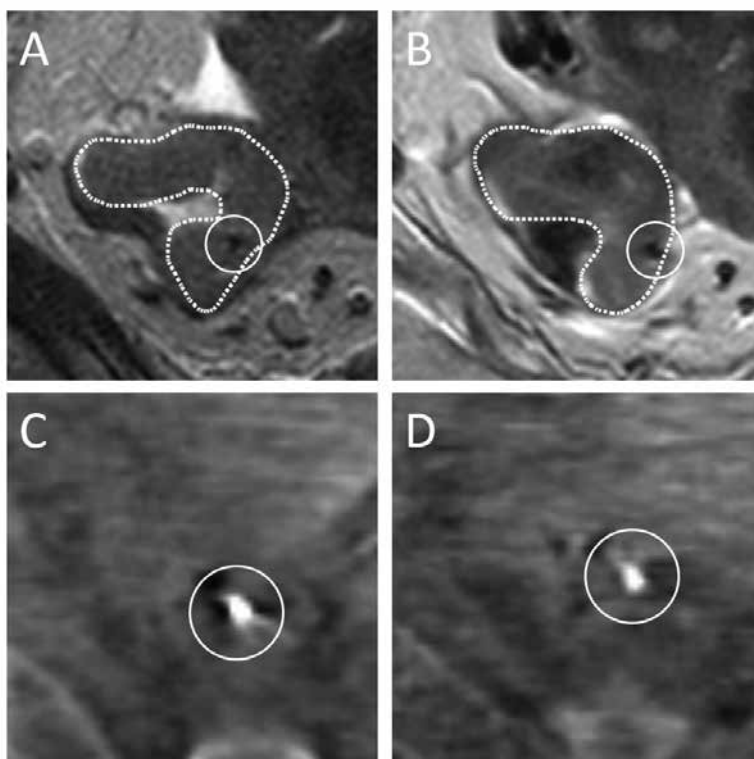
Figure 1. Examples of a GTV delineation and a fiducial on the T2-TSE sequence of both MRI exams (A and B) and the same fiducial on two pre-irradiation CBCT scans (C and D) for patient 19.

For the interfraction COG_{GTV} displacement relative to bony anatomy, the systematic error was 3.0 mm (LR), 8.7 mm (AP) and 9.4 mm (CC) for patients with a tumor in the mid- and upper rectum, while it was 1.3 mm (LR), 4.7 mm (AP) and 4.9 mm (CC) for patients with a tumor in the lower rectum. Similarly, for the interfraction fiducial displacement relative to bony anatomy on CBCT, systematic and random errors were 3.8 and 3.4 mm (LR), 6.1 and 5.1 mm (AP) and 5.5 and 5.6 mm (CC) for the mid- and upper group and 3.1 and 1.1 mm (LR), 1.6 and 2.3 mm (AP) and 2.8 and 2.9 mm (CC) for the lower rectum group. The standard deviation of the interfraction fiducial displacements relative to bony anatomy was significantly higher for patients with a tumor in the mid- and upper rectum compared to patients with a tumor in the lower rectum in the LR (p<0.01), AP (p=0.03) and CC (p=0.04) direction. An overview of the inter- and intrafraction fiducial displacements relative to bony anatomy split according to tumor location is shown in Figure 2 and Figure 3.

Systematic and random errors of the intrafraction fiducial displacement relative to bony anatomy were ≤2.1 mm in all directions.

Setup correction scenarios

For setup correction based on bony anatomy, the estimated margins were 8.3 mm (LR), 19.5 mm (AP) and 21.9 mm (CC) using the COG_{GTV} displacement relative to bony anatomy, and 11.3 mm (LR), 15.7 mm (AP) and 15.8 mm (CC) using the fiducial displacement relative to bony anatomy (Table 3). For setup correction based on fiducials, a reduction to 8.3 mm (LR and AP) and 12.8 mm (CC) was observed. Setup correction based on a direct visualization of the GTV would further reduce required margins to 3.0 mm (LR), 4.7 mm (AP) and 5.5 mm (CC).
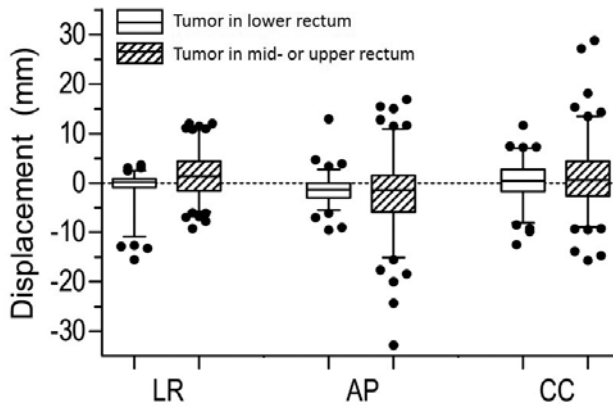

Figure 2. Boxplots of the interfraction fiducial displacements relative to bony anatomy on CBCT in the LR, AP and CC direction, split according to tumor location.

Figure 3. Boxplots of the intrafraction fiducial displacements relative to bony anatomy on CBCT in the LR, AP and CC direction, split according to tumor location.
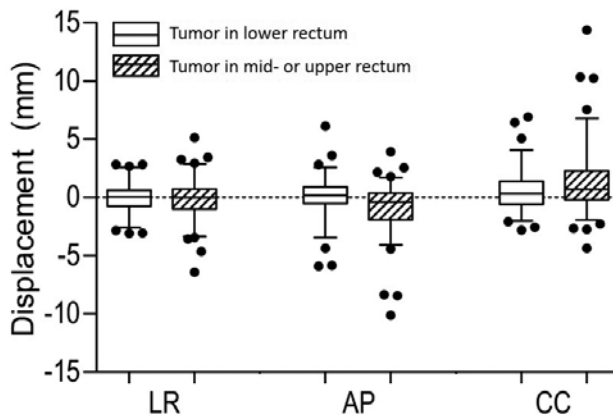
Table 3. Systematic error, random error and corresponding margin for different setup correction scenarios

		LR (mm)	AP (mm)	CC (mm)
Setup correction based on bony anatomy (COG$_{GTV}$ MRI data)	Σ	2.9	7.3	8.2
	σ	1.4	1.7	2.1
	Margin	8.3	19.5	21.9
Setup correction based on bony anatomy (fiducial CBCT data)	Σ	3.7	5.0	4.9
	σ	3.0	4.5	5.1
	Margin	11.3	15.7	15.8
Setup correction based on fiducials	Σ	2.9	2.8	4.5
	σ	1.5	1.9	2.3
	Margin	8.3	8.3	12.8
Setup correction based on GTV	Σ	0.8	1.4	1.6
	σ	1.4	1.7	2.1
	Margin	3.0	4.7	5.5

LR = left-right, AP = anterior-posterior, CC = craniocaudal, **Σ** = systematic error, **σ** = random error

DISCUSSION

The aim of this study was to evaluate the feasibility of fiducials as a surrogate for GTV position in rectal cancer. Despite fiducial displacement relative to the COG$_{GTV}$, an advantage for fiducial setup correction was observed in the AP and CC direction compared to bony anatomy setup correction. Consequently, the use of fiducials in a GTV boost setting allows for more precise irradiation of the GTV and sparing of organs at risk. More organ motion of the proximal rectum compared to the distal rectum is reported [33–35]. Although only a small number of patients were included in our study, a similar difference was observed. This suggests that the advantage of setup correction based on fiducials may be larger in patients with a proximal tumor.

The interfraction systematic error of the COG$_{GTV}$ relative to bony anatomy, as based on MRI, was substantially larger than the systematic and random errors of the fiducial displacements on CBCT. This is mainly due to large displacement of the COG$_{GTV}$ in two patients on MRI and may be explained by the absence of patient preparation before the MRI exams. For the calculation of the displacement of the COG$_{FID}$ as a result of changes in fiducial configuration, the COG$_{FID}$ was used as a reference point, assuming that all fiducials contributed equally to changes in fiducial configuration.

There is an inherent inaccuracy in determining exact fiducial locations on MRI, for instance due to the asymmetrical artifacts of the fiducials [36]. With help of the other available sequences, we delineated the fiducials on the tT2-TSE scan as it had the smallest artifacts [27]. Therefore, we believe that the inaccuracy in selecting the exact fiducial location has a minor effect on the observed fiducial displacements on MRI.

In the last two decades, organ motion in rectal cancer patients has been actively investigated and most studies focus on the movement of the clinical target volume (CTV) relative to bony anatomy [11,33,34,37–39]. Only a few papers have investigated the position variability of the GTV to determine the required margins for a GTV boost. Kleijnen *et al.* studied the motion of the rectum and GTV based on repeated MRI data [40–42]. They evaluated the intra- and interfraction displacement of the GTV relative to bony anatomy on time intervals of 1 minute, 9.5 minutes, 18 minutes and 1-4 days using daily MRI exams in 16 patients. They report a required margin of around 8 mm in all directions for both the 9.5 minute and 1-4 days timepoints [33]. However, a direct comparison is difficult since they used a different method to calculate the displacements and corresponding margins and they did not report the tumor location for each patient.

Furthermore, Kleijnen *et al.* report that although setup errors based on the rectal wall were slightly reduced compared to bony anatomy, a similar PTV margin was found. More importantly, the rectal wall could not be used as a surrogate for the GTV position, because displacement of the rectal wall and the GTV along the direction of the rectal wall will not be detected due to the absence of anatomical landmarks on the rectal wall [41]. They conclude that in order to further reduce uncertainties in a GTV boost setting, direct or indirect online tumor visualization is needed. In our study, we have shown that fiducials as an indirect visualization of the GTV reduces uncertainties. However, an uncertainty of the GTV position relative to the fiducials remains.

The suggested margins for setup correction based on bony anatomy as reported by Kleijnen *et al.* [42] are lower than those in our study, especially in the AP direction. However, a direct comparison is difficult since they did not report on the tumor location and intrafraction displacement of the tumor. Brierley *et al.* assessed the interfraction displacement of the rectum, mesorectum and GTV relative to bony anatomy [35]. They found that the GTV displacement was greatest in the CC direction, which is confirmed by the results in our study.

A limitation of the use of fiducials might be the low retention rate. In our study, a total of 64 fiducials were inserted, of which 35 fiducials were still in situ at the end of radiotherapy [24]. Furthermore, the insertion of fiducials is an invasive procedure. Previous studies on fiducial insertion in the rectum report no serious adverse events [22,24,25]. In one study, a small amount of bleeding that resolved spontaneously was reported in one out of 54 patients [23].

A limitation of this study is the small number of patients. Therefore, the determined margins and the observed difference between proximal and distal tumors would need confirmation in a larger study. As only 3 fiducials in the mesorectum were identified on both MRI exams, no conclusions can be drawn about fiducial displacement with respect to the tumor between fiducials implanted in the tumor and the mesorectum. Furthermore, we evaluated the displacement of the fiducials relative to the GTV only for the first week of radiotherapy. If fiducials would be used for the full duration of a long-course radiotherapy schedule, the displacement of the fiducials relative to the GTV should be investigated for all five weeks. Because of logistical reasons, the time between the MRI exams differed between patients. However, the difference is mainly due to the time range of the first MRI exam relative to the start of radiotherapy. Finally, the estimated margins presented in this paper are based on the position of the fiducials and GTV and do not include other remaining errors involved in the treatment process.

CONCLUSIONS

The results of this study show that despite the observed fiducial displacement relative to the GTV, the use of fiducials as a surrogate for GTV position reduces required margins in the AP and CC direction for a GTV boost using image-guided radiotherapy of rectal cancer. The reduction of required margins may be higher in patients with a proximal compared to a distal tumor. However, this needs to be confirmed in a larger study.

REFERENCES

1. Van Gijn W, Marijnen CAM, Nagtegaal ID, Kranenbarg EMK, Putter H, Wiggers T, *et al.* Preoperative radiotherapy combined with total mesorectal excision for resectable rectal cancer: 12-year follow-up of the multicentre, randomised controlled TME trial. *Lancet Oncol* 2011;12:575–82.

2. Bosset JF, Calais G, Mineur L, Maingon P, Stojanovic-Rundic S, Bensadoun RJ, *et al.* Fluorouracil-based adjuvant chemotherapy after preoperative chemoradiotherapy in rectal cancer: Long-term results of the EORTC 22921 randomised study. *Lancet Oncol* 2014;15:184–90.

3. Sauer R, Liersch T, Merkel S, Fietkau R, Hohenberger W, Hess C, *et al.* Preoperative versus postoperative chemoradiotherapy for locally advanced rectal cancer: Results of the German CAO/ARO/AIO-94 randomized phase III trial after a median follow-up of 11 years. *J Clin Oncol* 2012;30:1926–33.

4. Sebag-Montefiore D, Stephens RJ, Steele R, Monson J, Grieve R, Khanna S, *et al.* Preoperative radiotherapy versus selective postoperative chemoradiotherapy in patients with rectal cancer (MRC CR07 and NCIC-CTG C016): a multicentre, randomised trial. *Lancet* 2009;373:811–20.

5. Maas M, Nelemans PJ, Valentini V, Das P, Rödel C, Kuo LJ, *et al.* Long-term outcome in patients with a pathological complete response after chemoradiation for rectal cancer: A pooled analysis of individual patient data. *Lancet Oncol* 2010;11:835–44.

6. Sanghera P, Wong DWY, McConkey CC, Geh JI, Hartley A. Chemoradiotherapy for Rectal Cancer: An Updated Analysis of Factors Affecting Pathological Response. *Clin Oncol* 2008;20:176–83.

7. Appelt AL, Ploen J, Vogelius IR, Bentzen SM, Jakobsen A. Radiation dose-response model for locally advanced rectal cancer after preoperative chemoradiation therapy. *Int J Radiat Oncol Biol Phys* 2013;85:74–80.

8. Hall MD, Schultheiss TE, Smith DD, Fakih MG, Wong JYC, Chen YJ. Effect of increasing radiation dose on pathologic complete response in rectal cancer patients treated with neoadjuvant chemoradiation therapy. *Acta Oncol (Madr)* 2016;55:1392–9.

9. Ortholan C, Romestaing P, Chapet O, Gerard JP. Correlation in rectal cancer between clinical tumor response after neoadjuvant radiotherapy and sphincter or organ preservation: 10-year results of the Lyon R 96-02 randomized trial. *Int J Radiat Oncol Biol Phys* 2012;83.

10. Burbach JPM, Den Harder AM, Intven M, Van Vulpen M, Verkooijen HM, Reerink O. Impact of radiotherapy boost on pathological complete response in patients with locally advanced rectal cancer: A systematic review and meta-analysis. *Radiother Oncol* 2014;113:1–9.

11. Nijkamp J, de Jong R, Sonke JJ, Remeijer P, van Vliet C, Marijnen C. Target volume shape variation during hypo-fractionated preoperative irradiation of rectal cancer patients. *Radiother Oncol* 2009;92:202–9.

12. Vestermark LW, Jacobsen A, Qvortrup C, Hansen F, Bisgaard C, Baatrup G, *et al.* Long-term results of a phase II trial of high-dose radiotherapy (60 Gy) and UFT/l-leucovorin in patients with non-resectable locally advanced rectal cancer (LARC). *Acta Oncol (Madr)* 2008;47:428–33.

13. Seierstad T, Hole KH, Sælen E, Ree AH, Flatmark K, Malinen E. MR-guided simultaneous integrated boost in preoperative radiotherapy of locally advanced rectal cancer following neoadjuvant chemotherapy. *Radiother Oncol* 2009;93:279–84.

14. Mohiuddin M, Paulus R, Mitchell E, Hanna N, Yuen A, Nichols R, *et al.* Neoadjuvant chemoradiation for distal rectal cancer: 5-year updated results of a randomized phase 2 study of neoadjuvant combined modality chemoradiation for distal rectal cancer. *Int J Radiat Oncol Biol Phys* 2013;86:523–8.

15. Engineer R, Mohandas KM, Shukla PJ, Shrikhande S V., Mahantshetty U, Chopra S, *et al.* Escalated radiation dose alone vs. concurrent chemoradiation for locally advanced and unresectable rectal cancers: Results from phase II randomized study. *Int J Colorectal Dis* 2013;28:959–66.

16. Burbach JM, Verkooijen HM, Intven M, Kleijnen J-PPJEJ, Bosman ME, Raaymakers BW, *et al.* RandomizEd controlled trial for pre-operAtive dose-escaLation BOOST in locally advanced rectal cancer (RECTAL BOOST study): study protocol for a randomized controlled trial. *Trials* 2015;16:58.

17. Tan J, Lim Joon D, Fitt G, Wada M, Lim Joon M, Mercuri A, *et al.* The utility of multimodality imaging with CT and MRI in defining rectal tumour volumes for radiotherapy treatment planning: A pilot study. *J Med Imaging Radiat Oncol* 2010;54:562–8.

18. Oelfke U. Magnetic Resonance Imaging-guided Radiation Therapy: Technological Innovation Provides a New Vision of Radiation Oncology Practice. *Clin Oncol* 2015;27:495–7.

19. Van Der Horst A, Wognum S, Dávila Fajardo R, De Jong R, Van Hooft JE, Fockens P, *et al.* Interfractional position variation of pancreatic tumors quantified using intratumoral fiducial markers and daily cone beam computed tomography. *Int J Radiat Oncol Biol Phys* 2013;87:202–8.

20. Jin P, van der Horst A, de Jong R, van Hooft JE, Kamphuis M, van Wieringen N, *et al.* Marker-based quantification of interfractional tumor position variation and the use of markers for setup verification in radiation therapy for esophageal cancer. *Radiother Oncol* 2015;117:412–8.

21. Beltran C, Herman MG, Davis BJ. Planning Target Margin Calculations for Prostate Radiotherapy Based on Intrafraction and Interfraction Motion Using Four Localization Methods. *Int J Radiat Oncol Biol Phys* 2008;70:289–95.

22. Moningi S, Walker AJ, Malayeri AA, Rosati LM, Gearhart SL, Efron JE, *et al.* Analysis of fiducials implanted during EUS for patients with localized rectal cancer receiving high-dose rate endorectal brachytherapy. *Gastrointest Endosc* 2015;81:765–9.

23. Dhadham GC, Hoffe S, Harris CL, Klapman JB. Endoscopic ultrasound-guided fiducial marker placement for image-guided radiation therapy without fluoroscopy: safety and technical feasibility. *Endosc Int Open* 2016;4:E378-82.

24. Rigter LS, Rijkmans EC, Inderson A, van den Ende RPJ, Kerkhof EM, Ketelaars M, *et al.* EUS-guided fiducial marker placement for radiotherapy in rectal cancer: feasibility of two placement strategies and four fiducial types. *Endosc Int Open* 2019;07:E1357–64.

25. Vorwerk H, Liersch T, Rothe H, Ghadimi M, Christiansen H, Hess CF, *et al.* Gold markers for tumor localization and target volume delineation in radiotherapy for rectal cancer. *Strahlentherapie Und Onkol* 2009;185:127–33.

26. Dutch Trial Registry; registration no. NL4473. Accessed September 16, 2019.

27. van den Ende RPJ, Rigter LS, Kerkhof EM, van Persijn van Meerten EL, Rijkmans EC, Lambregts DMJ, *et al.* MRI visibility of gold fiducial markers for image-guided radiotherapy of rectal cancer. *Radiother Oncol* 2019;132:93–9.

28. Klein S, Staring M, Murphy K, Viergever MA, Pluim JPW. Elastix: A toolbox for intensity-based medical image registration. *IEEE Trans Med Imaging* 2010;29:196–205.

29. Van Herk M. Errors and Margins in Radiotherapy. *Semin Radiat Oncol* 2004;14:52–64.

30. Salerno G, Sinnatamby C, Branagan G, Daniels IR, Heald RJ, Moran BJ. Defining the rectum: surgically, radiologically and anatomically. *Colorectal Dis* 2006;8 Suppl 3:5–9.

31. Van Herk M, Remeijer P, Rasch C, Lebesque J V. The probability of correct target dosage: Dose-population histograms for deriving treatment margins in radiotherapy. *Int J Radiat Oncol Biol Phys* 2000;47:1121–35.

32. Nijkamp J, Swellengrebel M, Hollmann B, De Jong R, Marijnen C, Van Vliet-Vroegindeweij C, *et al.* Repeat CT assessed CTV variation and PTV margins for short- and long-course pre-operative RT of rectal cancer. *Radiother Oncol* 2012;102:399–405.

33. Chong I, Hawkins M, Hansen V, Thomas K, McNair H, O'Neill B, *et al.* Quantification of organ motion during chemoradiotherapy of rectal cancer using cone-beam computed tomography. *Int J Radiat Oncol Biol Phys* 2011;81:431–8.

34. Brierley JD, Dawson LA, Sampson E, Bayley A, Scott S, Moseley JL, *et al.* Rectal motion in patients receiving preoperative radiotherapy for carcinoma of the rectum. *Int J Radiat Oncol Biol Phys* 2011;80:97–102.

35. Gurney-Champion OJ, Lens E, Van Der Horst A, Houweling AC, Klaassen R, Van Hooft JE, *et al.* Visibility and artifacts of gold fiducial markers used for image guided radiation therapy of pancreatic cancer on MRI. *Med Phys* 2015;42:2638–47.

36. Nuyttens JJ, Robertson JM, Yan D, Martinez A. The variability of the clinical target volume for rectal cancer due to internal organ motion during adjuvant treatment. *Int J Radiat Oncol Biol Phys* 2002;53:497–503.

37. Raso R, Scalco E, Fiorino C, Broggi S, Cattaneo GM, Garelli S, *et al.* Assessment and clinical validation of margins for adaptive simultaneous integrated boost in neo-adjuvant radiochemotherapy for rectal cancer. *Phys Medica* 2015;31:167–72.

38. Daly ME, Murphy JD, Mok E, Christman-Skieller C, Koong AC, Chang DT. Rectal and bladder deformation and displacement during preoperative radiotherapy for rectal cancer: Are current margin guidelines adequate for conformal therapy? *Pract Radiat Oncol* 2011;1:85–94.

39. Kleijnen J-PJE, van Asselen B, Burbach JPM, Intven M, Philippens MEP, Reerink O, *et al.* Evolution of motion uncertainty in rectal cancer: implications for adaptive radiotherapy. *Phys Med Biol* 2016;61:1–11.

40. Kleijnen J-PJE, van Asselen B, Intven M, Burbach JPM, Philippens MEP, Lagendijk JJW, *et al.* Does setup on rectal wall improve rectal cancer boost radiotherapy? *Radiat Oncol* 2018;13:61.

41. Kleijnen J-PJE, van Asselen B, Van den Begin R, Intven M, Burbach JPM, Reerink O, *et al.* MRI-based tumor inter-fraction motion statistics for rectal cancer boost radiotherapy. *Acta Oncol (Madr)* 2019;58:232–6.

Chapter 6

Radiotherapy quality assurance for mesorectum treatment planning within the multi-center phase II STAR-TReC trial: Dutch results

Roy P.J. van den Ende
Femke P. Peters
Ernst Harderwijk
Heidi Rütten
Liza Bouwmans
Maaike Berbee
Richard A.M. Canters
Georgiana Stoian
Kim Compagner
Tom Rozema
Mariska de Smet
Martijn P.W. Intven
Rob H.N. Tijssen
Jacqueline Theuws
Paul van Haaren
Baukelien van Triest
Dave Eekhout
Corrie A.M. Marijnen
Uulke A. van der Heide
Ellen M. Kerkhof

ABSTRACT

Background

The STAR-TReC trial is an international multi-center, randomized, phase II study assessing the feasibility of short-course radiotherapy or long-course chemoradiotherapy as an alternative to total mesorectal excision surgery. A new target volume is used for both (chemo)radiotherapy arms which includes only the mesorectum. The treatment planning QA revealed substantial variation in dose to organs at risk (OAR) between centers. Therefore, the aim of this study was to determine the treatment plan variability in terms of dose to OAR and assess the effect of a national study group meeting on the quality and variability of treatment plans for mesorectum-only planning for rectal cancer.

Methods and materials

Eight centers produced 25x2 Gy treatment plans for five cases. The OAR were the bowel cavity, bladder and femoral heads. A study group meeting for the participating centers was organized to discuss the planning results. At the meeting, the values of the treatment plan DVH parameters were distributed among centers so that results could be compared. Subsequently, the centers were invited to perform replanning if they considered this to be necessary.

Results

All treatment plans, both initial planning and replanning, fulfilled the target constraints. Dose to OAR varied considerably for the initial planning, especially for dose levels below 20 Gy, indicating that there was room for trade-offs between the defined OAR. Five centers performed replanning for all cases. One center did not perform replanning at all and two centers performed replanning on two and three cases, respectively. On average, replanning reduced the bowel cavity V20Gy by 12.6%, bowel cavity V10Gy by 22.0%, bladder V35Gy by 14.7% and bladder V10Gy by 10.8%. In 26/30 replanned cases the V10Gy of both the bowel cavity and bladder was lower, indicating an overall lower dose to these OAR instead of a different trade-off. In addition, the bowel cavity V10Gy and V20Gy showed more similarity between centers.

Conclusions

Dose to OAR varied considerably between centers, especially for dose levels below 20 Gy. The study group meeting and the distribution of the initial planning results among centers resulted in lower dose to the defined OAR and reduced variability between centers after replanning.

BACKGROUND

Only 2% of the patients with early stage rectal cancer treated with total mesorectal excision (TME) surgery experience local failure and 12% develop a distant failure [1–3]. However, TME surgery can

result in significant morbidity and mortality [4–6]. For a distal tumor, approximately 40% of patients require a permanent stoma. Complications of TME surgery include anastomotic leaks, urinary and fecal incontinence and sexual dysfunction. Therefore, research for this early stage rectal cancer patient group has focused on alternative strategies, such as limited resections and active surveillance of good responders after chemoradiotherapy [7–10].

The STAR-TReC trial is an international multi-center, randomized, phase II study assessing the feasibility of short-course radiotherapy (SC-RT) or long-course chemoradiotherapy (LC-CRT) with subsequent two-stage response assessment as an alternative to TME surgery. Patients are randomized between; a) TME b) organ preservation utilizing LC-CRT and c) organ preservation utilizing SC-RT (ClinicalTrials.gov Identifier: NCT02945566) [11]. A novel target volume is used which includes only the mesorectum [12].

Before patient accrual, each center had to go through a radiotherapy quality assurance (QA) program led by national radiotherapy trial teams, including a delineation and a treatment planning case. The results for the treatment planning showed substantial variation in dose to organs at risk (OAR), suggesting that different trade-offs were made in each center. Therefore, the Dutch radiotherapy trial team (FP, CM and EK) decided to extend the QA program with four additional planning cases and organized a study group meeting for the Dutch centers in the STAR-TReC trial. The aim of this study was to determine the variability in treatment plans in terms of dose to OAR and to determine the effect of a study group meeting on the quality and variability of treatment plans for mesorectum-only planning for rectal cancer.

METHODS AND MATERIALS

Participating centers and patients

Eight centers participated in this study. We selected 5 cases, including the treatment planning case of the radiotherapy QA program, according to the STAR-TReC inclusion criteria with a small (< 4 cm) T1-3bN0M0 tumor without involvement of the mesorectal fascia or extra-mural vascular invasion.

Target volume and OAR

The STAR-TReC trial utilizes an adapted definition of the clinical target volume (CTV) that only includes the mesorectum from two centimeters below the tumor up to the S2-3 interspace level. This is a smaller CTV compared to the current standard for radiotherapy of rectal cancer and it is specially tailored for early stage disease, with the goal of organ preservation. The development of this new mesorectal CTV definition was described in Peters *et al.* [12]. The planning target volume (PTV) was defined as the CTV plus a margin of 15 mm in the anterior direction and 10 mm in the posterior, lateral and craniocaudal directions. The defined OAR were the bowel cavity, bladder and femoral heads. The bowel cavity was delineated using adapted RTOG guidelines, including abdominal contents and excluding major vasculature, muscles and bones, other pelvic organs (e.g. bladder, prostate, vagina, uterus) and the CTV.

The bowel cavity volume was delineated up to 2 cm above the superior extent of the PTV and inferiorly where small bowel or colon was visible. The whole bladder was delineated including the bladder wall. The femoral heads were delineated to the most inferior extent of the lesser trochanter. The CTV and the OAR of all 5 cases were delineated by one observer (FP) on the planning CT scan.

Treatment planning

We sent the planning CT scans with the corresponding delineations to each participating center, so that each center performed treatment planning based on the same delineations. They were asked to produce LC-CRT treatment plans of 25x2 Gy according to the STAR-TReC study protocol. The participating centers were experienced centers in the treatment of rectal cancer patients. Different planning systems and treatment delivery techniques were used among the centers, as shown in Table 1. Treatment plans were produced by radiotherapy technologists with 0 – 20 years of treatment planning experience. Participating centers used the same criteria regarding delivery efficiency as they would use in clinical practice, the constraints regarding delivery efficiency are shown in Table 1.

The target volume constraints were defined according to the ICRU 83 criteria, focusing on full coverage of the target volume with CTV V95% = 100%, PTV V95% ≥ 99%, PTV V90% = 100%, PTV V105% ≤ 1% and 98% ≤ PTV D50% ≤ 102%. There is lack of data on the association of dose to bowel, bladder and femoral heads and the risk of late complications for dose levels up to 50 Gy. Therefore, the study protocol had no mandated OAR constraints but specified optimization objectives for the OAR adapted from Appelt *et al.* [13]: bowel cavity V20Gy < 190 cc, V30Gy < 130 cc, V45Gy < 100 cc, bladder V35Gy < 22%, V50Gy < 7% and femoral head left and right V25Gy < 14%.

Study group meeting

After all centers had completed the treatment planning on all cases, we organized a study group meeting to discuss the planning results. A radiation-oncologist, a medical physicist and a radiotherapy technologist with rectal cancer expertise of each participating center were invited for this meeting. During the meeting, we visualized the values of the DVH parameters of all treatment plans and the dose distributions of specific cases to discuss the differences.

We distributed the values of the DVH parameters of all treatment plans among all centers so that results could be compared. Subsequently, we invited the participating centers to perform replanning if they considered this to be necessary.

Treatment plan comparison

Each participating center returned for each case the DVH parameters and the dose distribution of the initial planning and replanning in DICOM format. To avoid differences in DVH parameters due to different treatment planning systems, we calculated the values of the DVH parameters using an independent DVH calculation on the submitted dose distributions. We assessed the accuracy of our independent

DVH calculation algorithm using a gamma-analysis between dose volume histograms calculated by the algorithm and dose volume histograms calculated by our treatment planning system for a dataset of eight patients with varying target volumes and organs at risk. We used a tolerance of 0.1 Gy and 1% volume. In addition, we compared the DVH parameters calculated by the algorithm with the DVH parameters submitted by the participating centers, which were calculated by their treatment planning systems.

To determine the effect of the study group meeting on the dose to OAR, we compared the values of the DVH parameters of the replanned cases to the initial plans. In addition to the DVH parameters of the OAR optimization objectives, we selected additional DVH parameters for a more detailed evaluation of the differences in low dose levels. The additional parameters included the V5Gy, V10Gy, and V15Gy for the bowel cavity as well as the bladder. No constraints or objectives were imposed on the additional DVH parameters.

To investigate the total volume of the V10Gy and V25Gy, we added a volume that included the patient contour of the planning CT scan. In addition, we added a volume that included the patient contour of the planning CT scan but excluded the PTV, bowel cavity, bladder and femoral heads to investigate if the dose to other normal tissue was increased while sparing the defined OAR. This volume is called "Non-defined OAR".

For the cases for which no replanning was performed, we reported the values of the DVH parameters of the initial planning of those centers as the result of the replanning.

Statistical analysis

We used SPSS Statistics 23 (IBM Corp. Released 2015. IBM SPSS Statistics for Windows, Version 23.0. Armonk, NY: IBM Corp.) for statistical analysis. A paired samples T-test was used to test for differences in the values of the DVH parameters between the initial planning and replanning. The significance threshold was set at $p < 0.002$, adjusted for multiple testing using the Bonferroni correction.

RESULTS

DVH calculation algorithm

The gamma passing rate of the dose volume histograms calculated by the independent DVH calculation algorithm was 99.99 ± 0.03%. On average, the relative difference between the DVH parameters calculated by the independent DVH calculation algorithm and the DVH parameters submitted by the centers was -0.5 ± 0.2%.

Initial planning

All plans satisfied the target volume constraints. Large differences in dose to OAR were observed, especially in the dose levels below 20 Gy, as shown in Figure 1. The differences were discussed at the study group meeting, where it was concluded that the variation was mostly due to differences in local practice and lack of evidence for OAR constraints. As there is insufficient evidence to support prioritizing the sparing of OAR at these low dose levels, the prioritization was left to the center's preference.

Replanning

Five centers performed replanning for all cases. Center 2 performed replanning on two cases, center 3 did not perform replanning at all and center 5 performed replanning on three cases. Center 1 used Pinnacle AutoPlanning for the replanning. All other centers performed replanning using the same treatment technique as the initial planning, as described in Table 1. All 30 replanned cases fulfilled the target volume constraints. For all cases, replanning resulted on average in a lower dose to the defined OAR (Table 2). The bowel cavity V5Gy, V10Gy, V15Gy, V20Gy, V30Gy and V45Gy and the bladder V10Gy, V15Gy and V35Gy were significantly lower in the replanning for all cases ($p < 0.001$). On average, replanning reduced the bowel cavity V20Gy by 12.6%, the bowel cavity V10Gy by 22.0%, the bladder V35Gy by 14.7% and the bladder V10Gy by 10.8%.

Figure 2 shows for each case the bowel cavity V10Gy and bladder V10Gy for the initial planning and the replanning of all cases. All vectors (except three; center 1 for case 1, center 8 for case 4 and center 4 for case 5) show that both the bowel cavity V10Gy and the bladder V10Gy was lower after replanning. This reduction was at the expense of the V10Gy in the non-defined OAR, which on average is higher after replanning for all cases, except case 3. The bowel cavity V15Gy and bladder V15Gy were lower in 25/30 replanned cases and the bowel cavity V30Gy and bladder V35Gy were lower in 23/30 replanned cases. The bowel cavity V10Gy and V20Gy showed more homogeneity between centers after replanning, as depicted in Figure 1.
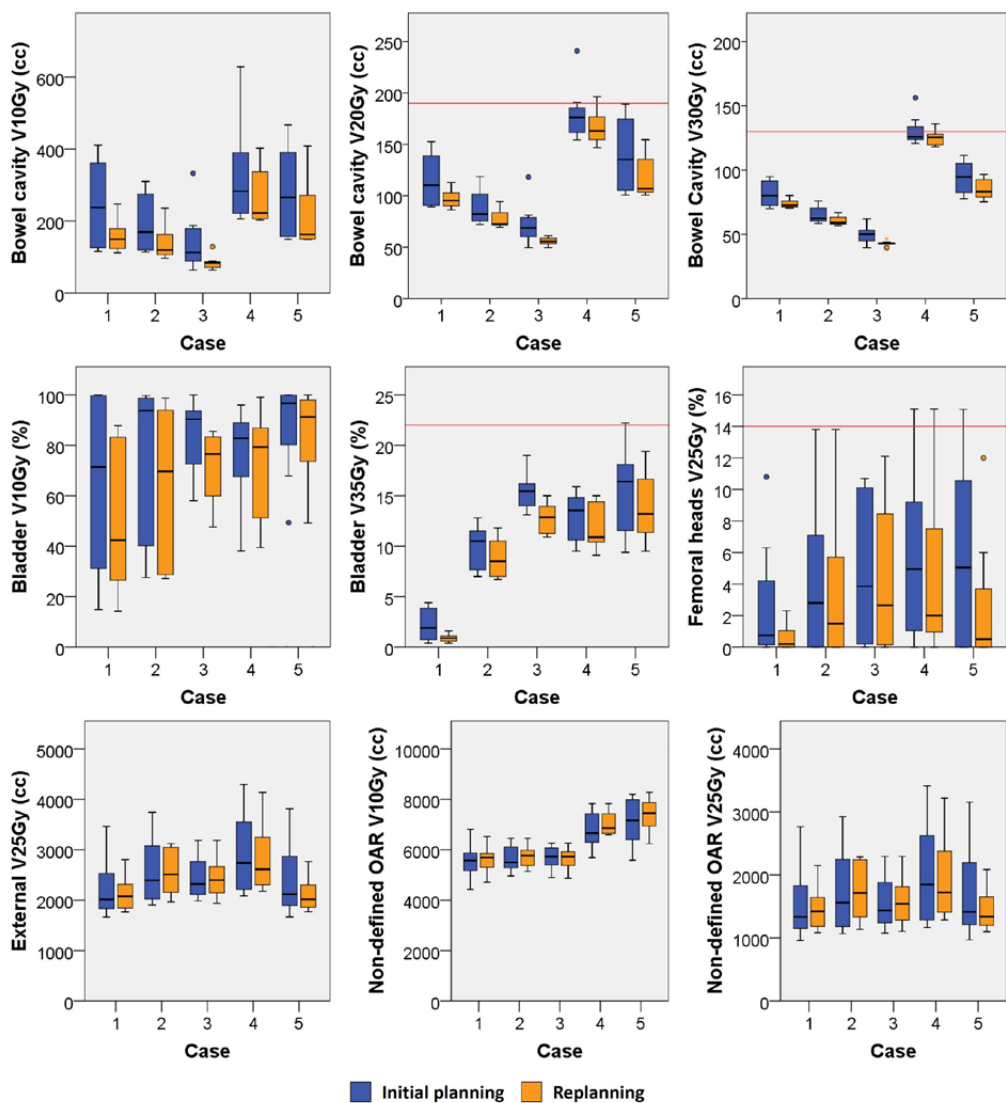
Figure 1. Planning results for the initial planning (blue) and replanning (orange) for each case. The red lines indicate the OAR optimization objective.

Table 1. Participating centers with corresponding planning parameters

Institute	TPS	Technique	Energy (MV)	Number of arcs/fields	Number of arcs/fields	Delivery efficiency	RTT experience (years)	Automated treatment planning
1	Pinnacle	AT	10	Dual full arc	2	Maximum delivery time 60 seconds	11	Yes, Pinnacle AutoPlanning[#]
2	Pinnacle	AT	6	One or two full arcs*	1 or 2*	Maximum delivery time 60-90 seconds per arc	15	No
3	Pinnacle	AT	10	Two dual partial arcs	4	Maximum delivery time 160 seconds	0-20	Yes, Pinnacle Auto-Planning
4	Pinnacle	AT	10	Two dual partial arcs	4	Maximum delivery time 100 seconds	5	No
5	Eclipse	AT	10	Two full arcs	2	Maximum 3 x prescribed dose in cGy for MU	10	No
6	Eclipse	AT	10	Two full arcs	2	Maximum 3 x prescribed dose in cGy for MU	20	Yes, RapidPlan
7	Monaco	AT	10	Two partial arcs	2	Maximum 4 x prescribed dose in cGy for MU	11	No
8	RayStation	IMRT	10	Five fields	5	Maximum 15 segments. Minimal segment area 35 cm^2, minimal 4 MU/segment	12	No

TPS = treatment planning system, AT = Arc Therapy, IMRT = Intensity Modulated Radiotherapy, MU = monitor units, RTT = Radiotherapy Technologist
*Depending on patient anatomy, [#] Only for the replanning

Table 2. Absolute difference between replanning and initial planning. A positive difference means a higher value for the replanning. All values are presented as mean (range).

|	Case 1	Case 2	Case 3	Case 4	Case 5
CTV V95 (%)	0.0 (0.0 - 0.0)	0.0 (0.0 - 0.0)	0.0 (0.0 - 0.0)	0.0 (0.0 - 0.0)	0.0 (0.0 - 0.0)
PTV V95 (%)	-0.3 (-0.9 - 0.2)	-0.1 (-0.3 - 0.0)	-0.2 (-0.7 - 0.0)	-0.1 (-0.3 - 0.0)	-0.1 (-0.3 - 0.0)
PTV V90 (%)	0.0 (0.0 - 0.0)	0.0 (-0.1 - 0.0)	0.0 (-0.1 - 0.0)	0.0 (0.0 - 0.0)	0.0 (-0.1 - 0.0)
Bowel cavity volume (cc)	992.0	754.4	721.3	1306.3	1273.2
Bowel cavity V5Gy (cc)	-120.9 (-371.9 - 0)	-78.9 (-317.1 - 22.9)	-106.2 (-299.6 - 0)	-107.8 (-426.1 - 44.5)	-141.5 (-529.2 - 0)
Bowel cavity V10Gy (cc)	-89 (-237.1 - 23.6)	-55.2 (-176.8 - 0)	-60.2 (-203.6 - 0)	-60.9 (-226.1 - 0)	-64.8 (-198.8 - 0)
Bowel cavity V15Gy (cc)	-32.4 (-68.5 - 5.2)	-23.5 (-92.5 - 0)	-28.4 (-106.1 - 0)	-22.7 (-66.4 - 0)	-33.9 (-105.5 - 0)
Bowel cavity V20Gy (cc)	-18.2 (-46.7 - 6.7)	-11.3 (-45.8 - 0)	-17.2 (-61.4 - 0)	-13.8 (-44.6 - 0)	-21.6 (-58.4 - 0.1)
Bowel cavity V30Gy (cc)	-7.9 (-22 - 6.8)	-4.6 (-18.3 - 0)	-6.9 (-19.6 - 0)	-5.4 (-20.3 - 0.8)	-9 (-25 - 0)
Bowel cavity V45Gy (cc)	-3.2 (-9.1 - 4.5)	-1.6 (-6.5 - 0)	-2.2 (-6.8 - 0)	-1.4 (-8.6 - 1.8)	-3.6 (-8.7 - 0)
Bladder volume (cc)	197.2	344.7	232.3	277.3	89.2
Bladder V5Gy (%)	-6.5 (-21.4 - 0)	-6.4 (-28.7 - 0)	-4.2 (-16.1 - 0)	-5.6 (-34.6 - 0)	0.1 (-1.1 - 2.2)
Bladder V10Gy (%)	-14.2 (-58.4 - 0)	-10.3 (-48.8 - 0)	-12.3 (-45.5 - 0)	-4.9 (-32.6 - 20)	-3.5 (-17 - 0.2)
Bladder V15Gy (%)	-14.8 (-59.2 - 0)	-7.5 (-33.5 - 1.1)	-13.1 (-33.6 - 0)	-6.1 (-22.2 - 1)	-3.4 (-13.8 - 0.1)
Bladder V35Gy (%)	-1.3 (-3.4 - 0.2)	-1.1 (-5 - 0.5)	-2.7 (-7.4 - 0)	-1 (-3.7 - 0)	-1.6 (-10.7 - 3.3)
Bladder V50Gy (%)	0 (0 - 0)	0.1 (-0.2 - 0.7)	0.3 (-1 - 1.8)	0.3 (-0.6 - 1.5)	0.1 (-1.3 - 0.8)
External volume (cc)	27105.6	21073.2	18660.9	23076.3	28088.9
External_V10Gy_(cc)	-61.9 (-645.1 - 645.2)	-13.3 (-362.9 - 409.3)	-142.5 (-335.9 - 0)	182.2 (-184.5 - 975.8)	201.3 (-313.9 - 636.5)
External_V25Gy_(cc)	-106.5 (-662.1 - 123.4)	-16.1 (-688.9 - 264.9)	-4.8 (-410.4 - 202.4)	-92.1 (-922 - 502)	-292.7 (-1624.6 - 163.7)
Non-defined OAR volume (cc)	24881.5	18795.5	16504.1	20541.4	26060.8
Non-defined OAR max dose (Gy)	0.2 (-0.4 - 1.1)	0.1 (-0.3 - 0.7)	-0.1 (-0.9 - 0.5)	0.0 (-0.6 - 1.3)	-0.1 (-1.6 - 1.2)
Non-defined OAR V10Gy (cc)	56.9 (-284.5 - 654.6)	81.2 (-264.2 - 461.5)	-46.5 (-258.6 - 57.3)	247.9 (-8.4 - 931.6)	271.2 (-208 - 845.8)
Non-defined OAR V25Gy (cc)	-77.2 (-615.5 - 173.8)	3.8 (-650.3 - 340.3)	23.1 (-390 - 254)	-71.8 (-888.6 - 512.8)	-273.9 (-1617.3 - 198.4)
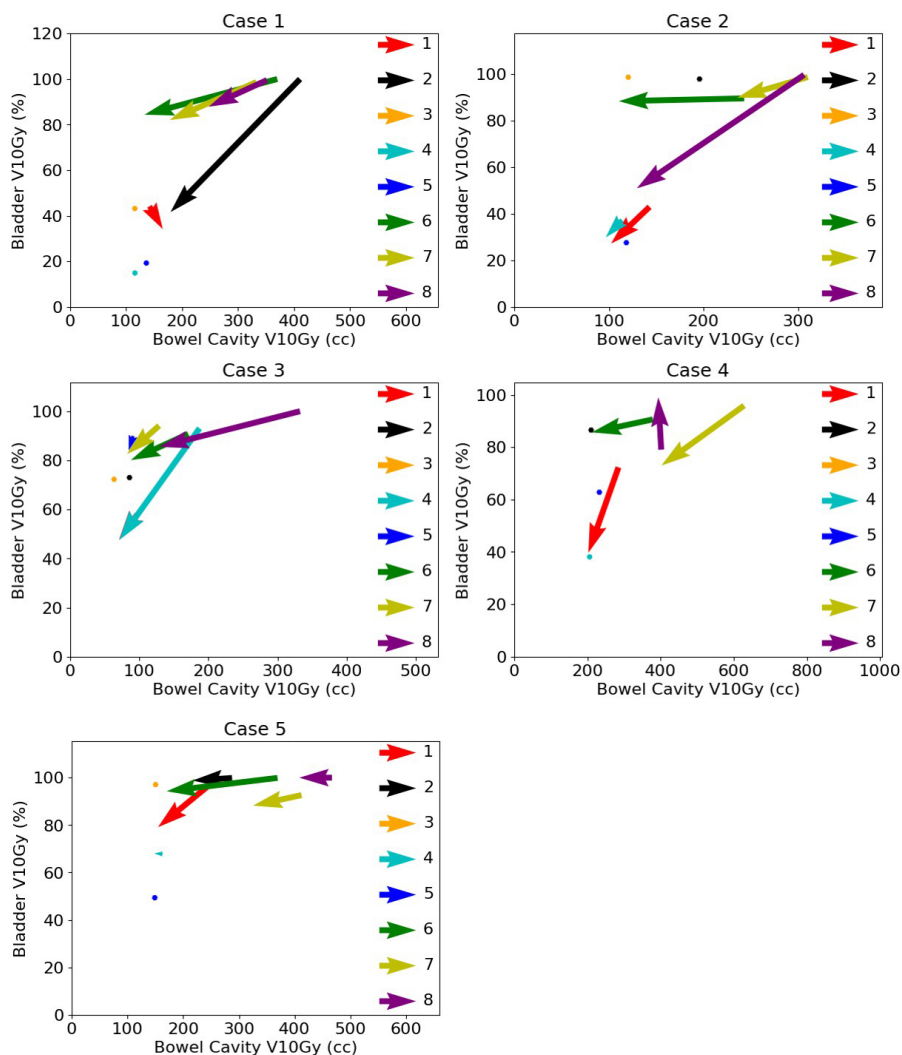
Figure 2. Vector representation for the initial planning and replanning for the bowel cavity V10Gy and the bladder V10Gy for all cases. A vector originates in the values of the DVH parameters of the initial planning and ends in the values of the replanning. The numbers 1 through 8 in the figure legends represent the centers. A plotted point indicates that the corresponding center did not perform replanning.

An example of the initial planning and replanning for one case is shown separately for all centers in Figure 3. For the same case, the difference in dose distribution between the initial planning and replanning is shown for center 4 and 6 in Figure 4. For center 4, the replanning reduced the dose deposition laterally, as shown on the axial images, while the V10Gy isodose is expanded into the pubic bone, as shown on the sagittal images. For center 6, replanning reduced the bowel cavity V10Gy and bladder V10Gy while the dose deposition is increased laterally.
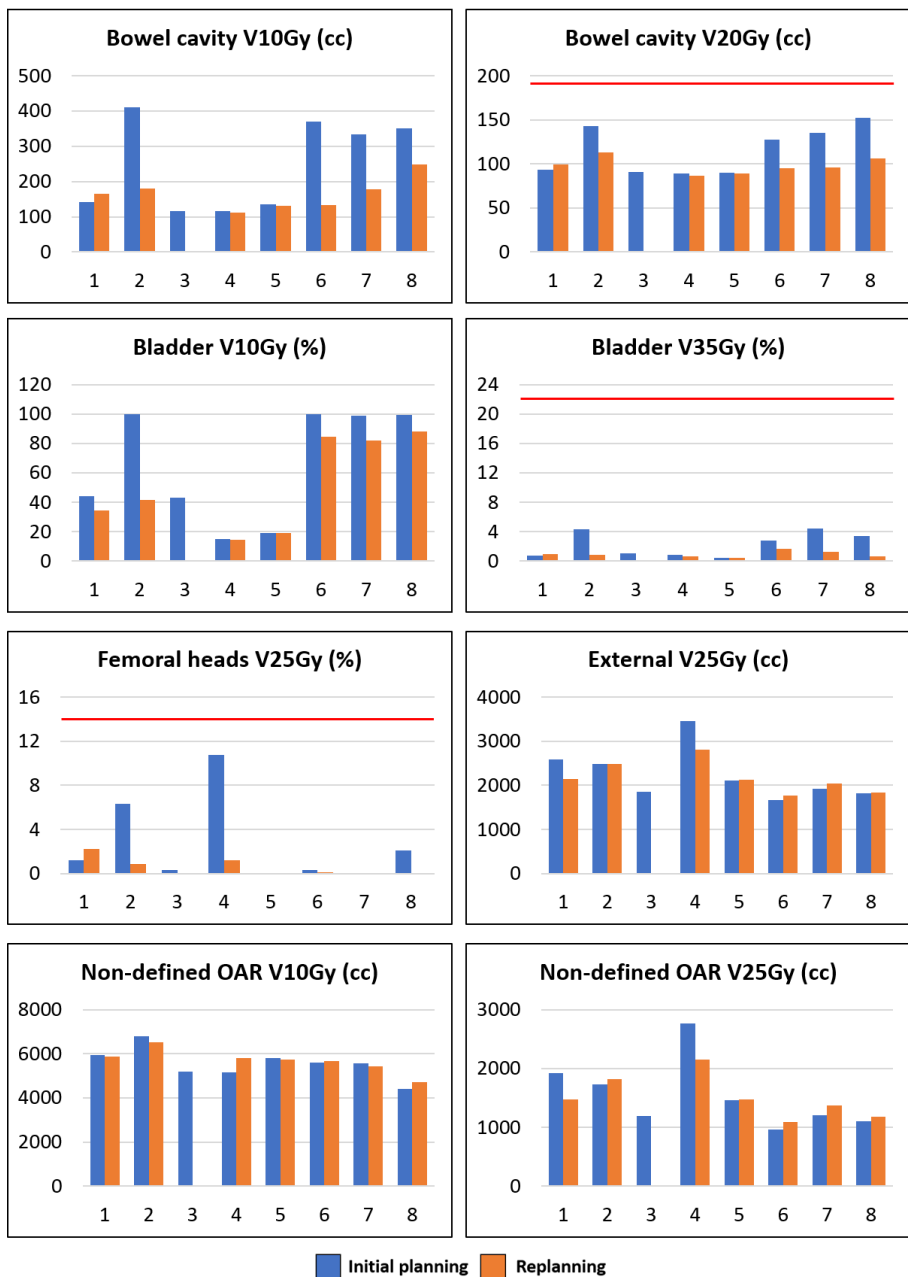
Figure 3. Planning results for the initial planning (blue) and replanning (orange) of case 1. The red lines indicate the OAR optimization objective.
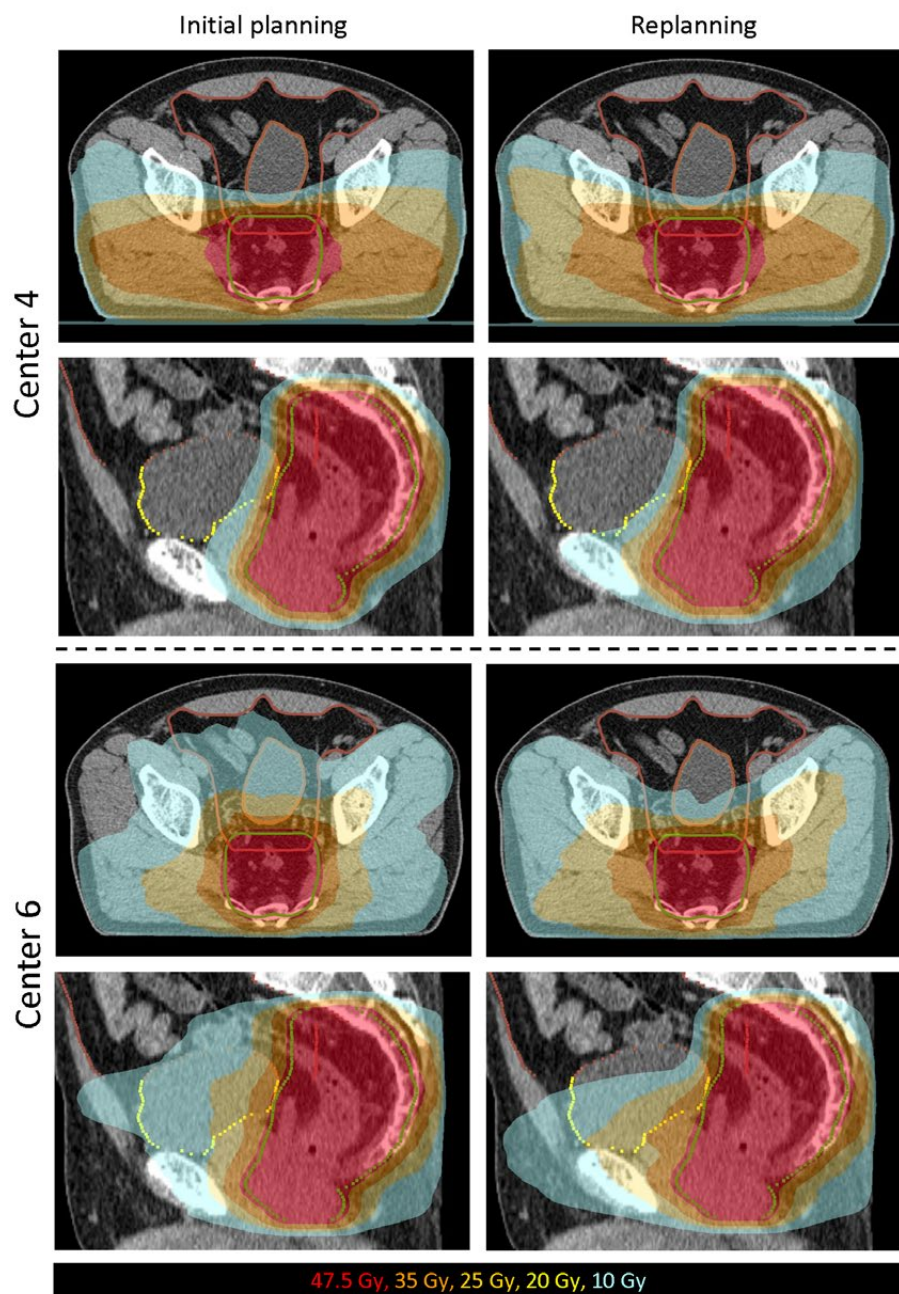
Figure 4. Dose distributions for the initial planning and replanning of case 1 for center 4 and center 6.

DISCUSSION

The aim of this study was to determine the variability in treatment plans in terms of dose to OAR and to determine the effect of a study group meeting on the quality and variability of treatment plans using a novel target volume for rectal cancer. We have shown that a large variability in dose to OAR occurred while the plans of all centers fulfilled the target constraints. After the study group meeting, replanning resulted in improved treatment plan quality due to lower doses to the defined OAR and smaller differences in dose to OAR between centers.

Optimization objectives for the dose to OAR in the STAR-TReC trial were provided only for dose levels above 20 Gy, which left room for variation in the distribution of the lower dose levels. As a result, radiation-oncologists made different choices regarding the distribution of these lower dose levels or these levels were not taken into account at all during the optimization.

It is not expected that the observed variations in dose to OAR have an impact on the trial hypothesis. However, the observed variations in low dose to the OAR may have an impact on toxicity. Therefore, optimization objectives might be added for the lower dose levels in the upcoming phase III study of the STAR-TReC trial in order to try to reach more consistent and possibly better treatment plans among centers and to prevent unnecessary large volumes of low dose to the OAR. To determine adequate dose volume constraints and prioritization for the OAR in the future, data will be gathered for correlation between dose to OAR and risk of complications within the STAR-TReC trial.

Evaluating a plan on dose volume constraints or objectives alone may not be a good indicator of plan quality, as some patients may have a favorable anatomy and the achieved parameters may not be the lowest possible organ dose volumes. On the other hand, in unfavorable patients, dose may not fulfill planning criteria or objectives while it is still the most optimal plan for that patient. In our study, this can be observed in Figure 1, where for case 4 the bowel cavity V20Gy approaches the objective for all centers. However, for the other patients the bowel cavity V20Gy is substantially lower than the objective. This shows that careful selection of a benchmark case for trial QA is important and raises the question whether one case is sufficient. Multiple cases enable the evaluation of different patient anatomies with corresponding degrees of possible OAR sparing.

To determine whether the dose to the defined OAR can be lowered further is difficult, even for experienced treatment planners. Plan quality is therefore dependent on planning time, experience of the treatment planner and the degree to which the treatment plan is being critically reviewed. The treatment plans in this study were made and reviewed extensively by expert planners and radiation-oncologists. These treatment plans may therefore not reflect treatment plans produced in clinical practice, as less detailed feedback or discussion of treatment plans is possible and plans may therefore be suboptimal. Automated treatment planning techniques, for example knowledge-based treatment planning, protocol-

based automatic iterative optimization or multicriteria optimization, could be used to determine whether a treatment plan can be further optimized [14].

Other studies describing trial QA report on the identification of delineation and/or dosimetric violations and that participating centers receive individual feedback regarding those violations [15–17]. Subsequently, the violations were resolved and treatment plan quality was improved. In our study, however, all target constraints and OAR objectives were fulfilled and the question was how to handle the variations in dose distribution for the OAR for which no guidelines were yet available. The study group meeting has enabled us to discuss the planning results and the considerations regarding dose distribution to defined and non-defined OAR face-to-face, by doing so learning from each other. Furthermore, sharing the planning results of the initial planning of all centers enabled centers to compare their results and helped them decide whether further optimization of the treatment plan was possible and desired for each case. Consequently, replanning led to improved plan quality as lower doses to defined OAR were observed while maintaining target volume constraints. Importantly, although no consensus guidelines were made on how to handle the variations in dose to OAR, the variation of dose levels below 20 Gy was reduced after replanning.

CONCLUSIONS

In the STAR-TReC trial, no constraints or objectives are defined for the OAR for lower dose levels since there is no clinical evidence to base constraints on. As a result, in this treatment planning study the dose to OAR varied considerably between centers, especially for dose levels below 20 Gy. After the study group meeting, treatment plan quality was improved as replanning resulted in lower dose to the defined OAR and reduced variability between centers. Therefore, for a novel target volume, we recommend to include more than one QA case and to share all planning results with participating centers, possibly at a study group meeting, to allow them to compare results and decide whether further optimization is possible.

REFERENCES

1. Bentrem DJ, Okabe S, Wong WD, Guillem JG, Weiser MR, Temple LK, et al. T1 adenocarcinoma of the rectum: transanal excision or radical surgery? *Ann Surg* 2005;242:472–7; discussion 477-9.

2. Van Gijn W, Marijnen CAM, Nagtegaal ID, Kranenbarg EMK, Putter H, Wiggers T, et al. Preoperative radiotherapy combined with total mesorectal excision for resectable rectal cancer: 12-year follow-up of the multicentre, randomised controlled TME trial. *Lancet Oncol* 2011;12:575–82.

3. Endreseth BH, Myrvold HE, Romundstad P, Hestvik UE, Bjerkeset T, Wibe A, et al. Transanal excision vs. major surgery for T1 rectal cancer. *Dis Colon Rectum* 2005;48:1380–8.

4. Lange MM, Maas CP, Marijnen CAM, Wiggers T, Rutten HJ, Klein Kranenbarg E, et al. Urinary dysfunction after rectal cancer treatment is mainly caused by surgery. *Br J Surg* 2008;95:1020–8.

5. Hendren SK, O'Connor BI, Liu M, Asano T, Cohen Z, Swallow CJ, et al. Prevalence of male and female sexual dysfunction is high following surgery for rectal cancer. *Ann Surg* 2005;242:212–23.

6. Peeters KCMJ, van de Velde CJH, Leer JWH, Martijn H, Junggeburt JMC, Kranenbarg EK, et al. Late side effects of short-course preoperative radiotherapy combined with total mesorectal excision for rectal cancer: Increased bowel dysfunction in irradiated patients - A Dutch Colorectal Cancer Group Study. *J Clin Oncol* 2005;23:6199–206.

7. Habr-Gama A, Gama-Rodrigues J, São Julião GP, Proscurshim I, Sabbagh C, Lynn PB, et al. Local recurrence after complete clinical response and watch and wait in rectal cancer after neoadjuvant chemoradiation: Impact of salvage therapy on local disease control. *Int J Radiat Oncol Biol Phys* 2014;88:822–8.

8. Glynne-Jones R, Hughes R. Critical appraisal of the "wait and see" approach in rectal cancer for clinical complete responders after chemoradiation. *Br J Surg* 2012;99:897–909.

9. Marijnen CAM. Organ preservation in rectal cancer: Have all questions been answered? *Lancet Oncol* 2015;16:e13–22.

10. Stijns RCH, Tromp MSR, Hugen N, de Wilt JHW. Advances in organ preserving strategies in rectal cancer patients. *Eur J Surg Oncol* 2018;44:209–19.

11. Rombouts AJM, Al-Najami I, Abbott NL, Appelt A, Baatrup G, Bach S, et al. Can we Save the rectum by watchful waiting or TransAnal microsurgery following (chemo) Radiotherapy versus Total mesorectal excision for early REctal Cancer (STAR-TREC study)?: protocol for a multicentre, randomised feasibility study. *BMJ Open* 2017;7:e019474.

12. Peters FP, Teo MTW, Appelt AL, Bach S, Baatrup G, de Wilt JHW, et al. Mesorectal radiotherapy for early stage rectal cancer: a novel target volume. *Clin Transl Radiat Oncol* 2020.

13. Appelt AL, Kerkhof EM, Nyvang L, Harderwijk EC, Abbott NL, Teo M, et al. Robust dose planning objectives for mesorectal radiotherapy of early stage rectal cancer – A multicentre dose planning study. *Tech Innov Patient Support Radiat Oncol* 2019;11:14–21.

14. Hussein M, Heijmen BJM, Verellen D, Nisbet A. Automation in intensity modulated radiotherapy treatment planning—a review of recent innovations. *Br J Radiol* 2018;91:20180270.

15. Joye I, Lambrecht M, Jegou D, Hortobágyi E, Scalliet P, Haustermans K. Does a central review platform improve the quality of radiotherapy for rectal cancer? Results of a national quality assurance project. *Radiother Oncol* 2014;111:400–5.

16. Habraken SJM, Sharfo AWM, Buijsen J, Verbakel WFAR, Haasbeek CJA, Öllers MC, et al. The TRENDY multi-center randomized trial on hepatocellular carcinoma – Trial QA including automated treatment planning and benchmark-case results. *Radiother Oncol* 2017;125:507–13.

17. Fenton PA, Hurkmans C, Gulyban A, Van Der Leer J, Matzinger O, Poortmans P, et al. Quality assurance of the EORTC 22043-30041 trial in post-operative radiotherapy in prostate cancer: Results of the Dummy Run procedure. *Radiother Oncol* 2013;107:346–51.

Chapter 7

General discussion

GENERAL DISCUSSION

The studies described in this thesis focus on the reduction of treatment-related uncertainties in image-guided high-dose-rate endorectal brachytherapy (HDREBT) and external beam radiotherapy (EBRT) for rectal cancer patients. Currently, the standard of care for rectal cancer patients consists of a surgical resection. Depending on disease stage, neoadjuvant (chemo)radiotherapy is given in order to reduce local recurrence rates. After standard chemoradiotherapy, 10-20% of patients develop a complete response. In these patients, a 'watch and wait' approach in which surgery is omitted seems safe. Dose response analyses suggest that escalating the dose to the gross tumor volume (GTV) leads to higher response rates. Various dose escalation techniques have been described in literature, including contact therapy, HDREBT and EBRT. For a dose escalation technique to be successful, it needs to lead to higher complete response rates in combination with limited acute and late toxicity. Therefore, the dose to healthy tissue should be as small as possible. In addition, if a boost dose can be delivered with higher accuracy, the dose to the GTV could be higher with similar dose to healthy tissue. Although the optimal treatment technique for dose escalation has not yet been determined, the work described in this thesis can be used to enhance the accuracy and decrease treatment related uncertainties related to a boost dose.

For HDREBT, most studies focus on oncological outcome and treatment-related toxicity. Although literature describes an adaptive approach using a treatment planning CT at each fraction, the dosimetric benefit of such an approach had not been investigated. Furthermore, the preferred image modality for target volume definition and treatment planning is MRI due to its superior soft tissue contrast. To realize a HDREBT workflow including MRI, a MRI-compatible fiducial marker was required that is visible on MRI imaging. Therefore, we have evaluated the visibility of four types of gold fiducial markers on MRI. Finally, the individual channels of the applicator are not visible on currently used anatomical MRI sequences. To be able to perform treatment planning on MRI, a method was needed to visualize the individual channels of the applicator on MRI. We have proposed a MRI sequence utilizing ultrashort echo times for visualization of the individual channels within the applicator.

With increased interest for organ preservation, improvements aimed at EBRT boost delivery are timely. Although some studies have evaluated the displacement of the GTV with respect to bony anatomy, most of them were based on CT and/or CBCT with inherent limited soft tissue contrast for GTV visualization. As a result, a wide range of PTV margins of 7-30 mm is described in literature. In addition, fiducial markers could be used as a surrogate for the GTV in order to perform setup correction based on fiducials instead of bony anatomy. However, data on the stability of fiducials relative to the GTV was lacking. Therefore, we have derived GTV displacement relative to bony anatomy using fiducials and provided data on the uncertainty of the GTV-fiducial spatial relationship. Together with the evaluation of the MRI visibility of four fiducial types, this thesis provides a basis for further research and subsequent clinical implementation of an EBRT GTV boost strategy using fiducial markers.

To facilitate organ preservation and avoid TME surgery in early stage rectal cancer patients, (chemo)-radiotherapy has to be given to control the tumor. The risk of pelvic lymph node involvement or distal mesorectal nodal involvement is low in this group of patients. Therefore, the typically large target volume may not be needed in this group of patients, and restricting the target volume to the peritumoral region of the primary tumor and mesorectum seems reasonable. In the STAR-TReC trial, a novel target volume is used which includes only the mesorectum [1]. Mesorectum only planning is intended for early stage rectal cancer with the aim of reducing the clinical target volume (CTV) and thereby reducing dose to the healthy tissue while maintaining local control. By showing the impact of a national study group meeting on the variability and quality of treatment plans for a novel target volume, we provide a basis for the realization of a more homogeneous treatment, potentially improving the quality of clinical trials on treatment outcome and toxicity.

High-dose-rate endorectal brachytherapy
Repeat imaging
The HDREBT procedure as described in literature uses a planning CT scan at each fraction and endoluminal clips to indicate the tumor position. Position verification prior to irradiation is performed with an X-ray, using the endoluminal clips and radiopaque markers inserted in the channels of the applicator. Although literature describes a transition from using a single-planning CT for all fractions to using a planning CT at each fraction, the difference in terms of target coverage and dose to organs at risk had not been evaluated [2–5]. In **Chapter 2**, we have shown that use of a single planning CT for all fractions can result in insufficient target coverage. The most important cause of limited target coverage was the presence of air and/or faeces between the applicator and the target volume. Air and/or faeces cannot be accurately assessed on the X-ray images used for position verification. Therefore, CT imaging at each fraction should be the minimal standard in HDREBT for rectal cancer.

Fiducial markers
Because of the limited soft tissue contrast of CT imaging, ideally a MRI should be used to define the target volume. However, the endoluminal clips create large artifacts on MRI, which limits target volume visibility. Therefore, an alternative marker allowing target volume visibility on MRI was needed. In addition, the alternative marker should be visible on MRI to determine the spatial relationship between the target volume and the fiducial marker. To determine a suitable alternative fiducial marker, we have evaluated the MRI visibility of four different MR-compatible gold fiducials in **Chapter 3**. The results of the study show that the Visicoil 0.75 and the Gold Anchor were the best visible fiducials on MRI and that a corresponding (CB)CT scan is required to provide an estimation of the fiducial localization on MRI. Although those fiducials were the best visible in the study, it can be argued whether the use of fiducials is clinically feasible, given the limited retention and visibility rate observed in **Chapter 3**. For future use of fiducial markers in the rectum, it is expected that the fiducial retention rate and visibility will improve for several reasons. First, the retention rate of fiducials in this study was better for fiducials that were inserted in the mesorectum, compared to fiducials inserted in the tumor, as shown by Rigter *et al.* [6].

Second, the use of a T1 3D sequence with prolonged echo time will increase the size of the artifacts that the fiducials create on MRI, which may enhance the fiducial visibility. We therefore recommend to insert fiducials in the mesorectum, in proximity of the tumor and to include a T1 3D sequence with prolonged echo time of at least 5 ms. Third, in brachytherapy, the planning CT and MRI are acquired with applicator in situ. This leads to a more similar anatomy between the CT and MRI, thereby increasing the accuracy of initial localization of fiducial markers on MRI.

Although the visibility of fiducials is expected to increase with a T1 3D sequence with prolonged echo time, manual fiducial identification on MRI remains a challenging and time-consuming procedure. In addition, fiducial marker appearance on MRI depends on sequence parameters and fiducial orientation with respect to the magnetic field [7]. Automatic fiducial detection could aid in the identification of fiducials and possibly eliminate the need for a corresponding (CB)CT. Multiple studies report on automatic fiducial detection on MRI in the prostate, with fiducial detection rates of 94-96% [8–10]. Since none report a marker detection rate of 100%, implementation of such a method would have to be in a semi-automatic workflow with an initial automatic fiducial detection on MRI with possible manual corrections. In addition, the proposed automatic fiducial detection methods would first have to be validated for the application in rectal cancer patients.

Given the increased interest in organ preservation strategies for rectal cancer patients, MRI will be increasingly used to determine whether a complete response has been reached. Among other sequences, a DWI sequence is used to assess tumor response. Since this sequence is sensitive to distortions in the magnetic field, fiducial markers that are placed (too) close to the tumor may hamper response assessment. As an alternative, a liquid marker that forms a semisolid gel after injection may be used [11,12]. These liquid markers are visible on MRI as a signal void due to the absence of water protons. This is different compared to gold fiducial markers, which cause signal voids due to absence of water protons *and* due to their alteration of the static magnetic field. Currently, only one study has evaluated the use of these liquid markers in rectal cancer [13], with positional stability as primary outcome. Preliminary results have been published in an abstract, in which the authors report that after 5 weeks of chemoradiotherapy, 96% of 74 liquid markers were still in situ and available for analysis. Marker pair distances, as a measure for marker stability, showed stable or negative slope of fits during chemoradiation. It was concluded that the liquid marker was feasible to act as a tumor location surrogate. However, stability with respect to the GTV was not reported in the abstract.

HDREBT MRI-only workflow
As the individual channels within the applicator are not visible on the currently used MRI sequences, delineation of the target volume and organs at risk, applicator reconstruction and treatment planning are still performed on CT. Image registration of the CT and MRI with applicator in situ is performed to aid in the target volume definition. A further improvement in HDREBT treatment planning would be a MRI-only workflow, in which the delineation of the target volume and organs at risk, applicator reconstruction

and treatment planning are all performed on MRI. This would eliminate any image registration errors between MRI and CT due to possible changes in applicator position. In addition, it would save time and increase patient comfort as the patient does not have to be transferred between CT and MRI. A MRI-only workflow can be realized if the fiducials can be identified on MRI without corresponding (CB)CT and if the individual channels within the applicator can be visualized. In the previous paragraph, improvements have been suggested to facilitate MRI fiducial identification without corresponding (CB)CT, including a T1 3D sequence with prolonged echo time and the use of automatic fiducial detection methods. In **Chapter 4**, we have proposed a MRI sequence utilizing an ultrashort echo time to visualize the applicator and the individual channels within it. We have shown that the applicator and the individual channels can be visualized, both in a phantom and in patients. By performing a rigid registration with an anatomical sequence, geometric fidelity was within acceptable range. Therefore, applicator reconstruction, delineation of target volume and organs at risk, and treatment planning can all be performed on MRI. However, before clinical implementation of such a workflow, the geometrical fidelity of all MRI sequences that are going to be used for treatment planning should be verified.

A next step in the HDREBT workflow would be to irradiate the patient while the patient is lying on the MRI scan table. This would eliminate the transfer of the patient between the MRI table and the treatment table, thereby reducing the chance of changes in applicator position between the planning MRI and the time of irradiation. In addition, fiducial markers would no longer be needed as both the target volume and the applicator can be visualized using MRI. Irradiation of the patient while the patient is lying in the MR bore would however require a MRI-compatible afterloader. The feasibility of such a procedure has been demonstrated using a prototype MRI-compatible afterloader [14]. However, the MRI-compatible afterloader is not clinically available yet.

Applicator design

The current most used applicator for HDREBT consists of eight catheters circumferentially placed near the edge of the applicator which allows selective use of channels for a more conformal treatment compared to one central channel. In addition, a shielding lead or tungsten insert can be placed in the central channel of the applicator to spare the contralateral healthy rectal wall. While EBRT techniques have evolved to become increasingly conformal using intensity modulated and dynamic arc radiotherapy, the applicator is limited in shielding options and is therefore far from conformal, which leaves substantial room for improvement. Several studies have proposed alternative applicator designs, aimed at increasing the conformality of the dose distribution. Webster *et al.* report on simulated dosimetric properties of several alternative applicator designs, mostly incorporating additional shielding [15]. In another paper, the same group describes dynamic modulated brachytherapy for rectal cancer [16]. The authors propose a design containing a long cylindrical tungsten alloy shield with a small window in which a ^{192}Ir can be encapsulated, resulting in a highly directional beam profile. The shield should then be rotated and translated within the applicator by a robot arm in order to irradiate a target volume. So far, the dosimetric properties of these alternative applicator designs have only been produced using in silico simulations and

are not currently clinically used, possibly because of the complexity. Belezzo *et al.* describe an alternative applicator design that can be used for contact radiotherapy using a ^{192}Ir source [17]. It contains multiple channels which allows planning optimization and tailoring of the dose distribution to the target volume. In addition, lateral shielding is incorporated, resulting in a uniform circular treatment surface with a 22 mm diameter. This applicator could result in more conformal treatments of small tumors. However, the applicator is not clinically used yet.

Future use of HDREBT

Altough literature reports promising results on the use of HDREBT as a neoadjuvant treatment, no randomized trials have yet been performed comparing neoadjuvant HDREBT to neoadjuvant EBRT [18–20]. The currently ongoing CORRECT trial will show us whether the promising results presented so far can be reproduced in a randomized trial. In the CORRECT trial, patients with resectable rectal cancer are randomized between neoadjuvant chemoradiotherapy or neoadjuvant 4x 6.5 Gy HDREBT [21]. The primary endpoint is pathological complete response rate. However, time to surgery is not reported.

Given the increased interest in organ preservation, HDREBT may play a role in delivering a boost dose to the GTV to enhance the complete response rates. There has only been one randomized trial on the use of a HDREBT boost, in which patients were randomized between chemoradiation with or without a HDREBT boost of 2x 5 Gy, prescribed at 10 mm from the applicator surface [22]. No difference in pathological complete response was reported. However, the major response rate (defined as Mandard tumor regression grade 1 and 2) was significantly higher in the HDREBT group (44% vs 28%) for patients with a T3 tumor with no increase in toxicity. No effect on the major response rate was observed in T4 tumors [23]. An explanation could be that larger tumors that extend widely into the mesorectum are inaccessible to brachytherapy and/or the dose prescription at 10 mm from the applicator surface did not allow full coverage of the tumor.

The potential use of HDREBT in an organ preservation setting will depend on the ability to limit long-term toxicity, since the rectum will not be removed. In the HERBERT trial, acute grade 2 and 3 proctitis was observed in 68.4% and 13.2% of patients respectively, while late grade 2 and grade ≥3 proctitis occurred in 48% and 40% of patients. The most severe toxicity was observed 12-18 months after treatment [24]. An analysis on the predictive factors for toxicity in this group of patients showed that brachytherapy CTV size and high doses at the mucosa of the CTV was correlated to endoscopic toxicity at the tumor site [25]. Due to the steep dose gradient and the aim to enclose the CTV with the 100% isodose, the dose at the mucosa can reach 400%. The dose to the contralateral wall was not correlated to endoscopic toxicity, which suggests that the dose was reduced sufficiently using the balloon that was placed between the applicator and the contralateral healthy rectal wall. The HERBERT trial was a dose escalation study, which partly explains the observed toxicity. In addition, no shielding was used and most patients in this study were treated with a single planning CT for all fractions, leading to uncertainties in the delivered dose to the CTV and surrounding healthy tissue. The added value of a HDREBT boost

after EBRT in elderly, frail patients will be further assessed in the HERBERT 2 trial. In this phase III trial, patients will be randomized between 13 x 3 Gy EBRT with or without a HDREBT boost of three weekly fractions of 7 Gy, at least 10 weeks after the end of EBRT. The primary endpoint is clinical complete response at 6 months after brachytherapy.

So far, the trials that have reported on the clinical outcome after HDREBT for rectal cancer vary in dose prescription methods, fractionation schemes, study endpoints and toxicity reporting [26,27]. In order to determine the added value of HDREBT in different clinical scenarios and to be able to compare different trials, consensus on the mentioned variables is urgently needed.

External beam radiotherapy

Higher doses to the tumor are suggested to result in higher complete response rates, which is interesting in the light of increased interest for organ preservation [28]. Due to the limited soft tissue contrast of imaging used for setup correction, such as CBCT, setup correction based on the GTV itself is not possible. Since fiducial markers are visible on (CB)CT imaging, they could be used as a surrogate for the GTV for setup correction in a GTV boost setting. Such an approach requires that the fiducials are representative of the GTV, and therefore stable with respect to the GTV. In addition, the spatial relationship between the fiducials and the GTV has to be determined, preferably on MRI, which means that they have to be visible on MRI. The visibility of fiducials on MRI as evaluated in **Chapter 3** has already been discussed in the previous paragraph.

Stability of fiducials relative to the GTV and inter- and intrafraction displacement

In **Chapter 5**, we have determined the stability of fiducials relative to the GTV and the inter- and intrafraction displacement of fiducials relative to bony anatomy. Subsequently, we have derived required margins in different setup correction scenarios in a GTV boost setting. The use of setup correction based on fiducials results in a substantial margin reduction compared to setup correction based on bony anatomy. The findings of this study were based on imaging that was mostly acquired in the first week of radiotherapy. While that makes it applicable for a boost during or directly after a short course radiotherapy schedule, it may not apply for a boost applied during or after a long-course chemoradiotherapy schedule. In a recent study it has been shown that tumor regression during LC-CRT occurred mostly during the first half of treatment [29]. The displacement of the fiducials relative to the GTV and the inter- and intrafraction displacement relative to bony anatomy may be different at the end of a LC-CRT schedule, after most GTV regression has taken place.

Dose escalation to the GTV can be achieved by using a simultaneous integrated boost (SIB) or a sequential boost. Boosting using a SIB with setup correction based on fiducials would require daily plan re-optimization to take into account the GTV position of that day. Alternatively, the boost dose could be given after the elective dose of each fraction. This would require setup correction twice for each fraction: once based on bony anatomy for the elective irradiation of the CTV and once for the GTV boost.

A sequential GTV boost could be given after all fractions of the elective CTV irradiation have been given. Given the GTV shrinkage during the treatment, a sequential boost would be applied on a smaller residual GTV, thereby minimizing the additional dose to the organs at risk. In addition, it would allow for selection of patients that could possibly benefit from a GTV boost.

A sub analysis in **Chapter 5** suggests a difference in GTV displacement between tumors located in the lower rectum and tumors located in the mid- and upper rectum. As a result, the potential margin reduction by performing setup correction based on fiducials is smaller for low-lying tumors, compared to higher tumors. This raises the question whether the use of fiducials is justified for lower tumors. However, the difference in inter- and intra-fraction displacement between tumors located in the lower rectum and tumors located in the mid- or upper rectum should be verified in a larger patient cohort. Finally, the introduction and clinical implementation of MRI systems with integrated linear accelerators will obviate the need for fiducial markers. With such systems, the GTV can be imaged (real time) with the superior soft tissue contrast of MRI. However, MRI systems with integrated linear accelerators are not widely available yet. Until such systems are widely available, a GTV boost should be given using setup correction based on fiducials in order to reduce margins, and therefore dose to healthy tissue.

STAR-TReC planning study

In the STAR-TReC trial, a novel target volume is used which only includes the mesorectum. There is lack of data on the association of dose to bowel, bladder and femoral heads and the risk of late complications for dose levels up to 50 Gy. In addition, there is no data regarding OAR constraints using this novel target volume. Therefore, there were no mandated OAR constraints but optimization objectives were specified for the dose to the OAR for dose levels of 20-45 Gy. As a result, there was substantial variation in the dose to organs at risk between centers after treatment planning for 5 cases, while all cases fulfilled target volume constraints. Furthermore, we demonstrated that a study group meeting with subsequent replanning led to better treatment plans, with decreased dose to the organs at risk and decreased variability between centers.

These observations show the added value of performing QA for a clinical study. The question remains whether the study group meeting itself led to higher quality treatment plans, or that only the distribution of initial planning results among centers could potentially lead to the same result. By comparing initial planning results, centers were able to determine whether a treatment plan could be further optimized. This illustrates the inherent limitations of manual optimization of the treatment plan. Although the experience of the planner certainly influences the plan quality, determining whether a plan can be further optimized can be even difficult for experienced planners. Automated treatment planning techniques, such as knowledge-based treatment planning, protocol-based automatic iterative optimization or multicriteria optimization can aid in the decision whether a plan can be further optimized [30]. The added value of automated treatment planning is also observed in the differences in dose to organs at risk between cases. While in some cases the objectives might be easily reached, in other cases the objectives

might be hard to satisfy, depending on patient anatomy. This shows the limitation of imposing fixed constraints/objectives for treatment planning. Nonetheless, automated treatment planning can aid in the decision whether a plan can be further optimized, but will still lead to a broad range of acceptable plans if there is a lack of evidence on dose volume constraints. Therefore, automated treatment planning is not expected to lead to a substantial decrease in variability. The lack of evidence also contributes to the observed variability in dose to the organs at risk. In order to develop dose volume constraints and optimization objectives for an organ preservation setting, toxicity and clinical outcome data has to be carefully collected.

The treatment plan quality achieved in **Chapter 6** may be higher compared to treatment plans produced in clinical practice, as in clinical practice less extensive discussion and time is spent on the treatment plan. In order to monitor treatment plan quality in a clinical trial, it can be beneficial to require regular QA of treatment plans. As an educational process, a similar QA as presented in **Chapter 6** can be performed, identifying differences between centers and followed by a discussion how to handle them.

REFERENCES

1. Peters FP, Teo MTW, Appelt AL, Bach S, Baatrup G, de Wilt JHW, *et al.* Mesorectal radiotherapy for early stage rectal cancer: a novel target volume. *Clin Transl Radiat Oncol* 2020.

2. Vuong T, Devic S, Moftah B, Evans M, Podgorsak EB. High-dose-rate endorectal brachytherapy in the treatment of locally advanced rectal carcinoma: Technical aspects. *Brachytherapy* 2005;4:230–5.

3. Devic S, Vuong T, Moftah B, Evans M, Podgorsak EB, Poon E, *et al.* Image-guided high dose rate endorectal brachytherapy. *Med Phys* 2007;34:4451–8.

4. Vuong T, Devic S. High-dose-rate pre-operative endorectal brachytherapy for patients with rectal cancer. *J Contemp Brachytherapy* 2015;7:181–6.

5. Nout RA, Bekerat H, Devic S, Vuong T. Is Daily CT-Based Adaptive Endorectal Brachytherapy of Benefit Compared to Using a Single Treatment Plan for Preoperative Treatment of Locally Advanced Rectal Cancer? *Brachytherapy* 2016;15:S83–4.

6. Rigter LS, Rijkmans EC, Inderson A, van den Ende RPJ, Kerkhof EM, Ketelaars M, *et al.* EUS-guided fiducial marker placement for radiotherapy in rectal cancer: feasibility of two placement strategies and four fiducial types. *Endosc Int Open* 2019;07:E1357–64.

7. Gurney-Champion OJ, Lens E, Van Der Horst A, Houweling AC, Klaassen R, Van Hooft JE, *et al.* Visibility and artifacts of gold fiducial markers used for image guided radiation therapy of pancreatic cancer on MRI. *Med Phys* 2015;42:2638–47.

8. Maspero M, Van Den Berg CAT, Zijlstra F, Sikkes GG, De Boer HCJ, Meijer GJ, *et al.* Evaluation of an automatic MR-based gold fiducial marker localisation method for MR-only prostate radiotherapy. *Phys Med Biol* 2017;62:7981–8002.

9. Ghose S, Mitra J, Rivest-Hénault D, Fazlollahi A, Stanwell P, Pichler P, *et al.* MRI-alone radiation therapy planning for prostate cancer: Automatic fiducial marker detection. *Med Phys* 2016;43:2218–28.

10. Dinis Fernandes C, Dinh C V., Steggerda MJ, ter Beek LC, Smolic M, van Buuren LD, *et al.* Prostate fiducial marker detection with the use of multi-parametric magnetic resonance imaging. *Phys Imaging Radiat Oncol* 2017;1:14–20.

11. De Roover R, Crijns W, Poels K, Peeters R, Draulans C, Haustermans K, *et al.* Characterization of a novel liquid fiducial marker for multimodal image guidance in stereotactic body radiotherapy of prostate cancer. *Med Phys* 2018;45:2205–17.

12. Riisgaard de Blanck S, Scherman Rydhög J, Richter Larsen K, Frost Clementsen P, Josipovic M, Camille Aznar M, *et al.* Safety and long-term visibility of a novel liquid fiducial marker for use in image guided radiotherapy of non-small cell lung cancer. *Clin Transl Radiat Oncol* 2018;13:24–8.

13. ClinicalTrials.gov; registration no. NCT03265418. Accessed December 2, 2019

14. Beld E, Seevinck PR, Schuurman J, Viergever MA, Lagendijk JJW, Moerland MA. Development and Testing of a Magnetic Resonance (MR) Conditional Afterloader for Source Tracking in Magnetic Resonance Imaging-Guided High-Dose-Rate (HDR) Brachytherapy. *Int J Radiat Oncol* 2018;102:960–8.

15. Gwynne S, Mukherjee S, Webster R, Spezi E, Staffurth J, Coles B, *et al.* Imaging for target volume delineation in rectal cancer radiotherapy - a systematic review. *Clin Oncol* 2012;24:52–63.

16. Webster MJ, Devic S, Vuong T, Yup Han D, Park JC, Scanderbeg D, *et al.* Dynamic modulated brachytherapy (DMBT) for rectal cancer. *Med Phys* 2013;40:.

17. Bellezzo M, Fonseca GP, Verrijssen AS, Voncken R, Van den Bosch MR, Yoriyaz H, *et al.* A novel rectal applicator for contact radiotherapy with HDR 192 Ir sources. *Brachytherapy* 2018;17:1037–44.

18. Vuong T, Richard C, Niazi T, Liberman S, Letellier F, Morin N, *et al.* High dose rate endorectal brachytherapy for patients with curable rectal cancer. *Semin Colon Rectal Surg* 2010;21:115–9.

19. Garfinkle R, Lachance S, Vuong T, Mikhail A, Pelsser V, Gologan A, *et al.* Is the pathologic response of T3 rectal cancer to high-dose-rate endorectal brachytherapy comparable to external beam radiotherapy? *Dis Colon Rectum* 2019;62:294–301.

20. Hesselager C, Vuong T, Påhlman L, Richard C, Liberman S, Letellier F, *et al.* Short-term outcome after neoadjuvant high-dose-rate endorectal brachytherapy or short-course external beam radiotherapy in resectable rectal cancer. *Color Dis* 2013;15:662–6.

21. ClinicalTrials.gov; registration no. NCT02017704. Accessed December 1, 2019

22. Jakobsen A, Ploen J, Vuong T, Appelt A, Lindebjerg J, Rafaelsen SR. Dose-effect relationship in chemoradiotherapy for locally advanced rectal cancer: A randomized trial comparing two radiation doses. *Int J Radiat Oncol Biol Phys* 2012;84:949–54.

23. Appelt AL, Vogelius IR, Pløen J, Rafaelsen SR, Lindebjerg J, Havelund BM, *et al.* Long-term results of a randomized trial in locally advanced rectal cancer: No benefit from adding a brachytherapy boost. *Int J Radiat Oncol Biol Phys* 2014;90:110–8.

24. Rijkmans EC, van Triest B, Nout RA, Kerkhof EM, Buijsen J, Rozema T, *et al.* Evaluation of clinical and endoscopic toxicity after external beam radiotherapy and endorectal brachytherapy in elderly patients with rectal cancer treated in the HERBERT study. *Radiother Oncol* 2018;126:417–23.

25. Rijkmans EC, Marijnen CAM, van Triest B, Ketelaars M, Cats A, Inderson A, *et al.* Predictive factors for response and toxicity after brachytherapy for rectal cancer; results from the HERBERT study. *Radiother Oncol* 2019;133:176–82.

26. Buckley H, Wilson C, Ajithkumar T. High-Dose-Rate Brachytherapy in the Management of Operable Rectal Cancer: A Systematic Review. *Int J Radiat Oncol Biol Phys* 2017;99:111–27.

27. Verrijssen AS, Opbroek T, Bellezzo M, Fonseca GP, Verhaegen F, Gerard JP, *et al.* A systematic review comparing radiation toxicity after various endorectal techniques. *Brachytherapy* 2018;18:71-86.e5.

28. Appelt AL, Ploen J, Vogelius IR, Bentzen SM, Jakobsen A. Radiation dose-response model for locally advanced rectal cancer after preoperative chemoradiation therapy. *Int J Radiat Oncol Biol Phys* 2013;85:74–80.

29. Van den Begin R, Kleijnen J-P, Engels B, Philippens M, van Asselen B, Raaymakers B, *et al.* Tumor volume regression during preoperative chemoradiotherapy for rectal cancer: a prospective observational study with weekly MRI. *Acta Oncol (Madr)* 2017;0:1–5.

30. Hussein M, Heijmen BJM, Verellen D, Nisbet A. Automation in intensity modulated radiotherapy treatment planning—a review of recent innovations. *Br J Radiol* 2018;91:20180270.

Chapter 8

Summary

SUMMARY

Improvements in the treatment of rectal cancer patients have led to increased survival. As a result, long-term outcome has become an increasingly important factor. In addition, the introduction of population screening will lead to earlier detection of the disease with probably improved survival as a result. Both preoperative (chemo)radiotherapy and TME surgery are associated with toxicity and complications. As a result, research for rectal cancer treatment has focused on the reduction of radiation dose to (healthy) tissue and less extensive surgery or omission of surgery in selected patients. The work described in this thesis can be used to decrease the uncertainties related to image-guided external beam radiotherapy and high-dose-rate endorectal brachytherapy (HDREBT) of rectal cancer.

HDREBT can be used to deliver high doses to the tumor while sparing surrounding organs at risk due to a steep dose gradient. Most publications on the use of HDREBT focus on oncological outcomes, but do not report on the technical aspects of the procedure. **Chapter 2, 3 and 4** of this thesis focus on improvements of the HDREBT treatment planning procedure in terms of required imaging and the transition to MRI-only treatment planning.

Chapter 2 compares the use of a single planning CT for all subsequent fractions and the use of a planning CT at each fraction (repeat CT) in terms of target volume coverage and dose to organs risk. In 8/22 fractions, a CTV D98 of at least 85% could not be achieved due to incorrect applicator balloon setup or remaining air and/or feces between the CTV and the applicator and an intervention would be necessary. Therefore, repeat CT imaging should be the minimal standard practice to check for a correct applicator setup. In addition, replanning based on repeat CT imaging resulted in more conformal treatment plans and is therefore recommended.

To be able to use MRI for treatment planning for HDREBT, MRI-compatible fiducial markers were needed as an alternative to endoluminal clips. In **Chapter 3**, the MRI visibility of four different gold fiducial markers is evaluated. Four observers identified fiducial locations on two MRI exams per patient in two scenarios: without and with corresponding (CB)CT available to provide an estimate of fiducial location on MRI. Fiducial identification was poor without a corresponding (CB)CT. With corresponding (CB)CT, the Visicoil 0.75 and the Gold Anchor were the most consistently identified fiducials and were best visible on T1 3D GRE images.

To enable MRI-only planning for HDREBT, the applicator and the individual channels need to be visible on MRI. However, the applicator creates a signal void on currently used anatomical MRI images. **Chapter 4** shows that an ultrashort-echo time (UTE) MRI sequence can be used to visualize the applicator and the individual channels for HDREBT treatment planning. On the UTE images, there was sufficient contrast to discern the individual channels within the applicator, both in a phantom and in patients. After rigid registration to a 3D T_1-weighted sequence, the residual 95th percentile of the geometric distortion

inside a 550 mm diameter sphere was 0.8 mm (LR), 1.0 mm (AP) and 0.9 mm (CC) mm, which is within acceptable range.

Complete response rates might be increased by delivering a higher dose to the tumor, which is beneficial in organ preservation strategies. Although extensive research has been performed on the inter- and intrafraction displacement of the CTV relative to the bony anatomy, limited research was performed on the inter- and intrafraction displacement of the GTV relative to bony anatomy to determine margins for an external beam radiotherapy GTV boost. As a result, a wide range of clinically used PTV margins of 7-30 mm is described in literature. Setup correction could potentially be performed based on the fiducials instead of bony anatomy. To do so, the fiducials need to be representative of the GTV and the fiducials should be visible on MRI to accurately determine the fiducial-GTV spatial relationship. In **Chapter 5**, the stability of fiducials relative to the GTV and the inter- and intrafraction displacement of fiducials relative to bony anatomy is determined. A fiducial displacement of around 3 mm (LR and AP) and 4 mm (CC) relative to the GTV was observed. In addition, large interfraction displacements of the GTV and the fiducials relative to bony anatomy were found. Therefore, despite the observed fiducial displacement relative to the GTV, the use of fiducials as a surrogate for GTV position reduces the required margins from 20 mm to 8 mm in the AP direction and from 20 mm to 13 mm in the CC direction. A sub analysis shows that this reduction in margin may be larger in patients with tumors located in the mid- and upper rectum compared to the lower rectum.

In order to facilitate organ preservation in early stage rectal cancer patients, (chemo)radiotherapy has to be given in order to control the tumor. It is doubtful whether the typically used large target volume is required for these patients and reduction of the target volume to only include the peritumoral region of the primary tumor and mesorectum seems reasonable. The significant volume reduction might lead to decreased treatment-related toxicity without compromising oncological outcome. This is currently being investigated in the STAR-TReC trial, which assesses the feasibility of short-course radiotherapy or long-course chemoradiotherapy with subsequent two-stage response assessment as an alternative to TME surgery. The radiotherapy target volume only includes the mesorectum. **Chapter 6** determines the treatment plan variability in terms of dose to OAR and assesses the effect of a national study group meeting on the quality and variability of treatment plans for mesorectum-only treatment planning. Eight centers produced treatment plans for five cases and a study group meeting for the participating centers was organized to discuss the planning results. At the meeting, the values of the treatment plan DVH parameters were distributed among centers so that results could be compared. Subsequently, the centers were invited to perform replanning if they considered this to be necessary. Dose to OAR varied considerably between centers, especially for dose levels below 20 Gy. The study group meeting and the distribution of the initial planning results among centers resulted in lower dose to the defined OAR and reduced variability between centers after replanning.

Appendices

SAMENVATTING

Verbeteringen van de behandeling voor patiënten met endeldarmkanker hebben geresulteerd in een verbeterde overleving. Daarnaast vindt door het bevolkingsonderzoek vroegere opsporing van endeldarmkanker plaats en hierdoor zal de overleving waarschijnlijk verder verbeteren. Door de (verwachte) verbeterde overleving worden de lange-termijn effecten van de behandeling steeds belangrijker. Preoperatieve (chemo)radiotherapie en totale mesorectale excisie (TME) chirurgie zijn geassocieerd met toxiciteit en chirurgische complicaties. Onderzoek naar de behandeling van endeldarmkanker is daarom gericht op het verlagen van de radiotherapie dosis op gezond weefsel en minder uitgebreide chirurgie of het achterwege laten van chirurgie in geselecteerde patiënten. Een radiotherapie behandeling van de endeldarm kan zowel via uitwendige als inwendige bestraling gegeven worden. Beide bestralingstechnieken hebben bepaalde behandelonderzekerheden, zoals het bepalen van de tumor op de beschikbare beeldvorming en de positionering van de patiënt op de bestralingstafel. Door deze behandelonzekerheden wordt er een veiligheidsmarge rondom het te bestralen doelvolume gebruikt om ervoor te zorgen dat de tumor daadwerkelijk de voorgeschreven dosis ontvangt. Het nadeel hiervan is dat naastgelegen gezond weefsel meer stralingsdosis ontvangt en een extra dosis op de tumor daardoor beperkt mogelijk is. De resultaten die zijn beschreven in dit proefschrift kunnen worden gebruikt om de behandelonzekerheden voor zowel uitwendige als inwendige bestraling van patiënten met endeldarmkanker te verlagen.

Inwendige bestraling met behulp van een applicator, ook wel brachytherapie, kan vanwege zijn steile dosis gradiënt gebruikt worden om een hoge stralingsdosis te geven aan de tumor terwijl omliggende organen gespaard worden. De meeste publicaties over het gebruik van brachytherapie bij endeldarmkanker richten zich op oncologische uitkomsten, maar rapporteren niet over de technische aspecten van de procedure. **Hoofdstuk 2, 3 en 4** richten zich op verbeteringen van de brachytherapie planningsprocedure bij endeldarmkanker voor wat betreft benodigde beeldvorming en de stap naar een planningsprocedure die uitsluitend gebaseerd is op MRI beeldvorming.

Hoofdstuk 2 vergelijkt het gebruik van een enkel CT onderzoek voor het plannen van alle bestralingsfracties met het gebruik van een CT onderzoek bij elke bestralingsfractie (herhaal CT), waarbij er gekeken wordt naar de dekking van het doelvolume en de dosis op de gezonde weefsels. Bij 8 van de 22 fracties kon een dekking van het doelvolume van minstens 85% niet behaald worden door een incorrecte plaatsing van de applicator ballon of resterende lucht en/of ontlasting tussen het doelvolume en de applicator. Bij deze 8 fracties zou een interventie nodig zijn om de positionering van de applicator te corrigeren. Het gebruik van een planning CT scan bij elke fractie zou daarom de minimale standaard moeten zijn om de positionering van de applicator te controleren. Ten slotte resulteerde herplannen op basis van de herhaal CT in meer conforme bestralingsplannen.

Om MRI te kunnen gebruiken bij het maken van het bestralingsplan zijn MRI-compatibele markers nodig als alternatief voor de huidige chirurgische clips om de tumor te markeren. In **Hoofdstuk 3** wordt de MRI zichtbaarheid van vier verschillende goudmarkers beoordeeld. Vier waarnemers hebben markerposities aangeduid op twee MRI onderzoeken per patiënt in twee scenario's: met en zonder de beschikbaarheid van een bijbehorend CT onderzoek om een schatting te geven van de markerposities op MRI. Het aanduiden van goudmarkers zonder bijbehorend CT onderzoek resulteerde in veel verschillen tussen de waarnemers. Met het gebruik van het bijbehorende CT onderzoek waren de Visicoil 0.75 en Gold Anchor de meest consistent aangeduide markers en deze waren het best zichtbaar op de T1 gewogen 3D GRE MRI beelden.

Om voor brachytherapie een bestralingsplan te kunnen maken dat uitsluitend gebaseerd is op MRI beeldvorming moeten de applicator en de individuele kanalen in de applicator zichtbaar zijn op de MRI beeldvorming. Echter, op de huidige gebruikte anatomische MRI beeldvorming is de applicator afgebeeld als een zwarte vlek door gebrek aan signaal. **Hoofdstuk 4** toont aan dat een MRI onderzoek met een ultrakorte echotijd gebruikt kan worden om de applicator en de individuele kanalen af te beelden. Dit MRI beeld geeft voldoende onderscheid tussen de individuele kanalen, zowel op beelden van een fantoom als beelden van patiënten met een applicator in de endeldarm. Na de fusie met een T1 gewogen 3D MRI onderzoek is de resterende geometrische verstoring binnen een bol met een diameter van 550 mm voor alle richtingen ongeveer 1 mm, wat een klinisch acceptabele afwijking is.

Het percentage patiënten waarbij de tumor volledig verdwenen is na (chemo)radiotherapie zou verhoogd kunnen worden door een hogere stralingsdosis te geven aan de tumor. Dit kan interessant zijn voor orgaansparende behandelingen, waarbij bij geselecteerde patiënten chirurgie achterwege wordt gelaten of minder uitgebreide chirurgie toegepast wordt. Er is uitgebreid onderzoek verricht naar de beweging van de gehele endeldarm ten opzichte van de botten, maar er is slechts beperkt onderzoek verricht naar de beweging van de tumor ten opzichte van de botten om veiligheidsmarges te bepalen voor een extra dosis op de tumor met uitwendige radiotherapie. Om die reden worden er in de literatuur uiteenlopende veiligheidsmarges van 7-30 mm beschreven. Positieverificatie voor een extra dosis op de tumor zou gebaseerd kunnen worden op geïmplanteerde markers in plaats van op botten. Om dit te realiseren moeten de markers representatief zijn voor de positie van de tumor en zichtbaar zijn op MRI om de markerposities ten opzichte van de tumor nauwkeurig te kunnen bepalen. In **Hoofdstuk 5** wordt de stabiliteit van de markers ten opzichte van de tumor en de beweging van de markers ten opzichte van de botten bepaald. Tussen bestralingsfracties werd een markerverplaatsing van 3 tot 4 mm ten opzichte van de tumor gevonden. Daarnaast werden er grote verplaatsingen van de tumor en de markers gevonden ten opzichte van de botten. Om die reden leidt het gebruik van markers als surrogaat voor de tumor tot een afname van de veiligheidsmarge van 20 mm naar 13 mm tot zelfs 8 mm, afhankelijk van de richting in de patiënt. Een subanalyse suggereert dat deze veiligheidsmarge meer afneemt bij patiënten met een tumor in het centrale en hooggelegen deel van de endeldarm vergeleken met patiënten met een tumor in het laaggelegen deel van de endeldarm.

Om patiënten met een vroeg stadium endeldarmkanker orgaansparend te kunnen behandelen, zullen deze patiënten (chemo)radiotherapie moeten krijgen om de tumor te bestrijden. Het is waarschijnlijk niet nodig om bij deze patiënten de reguliere grote doelvolumes te gebruiken, dus het beperken van het doelvolume tot enkel het gebied van de primaire tumor en het mesorectum lijkt redelijk. De flinke afname van het doelvolume zou kunnen leiden tot verminderde toxiciteit zonder verslechterde oncologische uitkomst. Dit wordt op dit moment onderzocht in de STAR-TReC studie, waarin de haalbaarheid van korte serie radiotherapie of lange serie chemoradiotherapie gevolgd door twee respons evaluaties als alternatief op TME chirurgie geëvalueerd wordt. In **Hoofdstuk 6** wordt voor bestralingsplannen met een doelvolume dat alleen bestaat uit het mesorectum de variabiliteit van dosis op de gezonde weefsels bepaald. Daarnaast wordt het effect van een nationale bijeenkomst op de kwaliteit en de variabiliteit van bestralingsplannen geëvalueerd. Acht radiotherapie afdelingen hebben ieder voor vijf patiënten bestralingsplannen gemaakt en vervolgens werd er een bijeenkomst georganiseerd voor de deelnemende radiotherapie afdelingen om de planningsresultaten te bespreken. Bij de bijeenkomst werden de dosisgegevens van de bestralingsplannen met elkaar gedeeld, zodat deze met elkaar konden worden vergeleken. Na de bijeenkomst werden de deelnemende afdelingen verzocht om voor iedere patiënt te bepalen of zij het bestralingsplan zouden willen herzien. De dosis op de gezonde weefsels was substantieel verschillend tussen de deelnemende afdelingen, in het bijzonder voor de lage dosis niveaus onder de 20 Gy. De bijeenkomst en het delen van de oorspronkelijke planningsresultaten onder de deelnemende afdelingen resulteerde in een lagere dosis op de gezonde weefsels en een lagere variabiliteit tussen de deelnemende afdelingen na het herzien van de bestralingsplannen.

De bevindingen beschreven in dit proefschrift kunnen worden gebruikt om de behandelonzekerheden voor zowel de uitwendige als inwendige bestraling van patiënten met endeldarmkanker te verlagen. Door het verlagen van de behandelonzekerheden kan het doelvolume meer conform worden bestraald waardoor er minder stralingsdosis op naastgelegen gezond weefsel komt en er een hogere extra dosis op de tumor mogelijk wordt.

LIST OF PUBLICATIONS AND CONFERENCE PRESENTATIONS

Publications

Clinical pedicle screw accuracy and deviation from planning in robot-guided spine surgery:
Robot-guided pedicle screw accuracy

J.D. van Dijk, **R.P.J. van den Ende**, S. Stramigioli, M. Köchling, N. Höss

Spine (Phila Pa 1976) 40: E986-991 (2015)

DOI: 10.1097/BRS.0000000000000960

Benefit of adaptive CT-based treatment planning in high-dose-rate endorectal brachytherapy
for rectal cancer

R.P.J. van den Ende, E.C. Rijkmans, E.M. Kerkhof, R.A. Nout, M. Ketelaars, M.S. Laman,

C.A.M. Marijnen, U.A. van der Heide

Brachytherapy 17:78–85 (2018)

DOI: 10.1016/j.brachy.2017.08.011

MRI visibility of gold fiducial markers for image-guided radiotherapy of rectal cancer

R.P.J. van den Ende, L.S. Rigter, E.M. Kerkhof, E.L. van Persijn van Meerten, E.C. Rijkmans,

D.M.J. Lambregts, B. van Triest, M.E. van Leerdam, M. Staring, C.A.M. Marijnen, U.A. van der Heide

Radiotherapy & Oncology 132, 93-99 (2019)

DOI: 10.1016/j.radonc.2018.11.016

Feasibility of gold fiducial markers as a surrogate for GTV position in image-guided radiotherapy
of rectal cancer

R.P.J. van den Ende, E.M. Kerkhof, L.S. Rigter, M.E. van Leerdam, F.P. Peters, B. van Triest,

M. Staring, C.A.M. Marijnen, U.A. van der Heide

International Journal of Radiation Oncology, Biology, Physics 105:1151-9 (2019)

DOI: 10.1016/j.ijrobp.2019.08.052

Predictive factors for response and toxicity after brachytherapy for rectal cancer; results from
the HERBERT study

E.C. Rijkmans, C.A.M. Marijnen, B. van Triest, M. Ketelaars, A. Cats, A. Inderson, **R.P.J. van den Ende**,

M.S. Laman, E.M. Kerkhof, R.A. Nout

Radiotherapy & Oncology 133: 176-182 (2019)

DOI: 10.1016/j.radonc.2019.01.034

EUS-guided fiducial marker placement for radiotherapy in rectal cancer: feasibility of two placement strategies and four fiducial types
L.S. Rigter, E.C. Rijkmans, A. Inderson, **R.P.J. van den Ende**, E.M. Kerkhof, M. Ketelaars, J. van Dieren, R.A. Veenendaal, B. van Triest, C.A.M. Marijnen, U.A. van der Heide, M.E. van Leerdam
Endoscopy International Open Nov;7(11), E1357-E1364 (2019)
DOI: 10.1055/a-0958-2148

Radiotherapy quality assurance for mesorectum treatment planning within the multicenter phase II STAR-TReC trial: Dutch results
R.P.J. van den Ende, F.P. Peters, E. Harderwijk, H. Rütten, L. Bouwmans, M. Berbee, R.A.M. Canters, G. Stoian, K. Compagner, T. Rozema, M. de Smet, M.P.W. Intven, R.H.N. Tijssen, J. Theuws, P. van Haaren, B. van Triest, D. Eekhout, C.A.M. Marijnen, U.A. van der Heide, E.M. Kerkhof
Radiation Oncology 15:41 (2020)
DOI: 10.1186/s13014-020-01487-6

Applicator visualization using ultrashort echo time MRI for high-dose-rate endorectal brachytherapy
R.P.J. van den Ende, E. Ercan, R. Keesman, E.M. Kerkhof, C.A.M. Marijnen, U.A. van der Heide
Accepted for publication in Brachytherapy
DOI: 10.1016/j.brachy.2020.06.010

Conference presentations

Benefit of repeat CT in high-dose rate brachytherapy as radical treatment for rectal cancer
R.P.J. Van den Ende*, E.C. Rijkmans, E.M. Kerkhof, R.A. Nout, M. Ketelaars, M.S. Laman, C.A.M. Marijnen, U.A. van der Heide
ESTRO 36, Vienna, Austria
*Oral presentation

Factors associated with complete response after brachytherapy for rectal cancer; the HERBERT study.
E.C. Rijkmans*, R.A. Nout, E.M. Kerkhof, A. Cats, B. van Triest, A. Inderson, **R.P.J. van den Ende**, M.S. Laman, M. Ketelaars, C.A.M. Marijnen
ESTRO 36, Vienna, Austria
*Poster presentation

MRI visibility of gold fiducial markers for image-guided radiotherapy for rectal cancer
R.P.J. van den Ende*, L.S. Rigter, E.M. Kerkhof, E.L. van Persijn van Meerten, E.C. Rijkmans, D.M.J. Lambregts, B. Van Triest, M.E. van Leerdam, M. Staring, C.A.M. Marijnen, U.A. Van der Heide
ESTRO 37, Barcelona, Spain
*Electronic poster

Proctitis after brachytherapy for rectal cancer: clinical and dosimetric factors - The HERBERT study
E.C. Rijkmans*, R.A. Nout, E.M. Kerkhof, A. Cats, B. van Triest, A. Inderson, **R.P.J. van den Ende**,
M.S. Laman, M. Ketelaars, C.A.M. Marijnen
ESTRO 37, Barcelona, Spain
*Oral presentation

Feasibility of gold fiducial markers as a surrogate for GTV position in image-guided radiotherapy of rectal cancer
R.P.J. van den Ende*, E.M. Kerkhof, L.S. Rigter, M.E. van Leerdam, F.P. Peters, B. van Triest,
M. Staring, C.A.M. Marijnen, U.A. van der Heide
AAPM Annual Meeting 2019, San Antonia, Texas, USA
*Electronic poster presentation

Applicator visualization for high-dose-rate endorectal brachytherapy using ultrashort echo time imaging
R.P.J. van den Ende, E. Ercan*, R. Keesman, E.M. Kerkhof, C.A.M. Marijnen, U.A. van der Heide
ESMRMB Congress 2020
*Oral presentation

DANKWOORD

Onderzoek doen en promoveren doe je gelukkig niet alleen, ik wil dan ook iedereen bedanken die direct of indirect een bijdrage hebben geleverd aan de totstandkoming van dit proefschrift.

Daarnaast wil ik in het bijzonder bedanken:
–   Mijn promotor prof. dr. van der Heide, Uulke, voor je goede adviezen en enthousiaste, laagdrempelige begeleiding. Ik heb bewondering voor het gemak waarmee jij nieuwe ideeën uit je mouw lijkt te schudden.
–   Mijn promotor prof. dr. Marijnen, Corrie, voor je waardevolle bijdragen en feedback, met name over de klinische kant van het project.
–   Mijn co-promotor dr. ir. Kerkhof, Ellen, voor je kritische blik en waardevolle feedback op mijn ideeën en geschreven stukken. Jouw geordende manier van werken waardeer ik enorm.
–   Tim, onze gedeelde hobby en interesses zorgden voor de nodige afleiding naast het werk. Ik geniet vooral van onze vaartochten wanneer niemand anders zo gek is om midden in de winter mee te gaan. Bedankt dat je mijn paranimf wil zijn.
–   Lisette, jouw geïnteresseerde, positieve instelling en bekende uitspraak 'traag maar gestaag' hebben vaak geholpen om de moed erin te houden. Bedankt dat je mijn paranimf wil zijn.
–   Mary en Lotte, voor de gezelligheid in K1-48!
–   De medewerkers van de afdeling Radiotherapie, in het bijzonder de onderzoeksgroep en de AIOS, voor de leuke tijd, zowel op de werkvloer als daarbuiten op congressen en de vele (vrijdagmiddag) borrels.
–   Marieke en Ton, voor het prachtige ontwerp van dit proefschrift.

Ten slotte (schoon)familie, vrienden en natuurlijk Marieke voor jullie gezelligheid, interesse, steun en afleiding.

CURRICULUM VITAE

Roy van den Ende werd op 19 april 1991 geboren in Delft. In 2009 behaalde hij het VWO diploma aan het ISW Tiendweg te Naaldwijk. Aansluitend startte hij de bachelor Technische Geneeskunde in Enschede gevolgd door de master Technical Medicine met specialisatie "Medical Imaging and Interventions". De master werd in 2015 afgesloten met een afstudeeronderzoek op de afdelingen Radiologie en Orthopedische Chirurgie van het Leids Universitair Medisch Centrum (LUMC), over de implementatie en het gebruik van een intraoperatieve CT scanner als toevoeging op een intraoperatief navigatiesysteem. Vanwege zijn interesse in beeldgestuurde interventies begon hij na het afronden van zijn studie aan zijn promotietraject bij de afdeling Radiotherapie van het LUMC, waarvan u het resultaat nu in handen heeft. In het laatste jaar van zijn promotieonderzoek is hij parttime gaan promoveren om ernaast als Technisch Geneeskundige te werken bij de afdeling Mondziekten, Kaak- en Aangezichtschirurgie van het LUMC. Per januari 2020 bekleed hij deze functie fulltime en houdt hij zich bezig met de implementatie en het gebruik van 3D technieken voor patiënt specifieke chirurgische planningen, 3D printen en intra-operatieve navigatie.